

ABSTRACT

FUNCTION OF DISINTEGRIN-LIKE DOMAIN OF KSHV gB IN

REGULATING VIRUS INFECTION

by

Lia R. Walker

November, 2015

Director of Dissertation: Dr. Shaw M. Akula

Major Department: Interdisciplinary Doctoral Program in Biological Sciences

KSHV, also referred to as human herpesvirus-8 (HHV-8), is the eighth and latest identified human herpesvirus. It is the causative agent for a variety of malignancies namely Kaposi's sarcoma (KS), primary effusion lymphoma (PEL), and multicentric Castleman disease (MCD). The processes and mechanisms involved in virus entry are among the many intricacies not fully understood regarding KSHV and other viruses. As in other herpesviruses, KSHV target cell entry is a complex process consisting of multiple steps which include: initial attachment/binding to the cell, virus:cell surface receptor interactions, virus internalization/uptake, and subsequent trafficking of the virus for nuclear delivery. Viral envelope glycoproteins interact with target cell surface receptor molecules to facilitate entry into cells. For instance, virus envelope associated glycoprotein B (gB) of KSHV is known to interact with integrins via its RGD (Arg-Gly-Asp; 27-29aa) integrin binding domain. RGD of KSHV functionally interacts with integrins $\alpha 3\beta 1$, $\alpha V\beta 3$, and $\alpha V\beta 5$ that have a role in initiating internalization. Cell surface receptors, like integrins, aid in a virus' ability to establish a successful infection. In addition to

RGD, KSHV gB also harbors the lesser studied integrin recognition motif, disintegrin-like domain (DLD; 66-85aa). As it pertains to virus entry in general, few studies have sought to establish a role for DLD, which is highly conserved among gB homologs. In the following studies, we employed phage display peptide library screening and recombinant viruses to determine that DLD of KSHV gB binds $\alpha 9\beta 1$ integrin on the surface of target cells in an interaction critical for infection. We go on to specify a role for DLD-binding $\alpha 9\beta 1$ in mediating KSHV entry by employing subcellular fractionation. The virus interactions with $\alpha 9\beta 1$ are crucial for endosomal trafficking of KSHV, as integrin $\alpha 9\beta 1$ was observed to have a role in late endosomal escape of KSHV for cytosolic delivery. These studies provide new insights in regards to KSHV infectious entry into target cells. Advancing our knowledge of virus entry is critical for a thorough understanding of KSHV pathogenesis.

FUNCTION OF DISINTEGRIN-LIKE DOMAIN OF KSHV gB IN
REGULATING VIRUS INFECTION

A Dissertation

Presented To the Faculty of the Interdisciplinary Doctoral Program in
Biological Sciences
East Carolina University

In Partial Fulfillment of the Requirements for the Degree
Doctor of Philosophy in Interdisciplinary Biological Science

by

Lia R. Walker

November, 2015

© Lia R. Walker, 2015

FUNCTION OF DISINTEGRIN-LIKE DOMAIN OF KSHV gB IN

REGULATING VIRUS INFECTION

by

Lia R. Walker

APPROVED BY:

DIRECTOR OF
DISSERTATION:

Shaw M. Akula, Ph.D.

COMMITTEE MEMBER:

Paul P. Cook, M.D.

COMMITTEE MEMBER:

Ronald S. Johnson, Ph.D.

COMMITTEE MEMBER:

MD A. Motaleb, Ph.D.

COMMITTEE MEMBER:

Baohong Zhang, Ph.D.

CHAIR OF THE INTERDISCIPLINARY
DOCTORAL PROGRAM IN BIOLOGICALSCIENCES:

Li Yang, PhD

DEAN OF THE
GRADUATE SCHOOL:

Paul J. Gemperline, PhD

ACKNOWLEDGEMENTS

With the utmost respect and gratitude, I would like to thank my mentor, Dr. Shaw Akula for noticing my potential and believing in me. His guidance, patience, and continued support have made the completion of this work possible. Additionally, I would like to thank my committee members for their valuable feedback and suggestions. I must also acknowledge both past and present members of the Akula lab for their willingness to offer encouragement and a helping hand.

To my wonderful parents, I thank you for your love, support, encouragement, and every sacrifice made to help me reach this point in my academic career! To my extended family, friends, and everyone who has uttered a prayer on my behalf and/or encouraged me along the way, thank you.

TABLE OF CONTENTS

LIST OF TABLES	ix
LIST OF FIGURES	x
LIST OF ABBREVIATIONS.....	xii
CHAPTER 1: REVIEW OF LITERATURE.....	1
Herpesvirus Overview	1
Kaposi's Sarcoma-Associated Herpesvirus	3
KSHV-Associated Diseases.....	4
KSHV Worldwide: Prevalence, Epidemiology, and Transmission	9
The KSHV Genome.....	11
KSHV Entry, a Receptor-Mediated Event.....	12
KSHV Latency and Reactivation.....	15
PRELUDE: THE KNOWN AND UNKNOWN INVOLVING KSHV gB's INTERACTIONS WITH INTEGRINS	18
CHAPTER 2: DISINTEGRIN-LIKE DOMAIN OF GLYCOPROTEIN B REGULATES KAPOSI'S SARCOMA-ASSOCIATED HERPESVIRUS INFECTION OF CELLS	21
Summary	22
Introduction.....	23
Results.....	24
Expression and purification of gB Δ TM Δ D	24
Phage display peptide library identifies integrin α 9 as a potential receptor for DLD in gB.....	25
Plate based binding assays demonstrate the DLD of KSHV gB to bind α 9 β 1	26
Inhibiting interactions between α 9 β 1 and the DLD of gB lowers KSHV infection	28
DLD of gB is critical to KSHV infection of cells.....	29
Discussion.....	31
Methods.....	35

Cells	35
Antibodies.....	36
Proteins and Peptides	36
Cloning and expression of recombinant gBATMΔDLD.H.....	36
Western blotting.....	36
PCR.....	36
Screening phage display peptide libraries to determine a novel receptor for gB	37
ELISA	37
Immunoprecipitation.....	37
Generating recombinant KSHV	37
Monitoring KSHV infection of cells.....	37
Flow cytometry	38
Acknowledgements.....	38
Author Contributions	38
CHAPTER 3: $\alpha 9\beta 1$ INTEGRIN MEDIATES POST-INTERNALIZATION STEP OF KSHV ENTRY.....	52
Summary.....	53
Introduction.....	54
Results	56
Anti- $\alpha 9$ and - $\beta 1$ integrin antibodies and soluble $\alpha 9\beta 1$ integrins do not inhibit KSHV internalization but do inhibit KSHV infectivity.....	56
KSHV particles are trafficked beyond the early endosome for late endosomal escape	58
Immunofluorescence microscopy demonstrates KSHV to localize in EEs and LEs.....	61
Discussion.....	62
Methods.....	64
Cells	64

Antibodies	64
Proteins and Reagents	65
Generating stable CHO cell line expressing human $\alpha 9$	65
Flow cytometry	65
Virus infection of cells	66
qRT-PCR.....	66
Monitoring KSHV by qPCR.....	67
Immunoprecipitation.....	67
Sucrose flotation gradient	67
Western blotting/marker analysis	68
Acid phosphatase activity assay.....	68
FITC-KSHV	69
Immunofluorescence microscopy	69
Author Contributions	70
SUMMARY	83
CHAPTER 4: ADDITIONAL DATA REACTIVATION OF VIRUSES IN RENAL TRANSPLANT RECIPIENTS	88
Abstract	88
Introduction	89
Methods	91
Study patients	91
Isolation of peripheral blood mononuclear cells (PBMCs)	91
qRT-PCR.....	92
DNA preparation and qPCR monitoring reactivation of BKV and JCV	92
Results and Discussion	93
I. Reactivation of herpesviruses post-renal transplantation	93
II. Incidence of polyomaviruses post-renal transplantation.....	94

Concluding Remarks.....	96
REFERENCES	99
APPENDIX A: SUPPLEMENTARY DATA FROM CHAPTER 2.....	129
Methods	129
Cells	129
Proteins	129
Peptides.....	129
Cloning and expression of recombinant gB Δ TM Δ D	130
Screening phage display peptide libraries to determine a novel receptor for gB.....	131
ELISA	132
Generating recombinant KSHV	132
Purifying KSHV for infection studies.....	134
Monitoring KSHV infection of cells.....	135
APPENDIX B: SUPPLEMENTARY DATA FROM CHAPTER 3.....	142
Methods	142
Reagents	142
Monitoring the effects of inhibitors on KSHV infection.....	142
APPENDIX C: IRB APPROVAL.....	144

LIST OF TABLES

CHAPTER 2: DISINTEGRIN-LIKE DOMAIN OF GLYCOPROTEIN B REGULATES KAPOSI'S SARCOMA-ASSOCIATED HERPESVIRUS INFECTION OF CELLS

Table 1. List of primers..... 50

Table 2. Amino acid sequences of the phage-displayed peptides isolated by screening DLD in
gB..... 51

CHAPTER 4: REACTIVATION OF VIRUSES IN RENAL TRANSPLANT RECIPIENTS

Table 1. List of primers..... 98

Table 2. Urinary viral loads 98

LIST OF FIGURES

PRELUDE: THE KNOWN AND UNKNOWN INVOLVING KSHV gB's INTERACTIONS WITH INTEGRINS

Figure 1. Role of RGD and DLD binding integrins in KSHV biology 20

CHAPTER 2: DISINTEGRIN-LIKE DOMAIN OF GLYCOPROTEIN B REGULATES KAPOSI'S SARCOMA-ASSOCIATED HERPESVIRUS INFECTION OF CELLS

Figure 1. Generating KSHV gB Δ TM Δ D..... 43

Figure 2. Expression and purification of gB Δ TM Δ D in baculovirus expression system..... 44

Figure 3. Phage encoding peptide PKADGRV bound gB Δ TM efficiently..... 45

Figure 4. Characterizing the gB: α 9 β 1 interactions by performing competitive ELISA..... 46

Figure 5. Role of integrin α 9 β 1 in wild type KSHV infection 47

Figure 6. Architecture and generation of recombinant BAC36 Δ D 48

Figure 7. DLD of gB is critical for KSHV infection 49

CHAPTER 3: α 9 β 1 INTEGRIN MEDIATES POST-INTERNALIZATION STEP OF KSHV ENTRY

Figure 1. Effect of anti-integrin antibodies and soluble α 9 β 1 on KSHV infection (A, B) and internalization (C, D) 75

Figure 2. Antibodies to integrin α 9 inhibit KSHV infection of CHO- α 9 cells, but not internalization 76

Figure 3. Schematic representation of the sucrose flotation assay for endosome purification 77

Figure 4. Detection of KSHV in endosomal fractions 78

Figure 5. Confirming the presence of KSHV in sucrose gradient fractions at different early time points..... 79

Figure 6. Antibodies to integrin $\alpha 9\beta 1$ inhibit KSHV escape from the late endosome 80

Figure 7. Antibodies against $\alpha 9$ and $\beta 1$ integrin subunits block KSHV nucleocapsid trafficking to the perinuclear region by 30min PI..... 82

SUMMARY

Summary Figure. 86

APPENDIX A: SUPPLEMENTARY DATA FROM CHAPTER 2

Supplemental Figure 1: Effect of RGD peptides and anti-RGDgB-N1 antibodies in blocking $\alpha v\beta 3$ integrin interactions with gB 136

Supplemental Figure 2: Expression of integrin $\alpha 9$ on the surface of HFF and HMVEC-d cells..... 137

Supplemental Figure 3: Inhibition of rKSHV.152 infection by different doses of antibodies to $\alpha 9$ 138

Supplemental Figure 4: $\alpha 5\beta 1$ integrin does not inhibit rKSHV.152 infection of cells 139

Supplemental Figure 5: Molecular cloning and mutagenesis involved in derivation of BAC36 Δ D and BAC36.T via PCR and sequencing..... 140

APPENDIX B: SUPPLEMENTARY DATA FROM CHAPTER 3

Supplemental Figure 1: Disruption of ‘normal’ endosome function inhibits KSHV infectious entry into HFF cells 143

LIST OF ABBREVIATIONS

293 cells	epithelial cells
+2ME	2-mercaptoethanol
$\alpha 3\beta 1$	alpha 3 beta 1; an RGD binding integrin
$\alpha V\beta 3$	alpha V beta 3; an RGD binding integrin
$\alpha V\beta 5$	alpha V beta 5; an RGD binding integrin
$\alpha 9\beta 1$	alpha 9 beta 1; an integrin identified as a receptor for the DLD in KSHV gB
ADAM	a disintegrin and metalloprotease
ADAMTS	a disintegrin and metalloprotease with thrombospondin motifs
AIDS	acquired immunodeficiency syndrome
Amp	ampicillin
AP-1	activating protein-1
BAC	bacterial artificial chromosome
BAC36	a bacterial artificial chromosome system harboring the KSHV genome used to generate recombinant virus
BAC36 Δ D-KSHV	recombinant KSHV lacking a functionally intact DLD of gB and containing an introduced tetracycline cassette
BAC36.T-KSHV	recombinant KSHV containing an intact DLD sequence and an introduced tetracycline cassette
BCBL cells	body-cavity-based lymphoma cell line
BKV	BK virus
BSA	bovine serum albumin
C	carboxyl domain
Cap	chloramphenicol
cART	combination antiretroviral therapy
CHO- $\alpha 9$ cells	Chinese hamster ovary cells stably expressing the human $\alpha 9$ integrin subunit
CHO cells	Chinese hamster ovary cells
CSA	chondroitin sulfate A
CSB	chondroitin sulfate B
Ct	threshold cycle
D+/R-	CMV-seropositive donor/CMV-seronegative recipient
D+/R+	CMV-seropositive donor/CMV-seropositive recipient
DC-SIGN	dendritic cell-specific intercellular adhesion molecule-3-grabbing non-integrin

DLD	disintegrin-like domain
DMEM	Dulbecco's modified Eagle's medium
DMSO	dimethyl sulfoxide
DNA	deoxyribonucleic acid
EBV	Epstein-Barr virus
EDTA	ethylenediaminetetraacetic acid
EEs	early endosomes
Egr-1	early growth response protein-1, a cellular transcription factor
ELISA	enzyme-linked immunosorbent assay
EphA2	ephrin receptor tyrosine kinase A2
ERK1/2	extracellular signal-related kinase 1/2
ESRD	end-stage renal disease
FAK	focal adhesion kinase
FBS	fetal bovine serum
FITC-KSHV	fluorescein isothiocyanate labeled KSHV
gB	glycoprotein B
gB Δ TM	soluble form of gB
gB Δ TM/pCDNA3.1(+)	plasmid encoding a recombinant gB (aa 1 to 702 lacking the transmembrane and cytoplasmic domains) that was amplified from the gB-pCDNA3.1(+)
gB Δ TM Δ D	soluble form of gB lacking intact DLD
gB Δ TM-DLD.M2/pCDNA3.1(+)	plasmid containing mutation to the DLD domain of gB
GFP	green fluorescent protein
gpK8.1A/B	glycoprotein K8.1A/B
GST	glutathione-S-transferase
HAART	highly active antiretroviral therapy
HBD	heparin binding domain
HCMV	human cytomegalovirus
HFF cells	human foreskin fibroblast cells
HHV	human herpesvirus
HHV-8	human herpesvirus-8 also known as KSHV
HMVEC-d	human dermal microvascular endothelial cells
HIV	human immunodeficiency virus

HS	heparan sulfate
HSV-1	herpes simplex virus-1
HSV-2	herpes simplex virus-2
ICTV	International Committee of Taxonomy of Viruses
IFA	immunofluorescence assay
IgG	immunoglobulin G antibody molecules
IL	interleukin
JCV	JC virus
KICS	KSHV inflammatory cytokine syndrome
KS	Kaposi's sarcoma
KSHV	Kaposi's sarcoma-associated herpesvirus
KSHV-MCD	KSHV multicentric Castleman disease
LANA	latency-associated nuclear antigen
LEs	late endosomes
LUR	long unique coding region
MAPK	mitogen activated protein kinase
MSM	men who have sex with men
MOI	multiplicity of infection
NaOH	Sodium hydroxide
NF- κ B	nuclear factor-kappa B
NI-NTA	nickle nitrilotriacetic acid
ORF	open reading frame
ORF8	gene encoding gB
ORF50	immediate early gene encoding for RTA
PBMC	peripheral blood mononuclear cells
PBS	phosphate buffered saline
PCR	polymerase chain reaction
PEL	primary effusion lymphoma
PFU	plaque forming units
pGET-rec	plasmid providing the recombineering enzymes, Gam, RecE, and RecT
PI	post infection
PI-3K	phosphatidylinositol 3-kinase

PML	progressive multifocal leukoencephalopathy
PMSF	phenylmethylsulfonyl fluoride
PNS	post-nuclear supernatant
PVAN	polyomavirus-associated nephropathy
PVDF	polyvinylidene difluoride
qPCR	quantitative real time PCR
qRT-PCR	quantitative reverse transcription PCR
Rab5	an EE marker
Rab7	LE marker
RGD	Arg-Gly-Asp motif
rKSHV.152	recombinant KSHV expressing green fluorescent protein
RNA	ribonucleic acid
RT	room temperature
RTA	replication and transcription activator
SDS-PAGE	sodium dodecyl sulfate-polyacrylamide gel electrophoresis
SF9	Spodoptera frugiperda ovarian cells
SIFA	surface immunofluorescence assay
SVMP	snake venom metalloprotease
Tet	tetracycline
TM	transmembrane region
TPA	12-O-tetradecanoyl phorbol-13-acetate
TRI-1	minor capsid protein KSHV ORF62-encoded triplex component I
TRITC	Tetramethylrhodamine
UMCIRB	University and Medical Center Institutional Review Board
VEGF	vascular endothelial growth factor
VZV	varicella zoster virus
xCT	human cysteine transporter system xCT

CHAPTER 1: REVIEW OF LITERATURE

Herpesvirus Overview

Herpesviruses are highly host-specific, large (125-295Kb), linear double stranded DNA viruses with certain shared biological properties (Davison, 2011; Hanson *et al.*, 2011; Lepa & Siwicki, 2012; Mettenleiter *et al.*, 2009; Wu *et al.*, 2014). As many as 300 of these enveloped viruses have been discovered (Davison, 2011), with well over 130 being characterized. Herpesviruses infect most vertebrates and a few invertebrates (Brown & Newcomb, 2011; Wu *et al.*, 2014). As of a 2009 update by the International Committee on Taxonomy of Viruses (ICTV), these viral pathogens are classified under the new order, *Herpesvirales*. This order is divided into three distinct families: *Herpesviridae* (subdivided into the alpha-, beta-, and gamma-*herpesvirinae* and containing mammal, bird, and reptile herpesviruses), *Alloherpesviridae* (fish and frog herpesviruses), and *Malacoherpesviridae* (invertebrate herpesviruses) (Davison, 2010; Davison *et al.*, 2009; Griffin *et al.*, 2010).

All herpesvirus exhibit structural commonality, comprising four layers: (i) an inner core containing double stranded viral DNA, (ii) an icosahedral capsid (125nm in diameter) surrounding the core and composed of 162 capsomers, (iii) a virus-encoded proteinaceous layer located between the capsid and the virus envelope called the tegument, and (iv) a lipid envelope studded with viral glycoproteins. Fully assembled, the herpesvirus virion is approximately 200-250nm in diameter (Bohannon *et al.*, 2013; Brown & Newcomb, 2011; Zaichick *et al.*, 2011). The standout fundamental theme unifying all herpesviruses is their ability to establish long-term latency after primary infection (Griffin *et al.*, 2010). In terms of their infectious cycle, herpesviruses share common methods of entry into host cells, delivery of their genome to the nucleus, establishment of prolonged latent infection, replication and capsid assembly inside the

nucleus, egress of genomes from the nucleus, maturation and envelopment in the cytosol, and ultimately exocytosis of mature and infectious virions. Notable differences among herpesviruses include variance in host range, tissue tropism, time course of lytic replication, and disease symptoms and severity (Zaichick *et al.*, 2011).

In particular, *Herpesviridae* subfamily classifications (alpha-, beta-, and gamma-*herpesvirinae*) are generally based on the host cell type in which latency is established, the length of replication cycles, and genome content (Kramer & Enquist, 2013). Alpha-herpesviruses are neuroinvasive pathogens that establish latency in the nervous systems of their mammalian hosts (Engel *et al.*, 2015; Kramer & Enquist, 2013). These viruses have a broad tissue tropism and host range and a relatively short replication cycle (i.e. hours) (Jin *et al.*, 2008). On the other hand, beta-herpesviruses have a long replication cycle (i.e. days) and limited host range. Additionally, beta-herpesviruses establish latency in mononuclear cells, secretory cells, epithelial cells, etc. (Fishman, 2013). The host range for gamma-herpesviruses is also limited (Cabello *et al.*, 2013), and these viruses widely establish latency in lymphocytes (Smith *et al.*, 2006) and have variable replication rates.

Historically, there was a general consensus that only eight herpesviruses infected humans as their natural host, namely human herpesviruses (HHV) (Kumari *et al.*, 2015; Tang & Mori, 2010). The herpesviruses identified in humans are herpes simplex virus-1 (HSV-1; HHV-1), herpes simplex virus-2 (HSV-2; HHV-2), varicella zoster virus (VZV; HHV-3), Epstein-Barr virus (EBV; HHV-4), cytomegalovirus (HCMV; HHV-5), human herpesvirus-6A/B (HHV-6A, HHV-6B), human herpesvirus-7 (HHV-7), and Kaposi's Sarcoma-associated herpesvirus (KSHV or HHV-8). HSV-1, HSV-2, and VZV are alpha-herpesviruses. HCMV, HHV-6A/B, and HHV-7 are beta-herpesviruses. EBV and KSHV are gamma-herpesviruses (Alibek *et al.*, 2014; Fishman,

2013; Penkert & Kalejta, 2011). Based on epidemiological, biological, and molecular characteristics, the classification of HHV-6A and HHV-6B has transitioned from viral variants to distinct viruses (Trempe *et al.*, 2015). Thus, many researchers are now considering there to be nine total human herpesviruses (Grose & Adams, 2014; Ohye *et al.*, 2014).

Kaposi's Sarcoma-Associated Herpesvirus

KSHV, the eighth identified human herpesvirus infecting a relatively small number of the human population (Dreyfus, 2013), is of particular interest to the present report. KSHV belongs to the gamma-2-herpesvirus subfamily and the genus *Rhadinovirus* along with its primate rhadinovirus relatives (Bruce *et al.*, 2015; Guito & Lukac, 2015; Neipel *et al.*, 1998). Primate rhadinoviruses have been observed in squirrel monkeys, African Green monkeys, rhesus macaques, etc. Notably, rhesus macaque rhadinovirus infects rhesus macaques and induces disease in a manner that resembles KSHV-associated pathologies. In fact, rhesus macaque rhadinovirus with its genetic similarities to KSHV serves as an animal model for understanding KSHV infection and pathogenesis (Estep & Wong, 2013). However, in terms of herpesviruses that infect humans, gamma-1-herpesvirus EBV is KSHV's closest human herpesvirus relative (Guito & Lukac, 2015; Jenner *et al.*, 2003).

With both sequence homology to and gene distinction from related gamma-herpesviruses, KSHV was identified as a new human herpesvirus in 1994 by Chang *et al.* via representational difference analysis (Chang *et al.*, 1994). Using this PCR-based subtraction hybridization technique, the team of researchers identified KSHV DNA sequences in lesions from patients with acquired immunodeficiency syndrome (AIDS)-Kaposi's Sarcoma (KS) but not in adjacent normal tissue. Befittingly named based on the KS biopsies from which it was discovered, KSHV has since been associated with all forms of KS (Chang *et al.*, 1994; Jenner & Boshoff, 2002; Moore &

Chang, 1995). Not long after its identification, the genome of the ‘new’ herpesvirus was cloned and sequenced (Ganem, 1997; Neipel *et al.*, 1998; Russo *et al.*, 1996). The KSHV genome was mapped using cosmid and phage genomic libraries from the BC-1 cell line (a B cell lymphoma cell line co-infected with KSHV and EBV; (Ueda *et al.*, 2011)) (Russo *et al.*, 1996).

KSHV-Associated Diseases

KSHV is considered the etiological agent for KS, primary effusion lymphoma (PEL), and KSHV-multicentric Castleman Disease (KSHV-MCD) (Cesarman *et al.*, 1995; Soulier *et al.*, 1995; Ueda *et al.*, 2011). All of these rare neoplastic disorders resulting from KSHV infection are most commonly observed in immunocompromised individuals (Kaplan, 2013).

KS is a malignant vascular tumor characterized by lesions occurring mainly on the skin, but it can also affect the mucosa and visceral organs (Makharoblidze *et al.*, 2015; Radu & Pantanowitz, 2013). Hallmarks of KS are angiogenesis, cell proliferation, and inflammation (Cancian *et al.*, 2013). Most human tumors are clonal outgrowths of a single cell type, but KS lesions are diverse in cell type (Ganem, 2010). The purplish-brown lesions progress from early stage flat patches to plaques to large nodules (in tumor stage) and histologically exhibit proliferation of infiltrating inflammatory cells, slit-like neovascular structures, and spindle-shaped endothelial cells (Cai *et al.*, 2010; Ganem, 2010; Gbabe *et al.*, 2014; Radu & Pantanowitz, 2013). KS lesions exhibit an abundant expression of pro-inflammatory cytokines (e.g.: interferon gamma [IFN γ], tumor necrosis factor alpha [TNF- α], interleukin-1 [IL-1], IL-6, and granulocyte-macrophage colony-stimulating factor [GM-CSF]), chemokines (e.g.: monocyte chemoattractant protein 1 [MCP-1] and IL-8), and pro-angiogenic growth factors (e.g.: vascular endothelial growth factor [VEGF], platelet-derived growth factor [PDGF], beta fibroblast growth factor [β FGF], transforming growth factor beta [TGF β]) (Cancian *et al.*, 2013; Sivakumar *et al.*, 2008). During

early stages of this chronic inflammation-associated malignancy, spindle cells (the predominant KSHV-infected cells in advancing KS lesions) secrete inflammatory cytokines and growth/angiogenic factors that fuel activation and proliferation of endothelial cells in an autocrine or paracrine manner. Further recruitment of inflammatory cells to the infection site advances the inflammatory process (Cancian *et al.*, 2013).

In 1872, KS was referred to as “idiopathic multiple pigmented sarcoma of the skin” by the Hungarian dermatologist, Moritz K. Kaposi. At the time of Kaposi’s reports, KS was believed to be a rare and slowly progressing tumor affecting mainly elderly men of Mediterranean and Eastern European origin who were more likely to die with KS rather than from it (Chang & Moore, 2014). Until the 1980s, only two forms of KS were readily noted, classic KS, as previously described by Kaposi, and an endemic and more aggressive form affecting adults as well as children in sub-Saharan Africa (Robey & Bower, 2015). However, with the emergence of the human immunodeficiency virus (HIV)/AIDS epidemic, KS quickly became a priority for scientific research (Chang & Moore, 2014); individuals with AIDS were at an astonishingly increased risk for developing KS (50,000 fold risk compared to the general population) (Shiels *et al.*, 2011). During the emergence of the HIV/AIDS epidemic, the incidence of KS reportedly increased over 1,000 fold in homosexual/bisexual men, intravenous drug users, and promiscuous individuals at high risk for contracting HIV (Karamanou *et al.*, 2013). By 1982, the United States (US) Center for Disease Control and Prevention characterized KS as an AIDS-defining illness (Robey & Bower, 2015).

Clinically, there are four recognized variants of KS which include: classic KS, African (endemic) KS, iatrogenic (transplantation-associated) KS, and AIDS (epidemic)-KS (Fatahzadeh & Schwartz, 2013). The aforementioned classic form of KS typically affects older (>60 years old)

HIV-*uninfected* men of Jewish, Mediterranean, and Eastern European decent (estimated male/female ratio: 15:1). Classic KS may persist over the course of many years, but it is considered non-life threatening. The lesions characteristic to this form of KS are usually present on the skin of the lower extremities and rarely infiltrate internal organs (Guttman-Yassky *et al.*, 2006; Regnier-Rosencher *et al.*, 2013); however, classic KS may be complicated by lympho-edema or hyperkeratosis (Hengge *et al.*, 2002).

African (endemic) KS was prevalent in equatorial countries of Africa long before the HIV/AIDS epidemic. Prior to the epidemic, endemic KS, like classic KS, primarily affected men, and tumor development was to some extent linked to environmental factors (e.g. barefoot walking on volcanic rock and clay soils composed of iron-oxide rich minerals) (Simonart, 2006). However, during the HIV/AIDS epidemic, endemic KS escalated alongside HIV (Singh *et al.*, 2014); it is now difficult to distinguish the endemic form of KS from AIDS-KS in sub-Saharan Africa (van Bogaert, 2012). Nonetheless, endemic KS has been divided into two subtypes. The first type mainly affects middle-aged adults and is locally aggressive on the skin. The second more aggressive and often fatal type of African KS mainly affects children (<10 years old) and is accompanied by lymphadenopathy (Szajerka & Jablecki, 2007).

Iatrogenic (transplantation-associated) KS is generally observed in the setting of solid organ transplantation upon treatment with immunosuppressive drugs, such as during renal transplantation (Bhutani *et al.*, 2015; Chen *et al.*, 2014). In addition to transplantation, iatrogenic KS also affects those individuals undergoing immunosuppressive therapies for autoimmune disorders and cancer (Saggar *et al.*, 2008). Cessation of immunosuppressive therapy reportedly leads to disease regression in some instances, but in other cases, there have been occurrences of aggressive/potentially fatal progression of iatrogenic KS (Restrepo & Ocazonez, 2011; Saggar *et*

al., 2008; Schwartz *et al.*, 2008). Additionally, with this particular form of KS, lymph node and visceral organ involvement is more common (Rescigno *et al.*, 2013).

AIDS-KS is deemed an AIDS-defining illness due to its close association with the AIDS. With this AIDS-KS, manifesting lesions are often present in the mouth and on the genitalia and internal organs (especially the lungs and gastrointestinal tract) (Robey & Bower, 2015). This form of KS is the most common malignancy in HIV-1 infected individuals. AIDS-KS is particularly frequent in homosexual and bisexual men who have sex with men (MSM) (Minhas & Wood, 2014). In the US alone, between 20-50% of AIDS patients developed KS during the early years of the epidemic (Bhutani *et al.*, 2015). However, after the introduction of highly active antiretroviral therapy (HAART) in 1996, there was a significant decline in AIDS-KS incidence (Restrepo & Ocazonez, 2011). In fact, in regions with access to combination antiretroviral therapy (cART), recent reports have shown an 80% decrease in AIDS-KS incidence since its peak occurrence during the early HIV/AIDS epidemic (i.e. the pre-HAART era) (Bhutani *et al.*, 2015). Unfortunately, in sub-Saharan Africa where resources are lacking and HIV infections have reached pandemic proportions, AIDS-KS continues to be a persisting public health problem. In some African countries, AIDS-KS is the most common cancer in males and second-most common malignancy among females (Bhutani *et al.*, 2015; Mosam *et al.*, 2010; Restrepo & Ocazonez, 2011).

KSHV is the causative agent for PEL, as well. PEL is a rare B cell non-Hodgkin's lymphoma originating in body cavities. This lymphoproliferative disorder causes lymphomatous effusions that typically affect surfaces of the pleura, peritoneum, and pericardium; on rare incidents, PEL may infiltrate joint spaces (Klepfish *et al.*, 2015). PEL mainly occurs in HIV infected individuals but also may affect solid organ transplant recipients, those inflicted with

chronic hepatitis C virus, and elderly individuals (Bhutani *et al.*, 2015). Though KSHV is deemed the etiological agent for PEL, nearly 50% of KSHV-positive PEL patients are also co-infected with EBV (Uppal *et al.*, 2015). Notably, all PEL derived cell lines are infected with KSHV and 70% are co-infected with EBV (Spadavecchia *et al.*, 2010).

KSHV-MCD is among one of the characterized Castleman disease variants that most often arises in the setting of an HIV-infection but can also occur in transplant recipients and other HIV-negative individuals (Bhutani *et al.*, 2015; Uldrick *et al.*, 2012). KSHV-MCD is a rare lymphoproliferative disorder characterized by symptoms of lymphadenopathy, splenomegaly, cytopenia, and inflammation (Carbone *et al.*, 2015). Excess cytokine production is believed to cause KSHV-MCD symptoms; specifically, human IL-6 and IL-10 dysregulation and KSHV-encoded viral IL-6 production is attributed to KSHV-MCD pathogenesis. Additionally, upregulation of nuclear factor-kappa B (NF- κ B), VEGF, and other factors is reportedly involved in KSHV-MCD pathogenesis (Bhutani *et al.*, 2015; Uldrick *et al.*, 2012).

More recently, a MCD-related KSHV-associated condition was described. With few exceptions, the clinical symptoms of KSHV inflammatory cytokine syndrome (KICS) are indistinguishable from that of KSHV-MCD (Polizzotto *et al.*, 2012; Sakakibara & Tosato, 2014). Likewise, KICS patients exhibit upregulated KSHV viral loads, viral IL-6, and homologs of human IL-6 and IL-10 quite comparable to levels observed in KSHV-MCD. The exact KICS:KSHV-MCD relationship is inconclusive, but it is presumed that KICS may be a being a prodrome or milder version of KSHV-MCD that at some point evolves into full-blown KSHV-MCD. Additionally, the possibility that KICS may be a contributing factor inducing the inflammatory symptoms observed in patients with severe KS or PEL is also being explored (Carbone *et al.*, 2015; Polizzotto *et al.*, 2012).

KSHV Worldwide: Prevalence, Epidemiology, and Transmission

KSHV is among the list of viral pathogens estimated to cause 12-25% of human cancers worldwide (La Ferla *et al.*, 2013; Morrison *et al.*, 2015). Unlike its other human herpesvirus counterparts, KSHV is not ubiquitous in the human population (Labo *et al.*, 2014; Moore & Chang, 2014; Morrison *et al.*, 2015) and its worldwide distribution is disproportionate (Minhas & Wood, 2014; Nalwoga *et al.*, 2015). Prevalence of KSHV infection is directly correlated to KS incidence and varies according to geographic location, ethnicity, and distinct behavioral risk factors (Labo *et al.*, 2014). Employing enzyme-linked immunosorbent assays (ELISAs) or immunofluorescent assays (IFAs), evaluation of KSHV seroprevalence is primarily assessed via antibody testing and typically relies on reactivity to one or more KSHV-encoded latent (e.g. latency-associated nuclear antigen [LANA]) and/or lytic antigens (e.g. K8.1 antigen) (Bhutani *et al.*, 2015; Labo *et al.*, 2014).

KSHV is overwhelmingly prevalent in sub-Saharan Africa with seropositivity rates >50%. Infection is moderately prevalent in Mediterranean regions (10-30%) and much less prevalent in Western and Northern Europe, Asia, and the US (<10%). Spiked KSHV prevalence is also reported among Brazilian Amerindians in South America as well as in some Chinese ethnic groups. Notably, even with reportedly low overall KSHV seroprevalence in the US and certain parts of Europe, prevalence is significantly elevated in MSM; some reports estimate 20-30% seropositivity in MSM in the US and Northern Europe (La Ferla *et al.*, 2013; Labo *et al.*, 2015; Labo *et al.*, 2014; Morrison *et al.*, 2015).

Despite KSHV's highly conserved genome, certain KSHV genomic regions containing sequence variations have been useful in molecular epidemiology studies as markers of strain diversity and epidemiologic patterns of viral spread. The open reading frame (ORF) K1 gene (K1) has the most variable region in the KSHV genome. Sequence variations of K1, a lytic gene unique

to KSHV, has allowed for the classification of KSHV into seven subtypes (A/A5, B, C, D, E, F, and Z) based on K1 sequence analysis/genotyping (Ouyang *et al.*, 2014). There is as much as a 30% difference among KSHV subtypes with variations majorly concentrated in two specific hypervariable regions of K1 (Ouyang *et al.*, 2014; White *et al.*, 2008). According to the accounts of several researchers, KSHV strain distribution seemingly varies geographically and ethnically in conjunction with historical human migration patterns (Betsem *et al.*, 2014; Fu *et al.*, 2009; Fukumoto *et al.*, 2011; Kajumbula *et al.*, 2006; Zong *et al.*, 1999). Specifically, KSHV subtypes A and C are observed in the US, Europe, the Middle East and Northern Asia. Subtypes B and A5 are present in Africa and French Guiana. KSHV subtype D is observed in Taiwan, the Pacific islands, and Australia. Subtype E is present in Ecuador and among Brazilian Amerindians. KSHV subtype F was identified in Uganda, and Z has been identified among Zambian children (Azadmanesh *et al.*, 2012; Ouyang *et al.*, 2014).

The non-uniform distribution of KSHV also suggests non-uniformity in its modes of transmission (Betsem *et al.*, 2014). Transmission of KSHV occurs via sexual and non-sexual routes. The bodily fluid in which KSHV is most abundant is saliva (considered the main vehicle for transmission (Pinzone *et al.*, 2015)), but it is also present in peripheral blood mononuclear cells (PBMCs), oropharyngeal mucosa, semen, cervico-vaginal secretions, and prostate glands (Minhas & Wood, 2014). In non-endemic regions, sexual transmission, with increasing risk according to the number of sexual partners and sexual practices (i.e. MSM), is presumably the main route of KSHV transmission (Minhas & Wood, 2014; Pinzone *et al.*, 2015). Though some studies argue the validity of sex being the mode of KSHV transmission among heterosexual individuals (Malope-Kgokong *et al.*, 2010; van Bogaert, 2012; Zhang *et al.*, 2014), other studies consider men in a heterosexual relationship who are concurrently bisexually active as a likely source for KSHV

transmission heterosexually (Munawwar *et al.*, 2014). In terms of non-sexual routes, KSHV transmission by blood transfusion may occur on rare occasions, and injection drug poses a risk for infection. As a consequence of immunosuppression, KSHV transmission is linked to solid organ transplantation as well (Fatahzadeh, 2012; La Ferla *et al.*, 2013; Pinzone *et al.*, 2015).

In endemic regions where KSHV affects the general population, transmission is mainly believed to occur via non-sexual transmission routes, such as mother-to-child/vertical transmission. However, the precise biological, social, environmental, etc. factors involved in non-sexual KSHV transmission are unknown (Malope-Kgokong *et al.*, 2010). In sub-Saharan Africa for instance, transmission is to some extent believed to occur via saliva exchange (Nalwoga *et al.*, 2015; Zhang *et al.*, 2014). In this region, studies have shown intrafamilial aggregation of KSHV, in which viral transmission likely occurs through the exchange of saliva (Betsem *et al.*, 2014; Crabtree *et al.*, 2014).

The KSHV Genome

KSHV has genomic organization similar to that of other rhadinoviruses. KSHV possesses a large double stranded DNA genome of approximately 170kb which is comprised of a central long unique coding region (LUR; approximately 140kb with 53.5% G+C content) flanked by multiple non-coding G+C-rich terminal repeat sequences (TRs) (Jha *et al.*, 2014; Uppal *et al.*, 2014). The LUR is the protein-coding region encoding 90 or so ORFs, 12 microRNAs (miRNAs), and antisense RNAs (Uppal *et al.*, 2014; Uppal *et al.*, 2015). Of the approximately 90 ORFs in the coding region, 60 are homologous to other rhadinoviruses, and there are 43 conserved genes among *Herpesviridae* (Krug & Pellett, 2014; Ouyang *et al.*, 2014). ORF4-75 are classified based on their homology to gamma-2 herpesvirus saimiri (Veetil *et al.*, 2014). The genome also consists of over 20 ORFs unique to KSHV, namely “K genes.” Viral genes have been shown to regulate the cell

cycle, inhibit apoptosis, promote angiogenesis, and facilitate immune evasion of infected cells (Wen & MacKenzie, 2013).

KSHV Entry, a Receptor-Mediated Event

The complex multi-step entry process for KSHV and many other viruses is considered cell type dependent (Bandyopadhyay *et al.*, 2014; Li *et al.*, 2015). It is seemingly a virus' overall intent to transport its genome to the nucleus of an uninfected host cell in a manner such that efficient viral replication can occur. Very few viruses have the ability to directly deliver their viral capsids to the cytosol via plasma membrane fusion. The majority of viruses, including KSHV, exploit existing endocytic mechanisms of the cell which presumably offers viruses the advantage of host immune system evasion (Mercer & Greber, 2013; Yamauchi & Helenius, 2013b). The major routes of endocytosis utilized by viruses include phagocytosis, macropinocytosis, caveolae-mediated endocytosis, and clathrin-mediated endocytosis (the most extensively studied and best characterized mechanism of endocytosis) (Bhattacharyya *et al.*, 2010; Hernaez & Alonso, 2010).

KSHV has an extensive cellular tropism and can establish a productive infection in various cell types both *in vivo* and *in vitro* (Chakraborty *et al.*, 2012; Hertel, 2011). These cell types include endothelial cells, epithelial cells, keratinocytes, fibroblasts and B cells, the only cell type in which long-term KSHV latency occurs, *in vivo* (Sin & Dittmer, 2013). Depending upon the cell type, KSHV utilizes different modes of endocytosis. For instance, KSHV entry into human foreskin fibroblast (HFF) cells is clathrin dependent (Akula *et al.*, 2003), whereas other mechanisms such as micropinocytosis have been implicated as the method of entry into endothelial cells (Dutta *et al.*, 2013; Raghu *et al.*, 2009). Nevertheless, most endocytosed viruses are delivered to the endosomes of target cells and experience low pH/acidification dependent membrane fusion to and penetration from either early or late endosomes for viral capsid delivery to the cytoplasm

prior to subsequent travel to the nucleus (Grove & Marsh, 2011; Veettil *et al.*, 2014; Yamauchi & Helenius, 2013b).

Herpesviruses, via their viral envelope glycoproteins, are able to initially attach and bind specific cellular entry receptors which in turn facilitates virus access to a target cell's interior. Virus internalization, endomembrane fusion, and subsequent trafficking are all believed to be driven by envelope glycoprotein interactions with cell surface receptor molecules (Zhang & Gao, 2012). KSHV ORFs 8, 22, 47, 39, and 53 encode conserved herpesvirus envelope glycoproteins gB, gH, gL, gM, and gN, respectively. Specific to KSHV alone are envelope glycoproteins ORF4 and gpK8.1A, as well as glycoproteins gpK8.1B, K1, K14, and K15; these glycoproteins are expressed during the lytic cycle of replication (Veettil *et al.*, 2014). Incidentally, KSHV is believed to infect a plethora of target cells due to its effective ability to interact with ubiquitously expressed cell surface molecules such as heparin sulfate (HS) during the preliminary phase of entry. For instance, KSHV gB, gpK8.1A, gH, and ORF4 are all shown to bind cell surface heparin sulfate molecules (Akula *et al.*, 2001a; Birkmann *et al.*, 2001; Hahn *et al.*, 2009; Hahn *et al.*, 2012; Spiller *et al.*, 2006; Wang *et al.*, 2001). Harboring a putative heparin binding domain (HBD), gB and gpK8.1A are typically considered the key envelope glycoproteins integral for the initial phase of infectious entry, as they facilitate attachment to cell surface HS proteoglycans via a charge-based interaction. This initial attachment to HS brings the virus within closer proximity to target cells such that perhaps more meaningful interactions with other receptor molecules, such as integrins (heterodimeric cell adhesion receptors composed of non-covalently associated α and β subunits (Barczyk *et al.*, 2010)), can occur to facilitate the actual entry process (Akula *et al.*, 2001a; Akula *et al.*, 2001b).

Of the human herpesvirus envelope glycoproteins, gB is the most highly conserved (Lopper & Compton, 2002; Wanas *et al.*, 1999). KSHV gB is unique compared to other conserved glycoproteins in that it exclusively possesses two distinct integrin recognition motifs: (i) RGD (Arg-Gly-Asp), the minimal peptide region known to interact with subsets of target cell surface integrins (Wang *et al.*, 2003); and (ii) disintegrin-like domain (DLD), the highly conserved, less common integrin binding domain initially identified within gB of HCMV (Feire *et al.*, 2004; Feire *et al.*, 2010). KSHV was the first herpesvirus shown to interact with adherent target cell integrins in a step initiating infectious virus entry (Akula *et al.*, 2002; Chakraborty *et al.*, 2012). Reportedly, KSHV gB:integrin interactions facilitate adhesion, cytoskeleton rearrangement, integrin activation, and enhanced intracellular signaling (i.e. focal adhesion kinase (FAK), Src, phosphatidylinositol 3-kinase (PI-3K), Rho GTPases, etc). Such signaling and reorganization prompts virus internalization and presumably generates a cellular environment receptive to infection (Boulant *et al.*, 2015; DiMaio *et al.*, 2011; Hussein *et al.*, 2015; Van den Broeke *et al.*, 2014). A multitude of studies have implicated KSHV gB interactions with RGD-binding integrins, $\alpha 3\beta 1$, $\alpha V\beta 3$, and $\alpha V\beta 5$, as valuable for infectious virus entry (Akula *et al.*, 2002; Chandran, 2010a; Garrigues *et al.*, 2008; Veettil *et al.*, 2008). However, both RGD and non-RGD-binding integrins are believed to aid equally in virus entry (Hussein *et al.*, 2015). For instance, KSHV gB via its DLD was recently shown to specifically interact with cell surface expressed non-RGD-binding $\alpha 9\beta 1$ integrin to promote infectious entry into cells (Walker *et al.*, 2014). Throughout the subsequent chapters of this work, the role(s) of integrin $\alpha 9\beta 1$ in KSHV entry and infection were further explored.

Apart from integrin-mediated entry, KSHV utilizes other cellular receptors for entry as well. For instance, KSHV envelope associated gH/gL engages the ephrin receptor tyrosine kinase

A2 (EphA2) for infectious entry into target cells (Hahn & Desrosiers, 2014; Hahn *et al.*, 2012). Additionally, dendritic cell-specific intercellular adhesion molecule-3-grabbing non-integrin (DC-SIGN) (Rappocciolo *et al.*, 2006) and human cysteine transporter xCT (xCT) (Kaleeba & Berger, 2006) among others, are also considered valuable entry receptors for KSHV (Garrigues *et al.*, 2014; Zhang & Gao, 2012).

KSHV Latency and Reactivation

KSHV infection of cells is established via endocytosis and delivery of viral DNA to the nucleus (Lu *et al.*, 2014) where KSHV replication occurs, post-entry (Chakraborty *et al.*, 2012). Like other herpesviruses, KSHV has a biphasic life cycle comprised of latent and lytic phases of replication that are distinguished based on divergent gene expression profiles (Owen *et al.*, 2014) (Purushothaman *et al.*, 2015; Uppal *et al.*, 2014; Uppal *et al.*, 2015). The dynamic between latent and lytic phases of replication allows the virus to persist for the duration of the host's lifetime (Frappier, 2015). Notably, KSHV establishes latency in the majority of infected cells (Steitz *et al.*, 2011); at any given instance, only a subpopulation (<5%) of infected cells display evidence of lytic gene expression (Cai *et al.*, 2010; Dyson *et al.*, 2008; Guito & Lukac, 2015; Sun *et al.*, 1999).

The default pathway of KSHV infection both *in vivo* and *in vitro* is latent (dormant) infection (Uppal *et al.*, 2014). Establishing latency allows KSHV to evade the host's immune surveillance, maintain persistent life-long infections, and promote tumorigenesis (Yang *et al.*, 2015). It is during this phase of replication that the KSHV genome persists in the nucleus of the infected host cell as a circular episome. Latency is also characterized by restricted gene expression without the production of infectious virions (Owen *et al.*, 2014; Purushothaman *et al.*, 2015; Uppal *et al.*, 2014). The few genes expressed during latency suppress KSHV lytic gene expression and encode proteins that promote cell survival and proliferation, thus preventing viral episome loss

(Owen *et al.*, 2014; Ye *et al.*, 2011). KSHV latent genes include ORF73 (LANA), ORF72 (viral cyclin; vCyc), ORF71 (vFLIP), and ORFK12 (kaposin) (Sin & Dittmer, 2013).

Latent phase of replication is reversible, and the quiescent state can be disrupted by certain environmental and physiological factors, such as hypoxia, oxidative stress, immune suppression, pro-inflammatory cytokine upregulation, co-infection with other viruses, etc. (Purushothaman *et al.*, 2015; Uppal *et al.*, 2014). The process by which a latent virus shifts to a lytic (productive) phase of replication is termed reactivation (Traylen *et al.*, 2011). For herpesviruses, the exact molecular mechanism by which virus reactivation from latency occurs is unknown (Dyson *et al.*, 2012). During lytic phase of infection, the full repertoire of KSHV genes are expressed, facilitating replication of linear genomes, production and egress of progeny virions, and cell death (Chen *et al.*, 2015; Uppal *et al.*, 2014).

Expression of lytic genes occurs in a sequential and temporally regulated manner, in the order of immediate early (IE), early (E), and late (L) genes (Uppal *et al.*, 2014). The genes expressed first after lytic reactivation, IE genes, regulate further expression of viral and cellular genes. E genes initiate replication of the viral genome, and L genes encode for structural proteins (Chang & Kung, 2014). Specifically, KSHV IE gene ORF50 encodes for replication and transcription activator (RTA). RTA is considered the molecular switch that actually initiates the transition from latent to lytic replication and is sufficient for activating the entire lytic program (Chen *et al.*, 2015; Li *et al.*, 2014). Notably, *in vitro*, KSHV latently infected cells in culture can undergo lytic reactivation in response to treatment with chemical inducers such as phorbol esters (e.g. 12-O-tetradecanoylphorbol-13- acetate; TPA) or histone deacetylase inhibitors (e.g. sodium butyrate) (Kati *et al.*, 2013). Among other cellular and viral factors, reactivation of KSHV from latency (i.e activation of RTA) is shown to require mitogen- activated protein kinase (MAPK)

signaling. The MAPK pathways mediate KSHV reactivation via activating protein (AP)-1 that binds specifically to the RTA promoter to initiate RTA expression and activate the lytic program. Conversely, MAPK inhibitors/RTA suppression prevents KSHV reactivation (Chen *et al.*, 2015; Giffin & Damania, 2014). Additionally, studies show that inhibition of early growth response-1 (Egr-1), a transcription factor and signaling component downstream of Raf>MEK>ERK1/2 (MAPK signaling) impedes KSHV reactivation as well (Dyson *et al.*, 2010; Dyson *et al.*, 2012).

In all, even after over 20 years since its identification as a new herpesvirus, several aspects of KSHV remain elusive. Fully comprehending the intricacies of KSHV entry, infection, and pathogenesis will allow for the advancement of therapeutic intervention strategies. However, without a thorough understanding of KSHV and other viruses alike, these opportunistic pathogens will continue to inflict havoc on their hosts.

**PRELUDE: THE KNOWN AND UNKNOWN INVOLVING KSHV gB's
INTERACTIONS WITH INTEGRINS**

Despite barriers that target cells possess, viruses strategically utilize distinct receptor molecules, which can be proteins, carbohydrates, or lipids (Dimitrov, 2004), to enter and subsequently infect cells (Grove & Marsh, 2011). Glycoprotein B (gB) is the most highly conserved glycoprotein among *Herpesviridae*. Among these gB homologs, only envelope associated KSHV gB possesses an RGD (Arg-Gly-Asp; 27-29aa; at the extracellular amino terminus coil region after the putative signal sequence) (Akula *et al.*, 2003; Garrigues *et al.*, 2008; Wang *et al.*, 2003; Zhang *et al.*, 2005) (Figure 1). Considered the major integrin binding motif, RGD is the minimal peptide region known to interact with subsets of host cell surface integrins (Akula *et al.*, 2003; Wang *et al.*, 2003). The RGD sequence recognizes at least half of the more than 20 known integrins (Ruoslahti, 1996). Specifically, RGD of KSHV gB interacts with integrins $\alpha 3\beta 1$, $\alpha V\beta 3$, and $\alpha V\beta 5$ that function in promoting KSHV internalization (Akula *et al.*, 2001a; 2002; Akula *et al.*, 2001b; Veetil *et al.*, 2008) (Figure 1).

Distinctively, KSHV gB harbors both RGD and DLD (RX5-7D/ELXXFX5C; 66-85aa; with a conservative D to E substitution) integrin recognition motifs (Figure 1). Initially identified within HCMV envelope gB, DLD of gB is conserved among many herpesvirus gB homologs (Feire *et al.*, 2004; Feire *et al.*, 2010). This lesser studied integrin recognition motif binds integrins RGD-independently (Eto *et al.*, 2002; Feire *et al.*, 2010). The DLD of gB strongly resembles the disintegrin loop of ADAMs (a disintegrin and metalloproteases), multifunctional proteins that contain a metalloprotease domain and a disintegrin motif that confers RGD-independent integrin-binding (Feire *et al.*, 2004). Disintegrins are non-enzymatic polypeptides with anti-cancer and anti-metastatic properties, widely distributed in the venoms of viperid snakes (Selistre-de-Araujo

et al., 2010). Actually, it was with the analysis of related domains of snake venom metalloproteases (SVMPs) that lead to the assumption that DLDs of other varieties would also be involved in integrin-mediated interactions (Wolfsberg *et al.*, 1995). Though highly conserved in gB of herpesviruses, DLD's role in virus entry has been minimally explored outside of the virus in which it was discovered. Herein we seek to: (i) define a role for DLD in KSHV infection of cells, (ii) identify integrin(s) with which DLD of KSHV gB interacts critical for entry and subsequent infection, and (iii) establish a role for DLD-binding integrin(s) during early stages of infection.

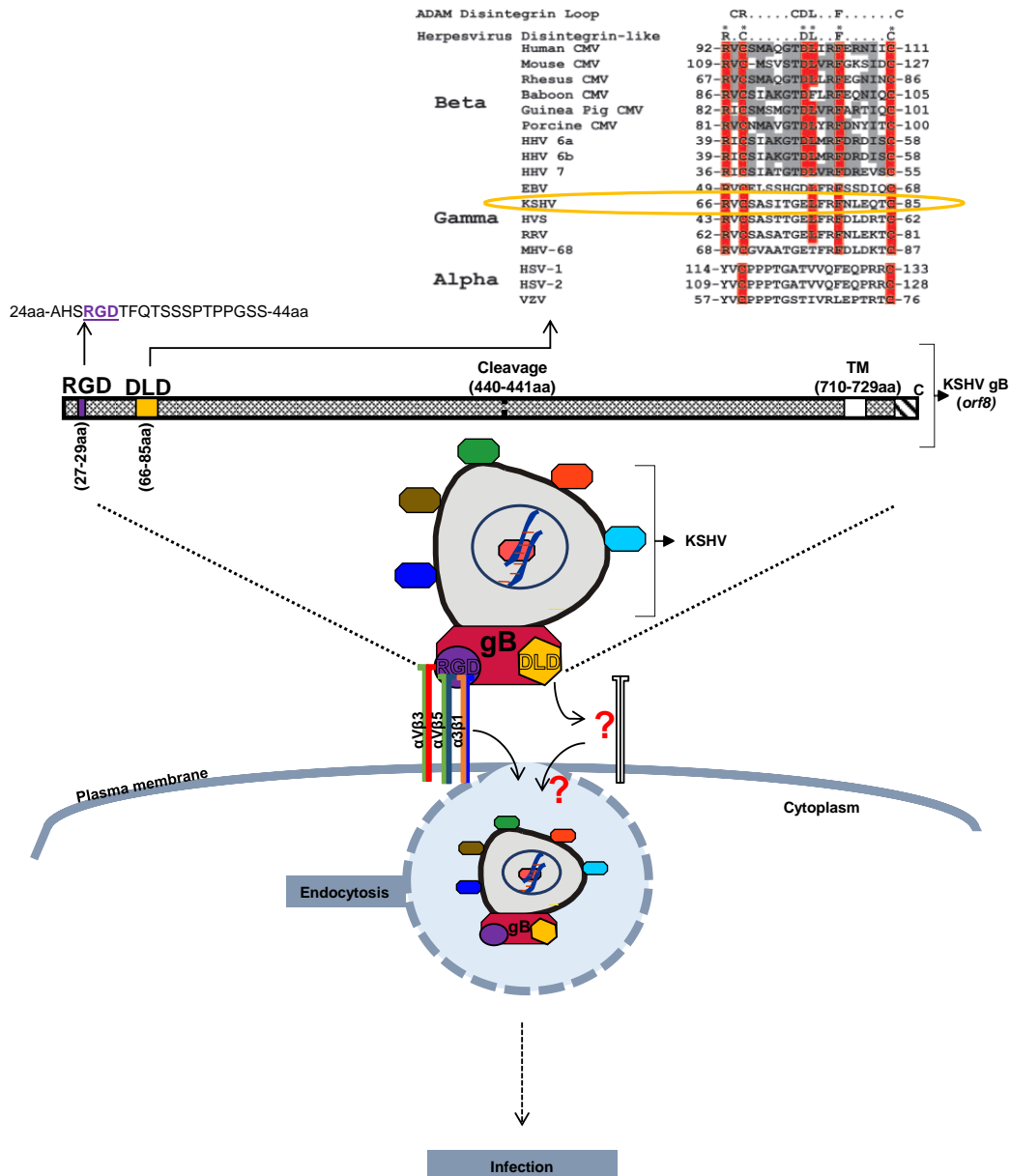


Figure 1. Role of RGD and DLD binding integrins in KSHV biology. Envelope associated KSHV gB harbors two distinct integrin binding domains: RGD (27-29aa) and DLD (66-85aa). KSHV gB is the only gB homolog with an RGD, whereas DLD is highly conserved among *Herpesviridae*. RGD physically interacts with integrins to initiate internalization. The role for the disintegrin-like function of gB as it pertains to receptor-driven KSHV entry and infection is unknown. This work tackles the following questions: (i) With what integrin(s) does DLD of KSHV gB interact; (ii) Is this DLD:integrin interaction critical for KSHV entry and subsequent infection; (iii) At what level does this interaction affect virus entry? The portion of this figure depicting conservation of the gB DLD was derived from (Feire *et al.*, 2004). TM: transmembrane region; C: carboxyl domain

**CHAPTER 2: DISINTEGRIN-LIKE DOMAIN OF GLYCOPROTEIN B REGULATES
KAPOSI'S SARCOMA-ASSOCIATED HERPESVIRUS INFECTION OF CELLS**

Lia R. Walker, Hosni A.M. Hussein, and Shaw M. Akula*

Department of Microbiology & Immunology, Brody School of Medicine at East Carolina
University, Greenville, NC, USA 27834.

This manuscript has been published:

J. Gen. Virol., August 2014 95: 1770-1782, doi: 10.1099/vir.0.066829-0

Running head: Disintegrin-like domain aid KSHV entry

Keywords: disintegrins, KSHV, integrins, entry

Word count: Summary (244); Main text (5491)

Journal's contents category: Animal viruses – Large DNA

Address correspondence to: Shaw M. Akula, Department of Microbiology & Immunology,
Brody School of Medicine, East Carolina University, Greenville, North Carolina, USA 27834.
Phone: (252)744-2702; Fax: (252) 744-3104; Email: akulas@ecu.edu

SUMMARY:

KSHV glycoprotein B (gB) is a lytic structural protein expressed on the envelope of mature virions and on the membrane of cells supporting lytic infection. In addition to this viral glycoprotein's interaction with integrins via its RGD (Arg-Gly-Asp) motif, KSHV gB possesses a disintegrin-like domain (DLD) which binds integrins as well. Prior to this study, there has been minimal research involving the less common integrin-binding motif, DLD, of gB as it pertains to herpesvirus infection. Via employing phage display peptide library screening and molecular biology techniques, DLD of KSHV gB was shown to specifically interact with non-RGD binding $\alpha 9\beta 1$ integrins. Similarly, monitoring wild type infection confirmed $\alpha 9\beta 1$:DLD interactions to be critical to successful KSHV infection of HFF and HMVEC-d cells compared to 293 cells. To further demonstrate the importance of DLD of gB in KSHV infection, two recombinant virus constructs were generated using a bacterial artificial chromosome (BAC) system harboring the KSHV genome (BAC36): BAC36 Δ D-KSHV (lacking a functionally intact DLD of gB and containing an introduced tetracycline cassette) and BAC36.T-KSHV (containing an intact DLD sequence and an introduced tetracycline cassette). Accordingly, BAC36 Δ D-KSHV presented significantly lower infection rates in HFF and HMVEC-d cells compared to the comparable infection rates achieved by wild type BAC36-KSHV and BAC36.T-KSHV. Thus, the present report has delineated a critical role for DLD of gB in KSHV infection which may lead to a better breadth of knowledge regarding the sophisticated mechanisms utilized by virus-encoded structural proteins in KSHV entry and infection.

INTRODUCTION

Since the 1994 discovery of Kaposi's sarcoma-associated herpesvirus (KSHV) in the Chang-Moore Lab (Chang *et al.*, 1994), efforts are continuously being made nearly 20 years later to understand the intricacies of this double-stranded DNA virus. KSHV, also referred to as Human herpesvirus-8 (HHV-8), belongs to the gamma-2-herpesvirus subfamily and is the eighth and latest addition to Herpesviridae (Russo *et al.*, 1996). KSHV causes a variety of cancers like Kaposi's sarcoma (KS), primary effusion lymphoma, and multicentric Castleman disease (Hamden *et al.*, 2005).

In general, envelope associated glycoproteins predominantly assist virus in the entry process (Bryan *et al.*, 2005). In this study, our focus is on KSHV gB, a lytic structural protein primarily expressed on the envelope of mature virions, but also present on the membrane of cells supporting lytic infection (Akula *et al.*, 2001a). KSHV virus binding and entry has been linked to gB mediated interactions not only with cell surface heparan sulfate (HS) molecules but also to integrins, transmembrane receptor molecules with involvement in processes such as adhesion, motility, and endocytosis (Akula *et al.*, 2001a; 2002; Hahn *et al.*, 2009). With KSHV being the first herpesvirus shown to exhibit an interaction with adherent target cell integrins—a preliminary step essential for successful viral infection—it is now known that via its RGD (Arg-Gly-Asp) motif, KSHV gB functionally interacts with a variety of cellular integrins, namely $\alpha 3\beta 1$, $\alpha \nu\beta 3$, and $\alpha \nu\beta 5$ (Chakraborty *et al.*, 2012). Unlike the RGD of gB, the disintegrin-like domain (DLD) is a less common integrin recognition motif that was initially identified within HCMV envelope gB (Feire *et al.*, 2010). The DLD in gB was found to bear a striking resemblance to the ADAM (a disintegrin and metalloprotease) disintegrin loop (Feire *et al.*, 2004). Members of the ADAM family are multifunctional proteins that contain a metalloprotease domain and a disintegrin motif

that confers RGD-independent integrin-binding (Feire *et al.*, 2004). It has been observed that KSHV gB possesses a DLD (RX5-7D/ELXXFX5C; 66-85aa; with a conservative D to E substitution) that is notably conserved among gB homologs of many herpesviruses; specifically beta and gamma herpesviruses (Feire *et al.*, 2010).

Thus, in seeking to delineate a role for DLD of KSHV gB, we hypothesized the DLD in KSHV gB to play a critical role in the virus infection of cells. Results from our study using phage display peptide library screening and molecular biology techniques implicate the ability of DLD in gB to specifically interact with $\alpha 9\beta 1$ integrins. Utilizing a bacterial artificial chromosome (BAC) system harboring the KSHV genome (BAC36), we generated two recombinant virus constructs, BAC36 Δ D-KSHV (containing alanine point mutations within the DLD sequence of gB and an introduced tetracycline cassette from vector pEX18TC) and BAC36.T-KSHV (containing an intact DLD sequence and the introduced tetracycline cassette from vector pEX18TC) as a means to decipher a potential role for the DLD of KSHV gB in infection of cells.

RESULTS

Expression and purification of gB Δ TM Δ D

The KSHV encoded 2,106bp region of the *orf8* gene encoding gB Δ TM lacking the transmembrane (TM) and carboxyl domains (Wang *et al.*, 2003) was used to generate a soluble gB lacking a functionally intact DLD, gB Δ TM Δ D (Fig. 1). This was a crucial step to characterize a role for DLD of KSHV gB. Coomassie staining of SDS-PAGE gels was conducted to analyze protein purity, and detection following standard Western blotting protocols (Fig. 2). When purified gB Δ TM Δ D protein treated with 2-mercaptoethanol (2ME; reducing conditions) was analyzed via Coomassie staining, bands of approximately 35-40, 68, and 104 kDa were observed as in the lane

with gB Δ TM (Fig. 2). Impurities such as other contaminating proteins were not detected in either the gB Δ TM Δ D or the gB Δ TM preparations. When gB Δ TM Δ D and gB Δ TM were resolved under non-reducing conditions (-2ME), the 35-40 and 68kDa bands disappeared while only 104kDa band and the multiple polypeptides of more than 180kDa were observed (Fig. 2). The migration pattern of gB Δ TM Δ D is comparable to what was observed when gB Δ TM was resolved in earlier studies (Dyson *et al.*, 2010; Wang *et al.*, 2003). The specificity of the gB proteins were confirmed by performing Western blotting experiments (Fig. 2). This implies that gB Δ TM Δ D, like gB Δ TM, expressed in Sf9 cells can form disulphide-linked dimers or multimers under non-reducing conditions. These results suggest that the alanine point mutations introduced to the DLD sequence of gB did not significantly change the molecular weight or the migration pattern of the protein on a gel compared to the wild type (gB Δ TM).

Phage display peptide library identifies integrin α 9 as a potential receptor for DLD in gB.

Ph.D phage display libraries was used to identify novel ligands for the DLD in gB. Three random peptide libraries, a linear (X)₇, a cyclic Cys (X)₇ Cys, and a linear (X)₁₂ were screened against the gBDLD peptide. The single most common peptide (based on the increased frequency; 20 out of 30) possessed a **PKA(P)DGR(H)V(L)** sequence (Table 2). Interestingly, the major conserved sequence among the peptides identified had a conserved sequence of PKADGRV (9 out of 30).

We tested the ability of the phage carrying peptides L3 (PKADGRV), F1 (DCKPKPDGRLRD), and F5 (PKADGHV) to bind gB Δ TM immobilized on 96 well plates. It was determined that the phage carrying peptides L3, F1, and F5 specifically bound gB Δ TM compared to BSA and gB Δ TM Δ D (Fig. 3A). However, the phage encoding peptide PKADGRV (peptide L3) bound more efficiently when compared to the other peptides (F1 and F5). The binding

of the phage encoding L3 peptide to gB Δ TM could be significantly blocked by including 1mM of synthetic peptide PKADGRV during the incubating step compared to using scrambled peptide (Fig. 3B). The effect of PKADGRV peptide was measured against the known positive control, gBDLD peptide (Fig. 3B). A protein blast search of this sequence identified α 9 integrin [Homo sapiens; NCBI Ref Seq: NM_002207.2] to possess such a motif (133-139aa). This was an interesting finding as we had predicted a non-RGD binding integrin (Yokosaki *et al.*, 1994) as a probable receptor capable of binding the DLD of gB at the beginning of the study.

Plate based binding assays demonstrate the DLD of KSHV gB to bind α 9 β 1.

The integrin α 9 commonly forms a heterodimer with β 1 integrin subunit, α 9 β 1 (Young *et al.*, 2001). Upon identifying the α 9 integrin as a plausible receptor for gB, we used various modified ELISAs to test the ability of soluble KSHV gB to bind α 9 β 1. The binding of α 9 β 1 to gB Δ TM was monitored using polyclonal antibodies to α 9 β 1 (H-198). ELISA studies identified α 9 β 1 to specifically bind 1 μ g/ml of gB Δ TM in a dose dependent manner (Fig. 3C) compared to gB Δ TM Δ D and non-specific controls, BSA or GST. Similar data was observed when monoclonal antibodies to α 9 β 1 (Clone #560201) were used in the ELISA (data not shown). Interestingly, ELISA studies demonstrated an RGD binding integrin α v β 3, to bind gB Δ TM and gB Δ TM Δ D to comparable extent (Fig. 3D), demonstrating a functional RGD motif in both the soluble forms of the gB tested. Based on these results, 1 μ g/ml of both gB Δ TM and α 9 β 1 were used in all of our other experiments described below. An Immunoprecipitation experiment was done to further authenticate the results from ELISA-based assays. Herein, it was found α 9 subunit to specifically bind gB Δ TM (Fig. 3E; *lane 1*) and not the gB Δ TM lacking a functional DLD (Fig. 3E; *lane 3*).

To confirm the specificity of the KSHV encoded gB: $\alpha 9\beta 1$ binding, we attempted to neutralize this interaction by conducting competitive ELISAs. In this case, different concentrations of various ligands or antibodies known to interact with gB, the DLD motif specifically, or $\alpha 9\beta 1$ were used. KSHV gB is known to interact with HS via a charge based interaction (Bryan *et al.*, 2005). HS, chondroitin sulfate-A or -B (CSA, CSB; control glycosaminoglycans) had little effect on the gB: $\alpha 9\beta 1$ interactions, as binding between gB Δ TM and $\alpha 9\beta 1$ still occurred (Fig. 4A).

KSHV gB interacts with a variety of integrins via its RGD domain. In order to determine if gB interactions via the RGD domain altered its ability to bind $\alpha 9\beta 1$, competitive ELISA using **GRGDSP** and **KQAGDV** (an irrelevant peptide) was performed. The results confirmed that increasing concentrations of RGD peptides did not alter the ability of $\alpha 9\beta 1$ to bind gB Δ TM (Fig. 4B). Interestingly, the RGD peptide significantly blocked the ability of $\alpha v\beta 3$ to bind gB Δ TM (Supplemental Figure 1).

VEGF and tenascin C are common known ligands for integrin $\alpha 9\beta 1$ (Andrews *et al.*, 2009; Vlahakis *et al.*, 2005). Our data suggests that increasing concentrations of VEGF and laminin does not alter the binding of $\alpha 9\beta 1$ to gB Δ TM (Fig. 4C). Tenascin C on the other hand, was shown to enhance the gB: $\alpha 9\beta 1$ binding interaction (Fig. 4C).

Finally, to confirm whether gB: $\alpha 9\beta 1$ binding is dependent on the DLD of gB, we conducted competitive ELISAs using rabbit antibodies to DLD of gB (anti-DLD). Here, results show that there was a significant inhibition in the ability of $\alpha 9\beta 1$ to interact with gB Δ TM when the gB Δ TM-coated wells were incubated with anti-DLD prior to performing ELISA (Fig. 4D). Incubating gB Δ TM-coated wells with anti-RGDgB-N1 or anti-gB-C (non-specific antibodies) did not alter the ability of $\alpha 9\beta 1$ to bind gB Δ TM (Fig. 4D). Also, the anti-RGDgB-N1 antibodies blocked $\alpha v\beta 3$

binding to gB Δ TM (Supplemental Figure 1), suggesting the specificity of antibodies to DLD of gB to block gB: α 9 β 1 interactions. ELISA when performed at RT or at 37°C (data not shown) yielded identical results.

Inhibiting interactions between α 9 β 1 and the DLD of gB lowers KSHV infection.

To confirm a critical role for the DLD: α 9 β 1 interactions in KSHV infection we utilized the recombinant KSHV that expressed green fluorescent protein (GFP) referred to as rKSHV.152 (Akula *et al.*, 2001b; Grange *et al.*, 2012; Vieira *et al.*, 2001) and three different cell types known to support KSHV infection of cells. They were HFF (fibroblasts), 293 (epithelial cells), and HMVEC-d (endothelial cells) cells. First, we determined if these cells actually did express α 9. PCR results demonstrated HFF and HMVEC-d cells to express α 9 compared to 293 cells (Fig. 5A). Both HFF and HMVEC-d cells express α 9 on their cell surface as monitored by flow cytometry (Fig. 5B) and IFA (Supplemental Figure 2). Interestingly, all of the above cells (including the commonly used B-cell line, BCBL-1) express the β 1 integrin subunit (Akula *et al.*, 2002). Next, we conducted rKSHV.152 infection-based studies in the above cells using appropriate antibodies (Fig. 5C). Expression of GFP by cells was considered as positive for rKSHV.152 infection (Akula *et al.*, 2001b). This expression of GFP was monitored using a fluorescent microscope. Number of GFP positive cells at 72 h post infection (hPI) in 293, HFF, and HMVEC-d cells that were untreated with antibodies were 260, 50, and 105, respectively. Antibodies to α 5 and a pre-immune IgG did not significantly alter rKSHV.152 infection of cells (Fig. 5C). Soluble heparin was used as a known inhibitor of KSHV binding and infection of all the target cells. Antibodies to β 1 and α V integrins significantly inhibited rKSHV.152 infection of cells in HFF and HMVEC-d cells compared to infection in 293 cells (Fig. 5C). Infection of HFF

by rKSHV.152 was significantly lowered by antibodies to $\alpha 9$. We observed only a modest inhibition of rKSHV.152 infection by antibodies to $\alpha 9$ in HMVEC-d cells. A dose dependent effect of the antibodies to $\alpha 9$ antibodies on rKSHV.152 infection is provided in the supplemental section (Supplemental Figure 3). These results suggest an involvement of $\alpha 9\beta 1$ integrin in the KSHV infectious process of HFF cells and to a modest extent in HMVEC-d cells. To further authenticate the above results, we tested the effect of incubating rKSHV.152 with the soluble $\alpha 9\beta 1$ integrin prior to infecting the target cells. A dose dependent inhibition of KSHV infection of cells was observed when rKSHV.152 was incubated with soluble $\alpha 9\beta 1$ compared to $\alpha 5\beta 1$ (Supplemental Figure 4) prior to infection of HFF and HMVEC-d compared to 293 cells (Fig. 5D). The soluble $\alpha 9\beta 1$ used in this study was in a lyophilized form that was resuspended in sterile PBS. Finally, we tested the effect of incubating KSHV with rabbit antibodies developed against the DLD peptide sequence of gB prior to infection of cells. Our results indicated incubating KSHV with antibodies to DLD or RGD of gB lowered KSHV infection of HFF and HMVEC-d cells compared to 293 cells (Fig. 5E). Overall, these results implicate a key role for $\alpha 9\beta 1$:DLD interactions in KSHV infection of HFF and HMVEC-d cells (with minor differences between cell types that is discussed in the discussion section).

DLD of gB is critical to KSHV infection of cells.

We hypothesized knocking down a functional DLD of gB in KSHV will result in a decrease in virus infection of cells. To test this hypothesis, we developed a recombinant virus that lacked a functional DLD in KSHV gB (BAC36 Δ D). As a control to the BAC36 Δ D, we also generated BAC36.T that had an uninterrupted and functional gB; but with a tetracycline cassette (as in BAC36 Δ D) introduced in the intron region between the *orf8* and *orf9*. In brief, employing overlap

PCR (Fig. 6A, B), a series of cloning experimentations, and recombination rendered BAC36 Δ D and BAC36.T clones, respectively (Fig. 6C). Prior to transformation via electroporation and tetracycline selection stages, the correct orientation of the inserted tetracycline cassette in *orf8 Δ DLD.Tet^r/TOPO* and *orf Δ 7.8. Δ 9.Tet^r/TOPO* positive clones was confirmed by restriction enzyme digestion using BamHI and NheI; clone #3.2 and clone #7.2, denoting *orf8 Δ DLD.Tet^r/TOPO* and *orf Δ 7.8. Δ 9.Tet^r/TOPO* respectively, contain the correctly oriented cassette and were subsequently used in the generation of BAC36 Δ D and BAC36.T clones (Supplemental Figure 5A). These clones were further compared with the BAC36 wild type and confirmed by performing a variety of PCR reactions. First, PCR amplified tetracycline gene in BAC36 Δ D and BAC36.T compared to the BAC36 (Supplemental Figure 5B). All of the recombinant viral genomes contained *orf8* gene as determined by PCR (Supplemental Figure 5B). Second, we confirmed that the targets-1 and -2 representing a portion of *orf7*, complete sequence of *orf8*, and the N-terminal sequence of *orf9* from the original BAC36 genome (Supplemental Figure 5B) was contained in BAC36 Δ D and BAC36.T (Supplemental Figure 5C). Third, we amplified *orf8* from BAC36, BAC36 Δ D, BAC36.T genome using T1(F) and T2(R) primers. As predicted, we amplified a 4005bp DNA fragment in the BAC36 genome, while amplifying a product of size 5698bp from both BAC36 Δ D and BAC36.T (Supplemental Figure 5D). The above results were authenticated by sequencing using appropriate primers to confirm the specific mutations in the *orf8* gene contained within the BAC36 Δ D (Supplemental Figure 5E).

We then tested the infection rates of the above different recombinant viruses generated in the lab. First, we analyzed cell surface expression of gB in BAC36-KSHV and BAC36 Δ D-KSHV infected cells by FACS. This is vital as the results demonstrated cell membrane expression of gB in TPA-induced 293 cells infected with BAC36-KSHV and BAC36 Δ D-KSHV was comparable

(Fig. 7A). Next, we monitored infection of BAC36-KSHV, BAC36 Δ D-KSHV, BAC36.T-KSHV in 293, HFF, and HMEVC-d cells as per standard procedures. Our results indicated a sharp decline in the BAC36 Δ D-KSHV infection of HFF and HMVEC-d cells compared to BAC36-KSHV and BAC36.T-KSHV, respectively (Fig. 7B). Interestingly, BAC36 Δ D-KSHV infection of 293 cells was not altered as compared to BAC36-KSHV and BAC36.T-KSHV (Fig. 7B). Number of GFP positive cells at 72 hPI of BAC36-KSHV in 293, HFF, and HMVEC-d cells that were 116, 28, and 57, respectively. Taken together, our results implicate a critical role for DLD of gB in KSHV infection of HFF and HMVEC-d cells.

DISCUSSION

In addition to the most common integrin recognition motif, RGD (Akula *et al.*, 2002; Garrigues *et al.*, 2008), KSHV gB also possesses DLD juxtaposed in the extracellular amino terminal coil region that has potential integrin-binding capabilities as well (Feire *et al.*, 2004). In fact, it was with the analysis of the related domains of snake venom metalloproteases (SVMPs) that sparked the assumption that DLDs of other varieties, such as in ADAMs, would also be involved in integrin-mediated interactions (Lu *et al.*, 2010; Wolfsberg *et al.*, 1995).

The DLD of KSHV gB (66-85aa) corresponds to 49-68aa residues within the EBV gB. EBV is a closely associated human herpesvirus to KSHV and both are classified as gamma herpesviruses. Earlier, the ectodomain (23-685aa out of 1-875aa full length) of EBV gB was crystallized (Backovic *et al.*, 2009). It was determined that the major portion (52-68aa) of the electron dense DLD of EBV gB is contained within the domain III region which is exposed and actually wraps around the helices to form a left-handed twist. Based on these findings, we predict DLD of KSHV gB to also be an exposed ectodomain available for interactions with host cell

receptor molecules. Outside of HCMV, the role of DLD in virus entry has been minimally explored. Thus, this study has sought to unearth the role of DLD of gB in KSHV infection.

Instead of employing antibody based assays, we utilized phage display peptide library to ascertain the putative receptor for DLD of KSHV gB. We determined DLD of gB to interact with host cell receptor molecule, integrin $\alpha 9$, by panning random libraries of phage displayed peptides against the gBDLD peptide fragment (Table 2; Fig. 3A,B). The results from screening the phage display peptide libraries were further authenticated by performing plate based binding assays (ELISAs) and immunoprecipitation experiments using both gB Δ TM and gB Δ TM Δ D (Fig. 3C-D).

The subunit $\alpha 9$ has been widely shown to combine with $\beta 1$ to form a single heterodimer (Young *et al.*, 2001) with non-RGD binding capabilities (Yokosaki *et al.*, 1994). For this study, insight regarding specificity of KSHV gB: $\alpha 9\beta 1$ interactions was provided from results of several competitive ELISAs. HS (Fig. 4A), a target cell membrane molecule whose interaction with KSHV is mediated in part by envelope gB (Bryan *et al.*, 2005), VEGF, a known ligand for $\alpha 9\beta 1$ (Vlahakis *et al.*, 2005), or laminin, an extracellular matrix protein (Fig. 4C), did not block the gB: $\alpha 9\beta 1$ interactions. Another known ligand for $\alpha 9\beta 1$, tenascin C (Andrews *et al.*, 2009), also failed to neutralize the gB: $\alpha 9\beta 1$ interaction (Fig. 4C). In the case of tenascin C however, enhanced binding was observed between gB Δ TM and $\alpha 9\beta 1$ in what we believe to be a result of an allosteric interaction (Fig. 4C), as suggested by an earlier report (Laskowski *et al.*, 2009). Tenascin C is an extracellular matrix (ECM) molecule that is often times expressed at elevated levels in solid tumors and is said to have a role in cancer formation (Orend & Chiquet-Ehrismann, 2006). Further studies will focus on appreciating gB: $\alpha 9$ interactions with respect to tenascin C expression.

Likewise, competitive ELISAs also confirmed the ability of KSHV gB to interact with integrin $\alpha 9\beta 1$ independent of its RGD domain (Fig. 4B). Our findings are reminiscent of results

produced by Eto et al., who found that mutating the RGD motif of the aforementioned ADAM-15, had no effect on the binding of $\alpha 9\beta 1$ to the protein's disintegrin domain (Eto *et al.*, 2002). Moreover, when using an antibody directed against the DLD in gB, competitive ELISA data showed a substantial down regulation in the gB: $\alpha 9\beta 1$ interactions, suggesting the specificity of this antibody (Fig. 4D). These results imply that the avid binding between gB and $\alpha 9\beta 1$ is in fact dependent on the DLD of KSHV gB (Fig. 4D).

In an effort to extrapolate plate based assays to viral infection, we attempted to test the role of integrin $\alpha 9\beta 1$ in wild type KSHV infection of different cells (Fig. 5). HFF and HMVEC-d cells express $\alpha 9\beta 1$ compared to 293 cells. KSHV infection of 293 cells was not altered by antibodies to $\alpha 9$, $\beta 1$ subunits, DLD target sequence; and soluble $\alpha 9\beta 1$ (Fig. 5C-E). In HFF cells, antibodies to $\alpha 9$, $\beta 1$ subunits, DLD target sequence; and soluble $\alpha 9\beta 1$ significantly lowered KSHV infection (Fig. 5C-E). In HMVEC-d cells, there was a significant decrease in KSHV infection of cells due to antibodies against $\beta 1$ subunit and the DLD target sequence with only a modest decrease in infection noticed due to antibodies against $\alpha 9$ and soluble $\alpha 9\beta 1$ (Fig. 5C-E). Taken together, from the above results we conclude the following: (i) The $\alpha 9\beta 1$:DLD of gB interactions may be required for an efficient KSHV infection of HFF cells. The DLD interactions may well play a supportive role to the RGD interactions with integrin(s) (Chandran, 2010b; Veettil *et al.*, 2008) in promoting virus entry; (ii) There may be another non-RGD binding integrin receptor(s) with which DLD of gB interacts in promoting virus infection of HMVEC-d cells; and (iii) KSHV utilizes diverse mechanisms to enter variety of target cells.

The use of soluble integrins and antibodies to define a crucial role for a receptor molecule is not without its limitations; primarily depending upon the purity, function, and the concentrations of the recombinant proteins or the antibodies. Hence, we generated BAC36 Δ D-KSHV (KSHV

lacking the functional DLD) to appreciate the physiological role for DLD in virus infection of cells (Fig. 7). Recently, upon sequencing the KSHV-BAC36 genome in its entirety, Yakushko *et al.* discerned a 9-kb long unique region (LUR) fragment duplication in the terminal repeat region of several viral stocks acquired by laboratories. However, we assume this to possess little to no complication to our generation of BAC36 Δ D and BAC36.T, as our modifications to BAC36 did not involve mutagenesis to viral genes located within the potential LUR duplication (Yakushko *et al.*, 2011). Here, the infection of BAC36 Δ D-KSHV was compared with BAC36-KSHV wild type and BAC36.T-KSHV in 293, HFF, and HMVEC-d cells (Fig. 7). Results depict comparable infection rates for BAC36-KSHV and BAC36.T-KSHV in all tested cell types (Fig. 7). However, the infection rates for virus lacking an intact DLD of gB were significantly lower in HFF and HMVEC-d cells compared to 293 cells (Fig. 7), which provides evidence that the DLD of KSHV gB and its interaction with $\alpha 9\beta 1$ has a substantially important role in regulating virus infection. Our results also confirm KSHV to utilize a mechanism of entry into 293 cells that is independent of $\alpha 9\beta 1$. Earlier studies also determined KSHV infection of 293 cells to be via binding heparin sulfate but independent of RGD integrins (Inoue *et al.*, 2003). At this stage, we can only hypothesize that such an efficient internalization of KSHV by 293 cells occurs as a result of a dynamic and biologically active cell membrane of a transformed cell line compared to primary cells such as HFF and HMVEC-d cells.

Multiple studies have determined RGD of gB interactions with $\alpha 3\beta 1$, $\alpha V\beta 3$, and $\alpha V\beta 5$ as a necessity for KSHV entry (Chandran, 2010a) (Veettil *et al.*, 2008). KSHV has also been shown to use DC-SIGN and the 12-transmembrane glutamate/cysteine exchange transporter protein xCT as receptor molecules in dendritic cells, macrophages, and activated B cells (Rappocciolo *et al.*, 2008; Rappocciolo *et al.*, 2006; Zhang & Gao, 2012). Recent studies by Hahn *et al.*, deciphered a

key role for gH/gL interactions with EphA2, a tyrosine kinase, in promoting virus entry (Hahn *et al.*, 2012). Like other viruses, KSHV has evolved to utilize different combinations of host cell receptor molecules to infect target cells, and integrin $\alpha 9\beta 1$ could well be the latest addition to KSHV's arsenal of host cell receptor molecules utilized for entry.

Though these findings delineate a critical role for the lesser studied integrin-binding domain (DLD) of gB in KSHV infection, this study has also opened a realm of other questions which await our further research. Importantly, we seek clarity regarding the manner by which the $\alpha 9\beta 1$:DLD induced cellular signaling alter initial stages of virus infection (i.e. virus binding, initial target cell entry, escape to the endosome, or eventual nucleo-transport). Additionally, we seek to understand how reactions involving DLD of gB and integrins support RGD-dependent interactions critical to virus entry. Do these seemingly mutually exclusive integrin-binding motifs within gB somehow work in concert to regulate virus infection? Moreover, ongoing studies will also monitor the possibility of integrin heterodimer, $\alpha 9\beta 7$, interacting with DLD of KSHV to regulate virus infection, as a recent report identified the ability of ADAM-2 in RPMI 8866 cells (which express little or no $\beta 1$) to interact with $\alpha 9\beta 7$ (Desiderio *et al.*, 2010). All further studies in this area will strive for a better understanding of the intricacies involved in the role of and mechanisms utilized by glycoproteins in KSHV entry and infection.

METHODS

Cells. Human foreskin fibroblasts (HFF), 293 cells, human vascular endothelial cells-dermal (HMVEC-Ds, CC-2543; Clonetics) and *Spodoptera frugiperda* ovarian cells (Sf9) were propagated as per standard laboratory protocols (Akula *et al.*, 2005).

Antibodies. An antibody to DLD peptide sequence of gB (anti-DLD) was generated in rabbits by Pi-Proteomics, LLC (Huntsville, AL) and used in ELISAs performed in this study. Rabbit antibodies to RGD containing sequence of gB (anti-RGDgB-N1) and a peptide sequence from the C-terminal domain in gB (anti-gB-C) was also used. Antibodies to full length gB, RGDgB-N1 and gB-C have been described in earlier studies (Akula *et al.*, 2002). Human $\alpha 9$ (H-198) rabbit polyclonal antibodies (Santa Cruz Biotechnology, Inc., Santa Cruz, CA), $\alpha 9$ monoclonal mouse IgG Clone #560201 (R & D Systems, Inc.), αV monoclonal mouse IgG (clone P3G8; Millipore), $\alpha 5$ monoclonal mouse IgG (Clone P1D6; Millipore), and $\beta 1$ monoclonal mouse IgG (Clone 6S6; Millipore), were also used in this study.

Proteins and Peptides. Refer supplemental section.

Cloning and expression of recombinant gB Δ TM Δ DLD.H. His-tagged, recombinant, and soluble KSHV gB Δ TM and gB Δ TM lacking the DLD (gB Δ TM Δ D) was expressed and purified from Sf9 cells as per earlier studies (Dyson *et al.*, 2010; Wang *et al.*, 2003).

Western blotting. Equal concentrations of soluble gB proteins (25 μ g) were resolved by SDS-PAGE gels prior to being transferred to a PVDF membrane that was probed using rabbit polyclonal antibodies to gB, and appropriate secondary antibodies as per earlier studies (Dyson *et al.*, 2012).

PCR. PCR assays were conducted using synthesized cDNA and specific primers (Table 1). PCR amplifications were performed using Platinum[®] Taq DNA Polymerase, High Fidelity (Life Technologies, Carlsbad, CA) and/or Advantage[®] cDNA PCR Kit (BD Biosciences Clontech, Palo

Alto, CA) at appropriate annealing temperatures and extension times. Amplified products were separated on agarose gels, and expression was monitored.

Screening phage display peptide libraries to determine a novel receptor for gB. A detailed protocol is provided in the supplemental section.

ELISA. To characterize the binding interactions between soluble gB and integrin $\alpha 9$, ELISA was performed as per standard protocols. A detailed protocol is provided in the supplemental section.

Immunoprecipitation. Soluble integrins (1 $\mu\text{g}/\text{ml}$) were incubated with different forms of 1 $\mu\text{g}/\text{ml}$ of recombinant gB for 2h at +4°C. The protein complexes were immunoprecipitated with appropriate antibodies (anti-gB, anti- αV , or pre-immune IgG) for an hour at +4°C, followed by addition of 100 μl of swollen Protein A-Sepharose beads and further incubating for another hour at +4°C. The beads were washed four times with Gold lysis buffer, boiled in sample loading buffer and resolved by a 10% SDS-PAGE gels. Proteins were transferred on to a PVDF membrane and Western blotted using appropriate antibodies as per earlier protocols (Akula *et al.*, 2002). The molecular weights of αV and $\alpha 9$ protein bands are 128 and 140kDa, respectively.

Generating recombinant KSHV. A detailed protocol is provided in the supplemental section.

Monitoring KSHV infection of cells. KSHV infection of different cells was recorded by counting the number of cells expressing GFP that is indicative of rKSHV.152 and BAC36 infection (Akula *et al.*, 2004; Akula *et al.*, 2001b; Grange *et al.*, 2012).

Flow cytometry. Target cells were washed, incubated in growth medium at 37°C for 30 min, centrifuged, and resuspended in cold PBS. The entire procedure involved the use of cold reagents and temperatures of +4°C. Cells (1×10^6) were incubated with different antibodies at 4°C for 30 min, washed, incubated with FITC-conjugated appropriate secondary IgG at 4°C for 30 min, washed, and analyzed in a FACScan flow cytometer (Becton Dickinson) with appropriate gating parameters.

ACKNOWLEDGMENTS

We thank Dr. Shou-Jiang (SJ) Gao (Keck School of Medicine, University of Southern California) to have graciously provided us with the BAC36 clone critical to this study. We also thank Dr. Kumaran Narayanan (Monash University) to have kindly provided us with the pGET-rec plasmid which again was a critical element of this project. Our sincere thanks go to Akarsh Manne and Dr. Ivan Ndamukong for their assistance and guidance in generating recombinant viruses. Finally, we thank Frank Williams who performed qRT-PCR for this study.

AUTHOR CONTRIBUTIONS

Conceived the idea: SMA; designed the experiments: LRW SMA; performed experiments: LRW; flow cytometry experiment: HAH; analyzed the data: LRW SMA; Wrote the first draft of the manuscript: LRW.

FIGURE LEGENDS

Figure 1. Generating KSHV gB Δ TM Δ D. The diagram shows the schematic of gB Δ TM and gB Δ TM Δ D mutant compared to the full length KSHV-gB (*orf8*).

Figure 2. Expression and purification of gB Δ TM Δ D in baculovirus expression system. The gB Δ TM Δ D and gB Δ TM were expressed in Sf9 cells and the protein purified from the harvested supernatant using a column containing Ni-NTA agarose beads. Protein purity was analyzed by Coomassie staining SDS-PAGE gels, and Western blotting procedures using rabbit polyclonal antibodies to full length gB. Experiments were performed under reducing (+2ME) and non-reducing conditions (-2ME). Under non-reducing conditions, an upward shift in the migration pattern of both the proteins is indicated by an asterisk mark. Arrows denote the bands corresponding to recombinant gB.

Figure 3. Phage encoding peptide PKADGRV bound gB Δ TM efficiently. (A) PFU recovered when 10^{11} PFU of phage carrying peptides L3, F1, and F5 were screened against immobilized gB Δ TM, gB Δ TM Δ D, or BSA (negative control) proteins on microplates. (B) PFU recovered when 10^{11} PFU of phage carrying peptide L3 was screened against immobilized gB Δ TM, gB Δ TM Δ D, or BSA on microplates in the absence or presence of 1mM solution of PKADGRV, gBDLD peptide, or scrambled peptide. Finally, ELISA was performed to determine the interactions between (C) $\alpha 9\beta 1$ or $\alpha v\beta 3$ (D) with immobilized gB Δ TM, gB Δ TM Δ D, BSA, or GST. Each point denotes the average \pm S.D. (*error bars*) of three experiments. Columns with different alphabets and asterisks on the data points denote the value to be statistically significant ($p < 0.05$) by least significant difference (LSD). (E) Immunoprecipitation experiments to demonstrate gB

interactions with $\alpha 9\beta 1$. Recombinant gB Δ TM (lane 1) compared to gB Δ TM Δ D (lane 3) specifically bound $\alpha 9$. As a positive control, gB interactions with $\alpha V\beta 3$ was tested.

Figure 4. Characterizing the gB: $\alpha 9\beta 1$ interactions by performing competitive ELISA. Using the constant concentration of 1 μ g/ml for both $\alpha 9\beta 1$ and bound gB Δ TM, ELISA was performed: (A) Increasing concentrations of HS in PBS (or CSA and CSB) were incubated in gB Δ TM-coated wells prior to incubating with $\alpha 9\beta 1$ and performing the ELISA. Increasing concentrations of GRGDSP and KQAGDV (an irrelevant peptide) (B); tenascin C, VEGF, and laminin (C) were incubated with $\alpha 9\beta 1$ for 30min at room temperature (in an additional step) prior to their addition into gB Δ TM-coated wells and performing ELISA. (D) gB Δ TM-coated plates were incubated with anti-DLD or additional non-specific antibodies prior to incubation with $\alpha 9\beta 1$ and performing ELISA. The results were read at 450nm (OD 450). Data presented in both the panels represent the average \pm S.D. (*error bars*) of three experiments. Asterisks on the data points denote the value to be statistically significant ($p < 0.05$) by LSD.

Figure 5. Role of integrin $\alpha 9\beta 1$ in wild type KSHV infection. (A) HFF, HMVEC-d, and BCBL-1 cells express $\alpha 9$. cDNA synthesized from target cells was subjected to PCR analysis to amplify a $\alpha 9$ PCR product ($\alpha 9$: ~190bp) that was resolved in a 2.1% agarose gel. (B) Flow cytometry analysis of the surface expression of $\alpha 9$ integrin subunit in 293, HFF, and HMVEC-d cells was performed by staining with Integrin $\alpha 9$ (H-198) rabbit polyclonal antibodies followed by incubation with goat anti-rabbit FITC, before examining by FACS. The average percentage number of cells positive for the $\alpha 9$ expression from three independent experiments is provided over the marker. A representative histogram plot (plots shaded purple and with green outline

denotes interactions with pre-immune IgG and anti- $\alpha 9$, respectively) for each cell type is depicted. (C-E) Inhibition of rKSHV.152 infection by 20 μ g/ml of different antibodies to integrins (C), soluble integrins (D), and anti-DLD antibodies (E) is shown. In all of the above experiments (panels C-E), infection was monitored at 72h post infection (PI) by recording the total number of cells expressing GFP under a fluorescent microscope. Data are presented as percentage of inhibition of virus infectivity obtained when the cells were preincubated with DMEM as control. Data represent the average \pm SD (*error bars*) of three experiments. Columns with different alphabets are statistically significant ($p < 0.05$) by LSD.

Figure 6. Architecture and generation of recombinant BAC36 Δ D. (A) A schematic architecture of how the target-3 PCR product was obtained is shown. (B) DNA agarose gel electrophoresis of purified targets to confirm predicted fragment sizes. Elution-purified target-1 (T1; 2967bp), target-2 (T2; 1055bp), and gel purified target-3 (T3; 4005bp) were resolved in a 1% agarose gel and stained by ethidium bromide. Bands of expected sizes were rendered. (C) Schematic depiction of the molecular biology processes involved in the construction of BAC36 Δ D and BAC36.T clones is provided. A detailed description concerning the construction of the clones is provided in the supplemental METHODS section.

Figure 7. DLD of gB is critical for KSHV infection. (A) Monolayers of 293 cells were infected with 0.1 MOI of BAC36-KSHV or BAC36 Δ D-KSHV. At the end of 48hPI, the cells were treated with TPA for 72h. These cells were analyzed for the surface expression of gB in 293 cells by staining with pre-immune IgG (shaded purple) rabbit polyclonal anti-gB antibodies (green outline) followed by incubation with goat anti-rabbit FITC, before examining by FACS. The average

percentage number of cells positive for the surface expression of gB from three independent experiments is provided over the marker. A representative histogram plot for each cell type is depicted. **(B)** Monolayers of 70-80% confluent 293, HFF, and HMVEC-d cells were infected with BAC36-KSHV, BAC36 Δ D-KSHV, and BAC36.T-KSHV. After 72h of infection, the total number of cells expressing GFP under a fluorescent microscope was counted. Data are presented as percentage of virus infection of target cells obtained when the respective cells were infected with BAC36-KSHV. Data represent the average \pm SD (*error bars*) of three experiments. Columns with different alphabets are statistically significant ($p < 0.05$) by LSD.

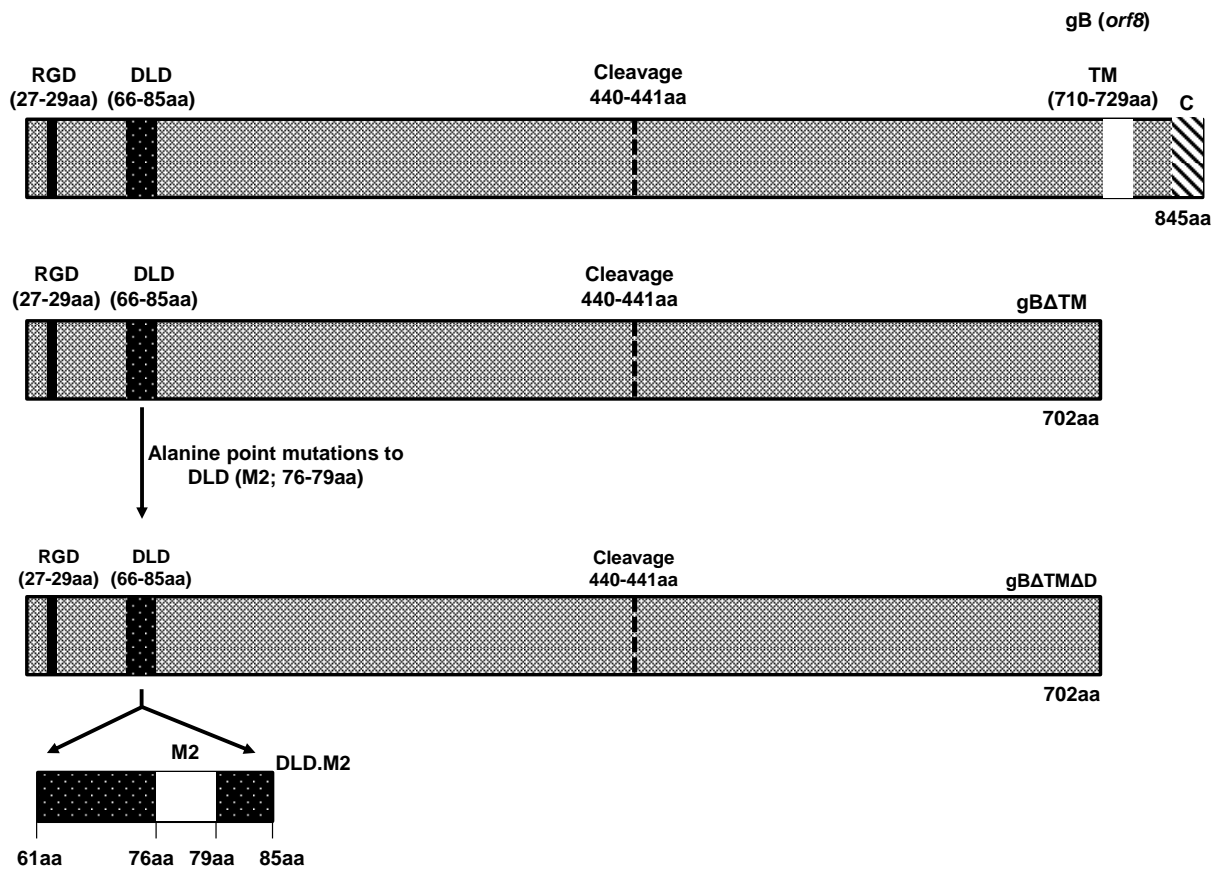


Figure 1

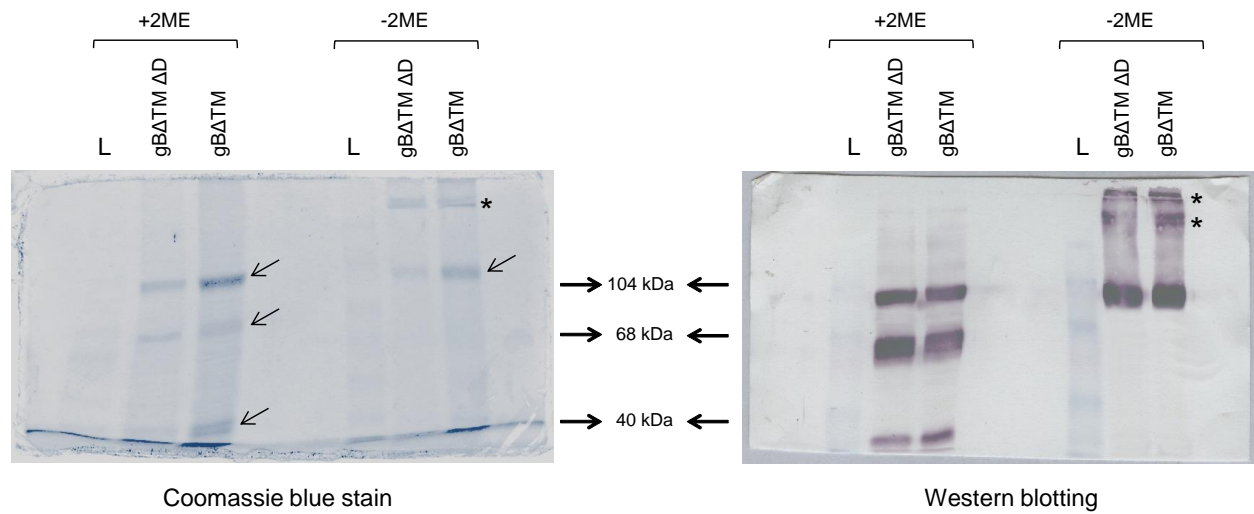


Figure 2

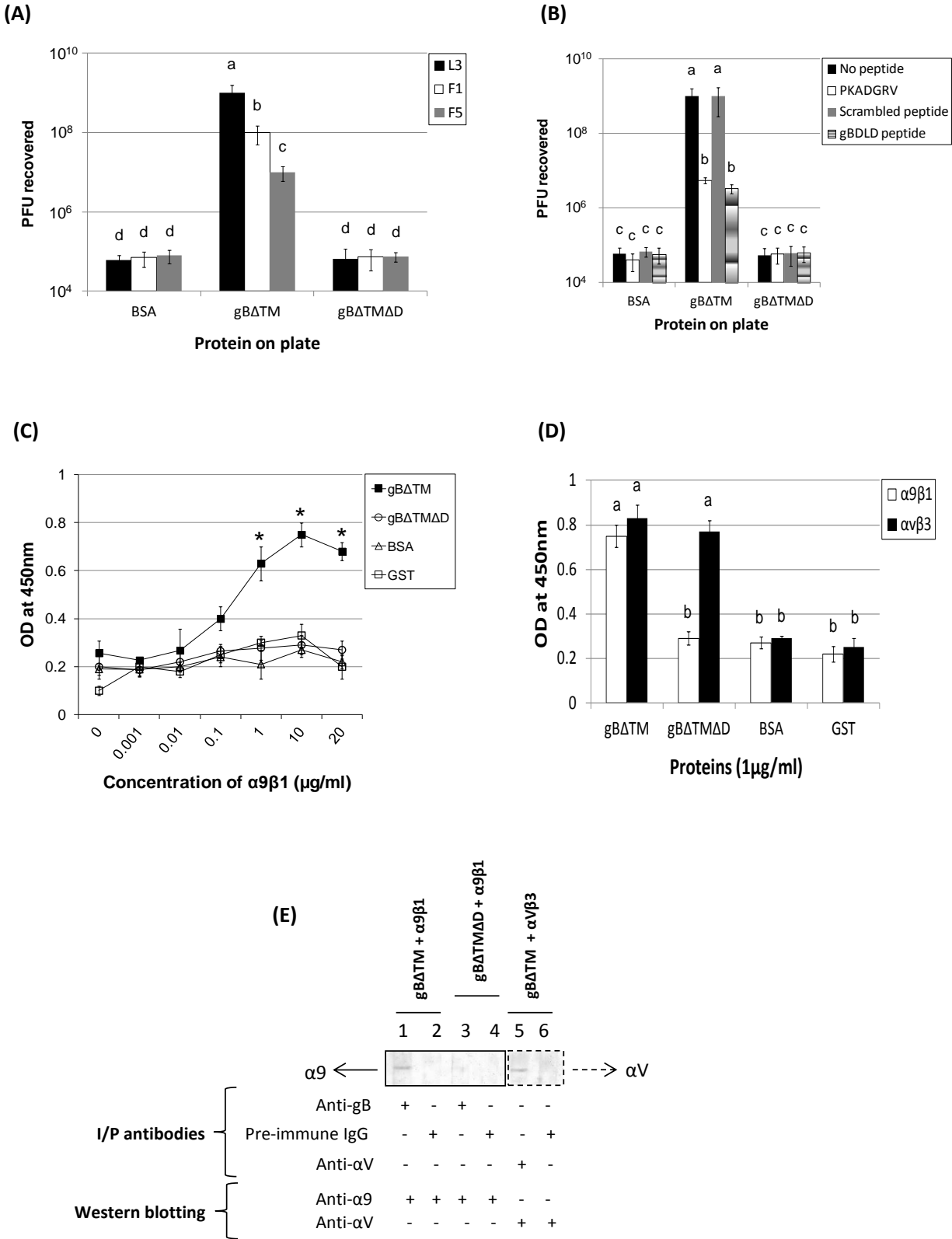


Figure 3

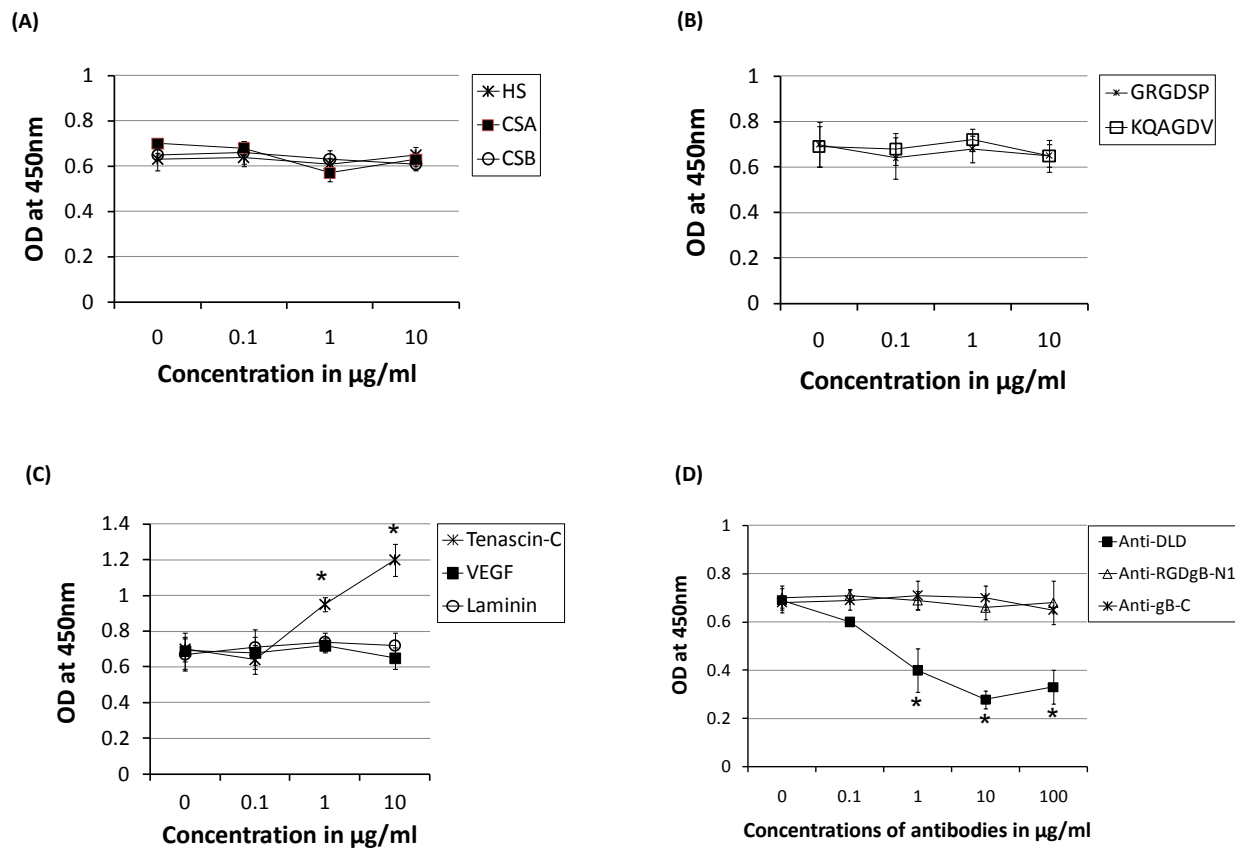


Figure 4

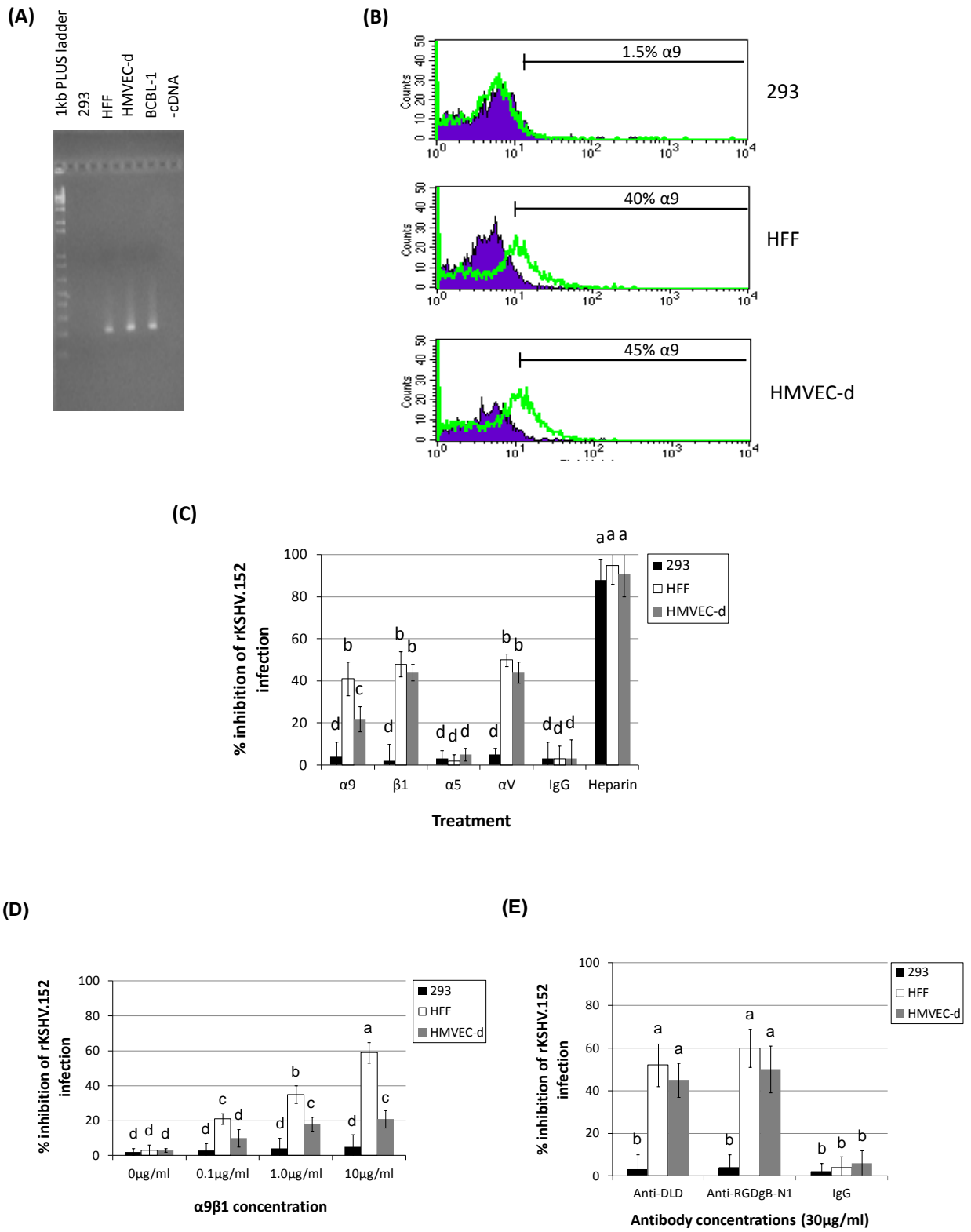


Figure 5

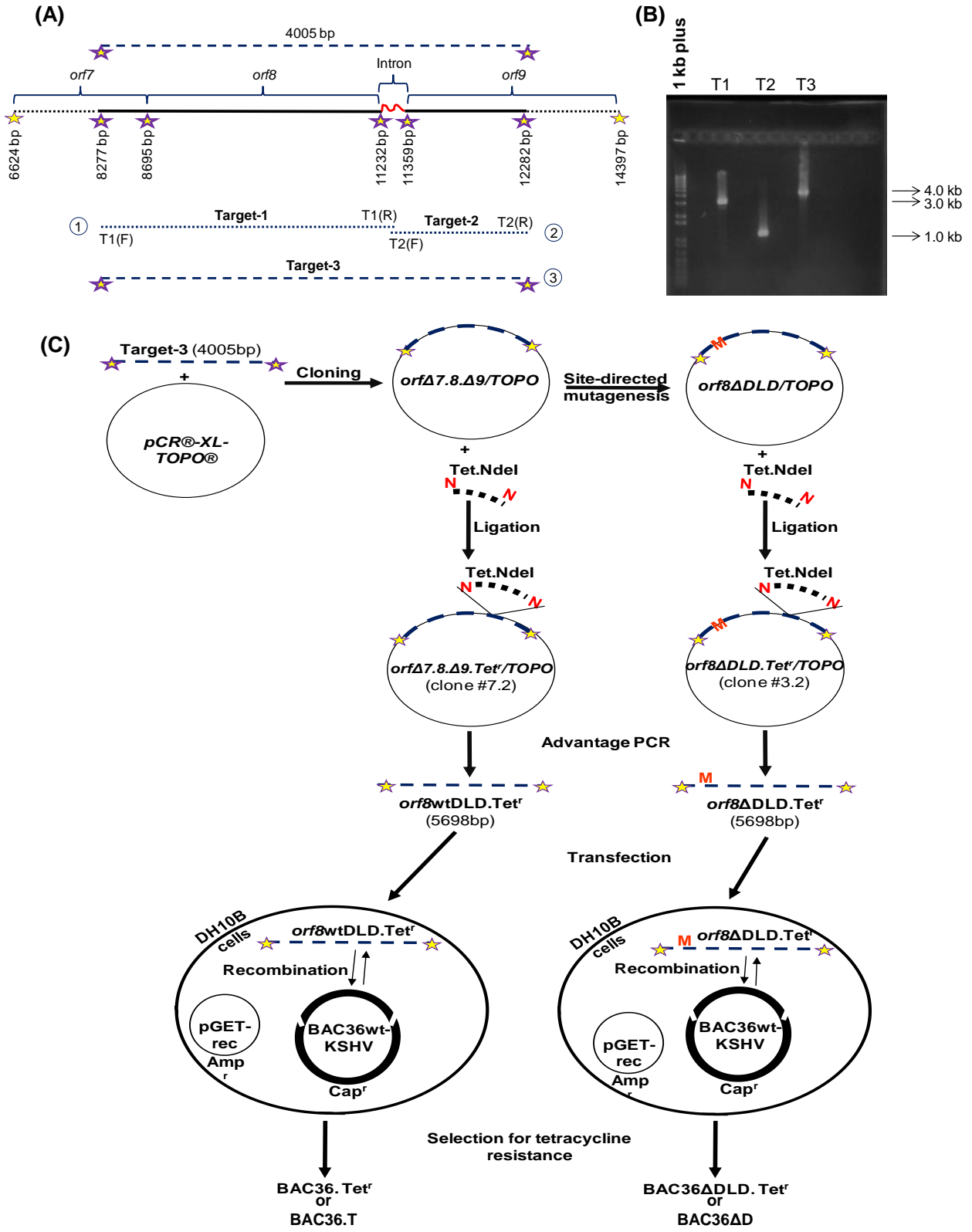
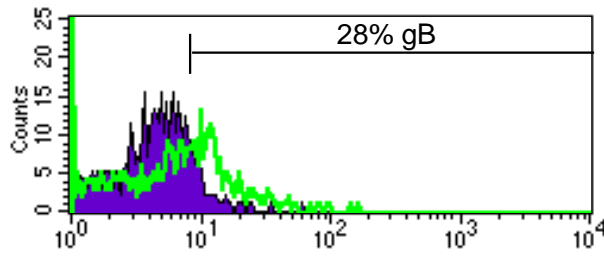
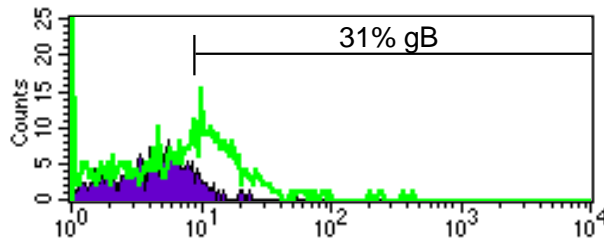


Figure 6

(A)



BAC36-KSHV infected 293 cells



BAC36ΔD-KSHV infected 293 cells

(B)

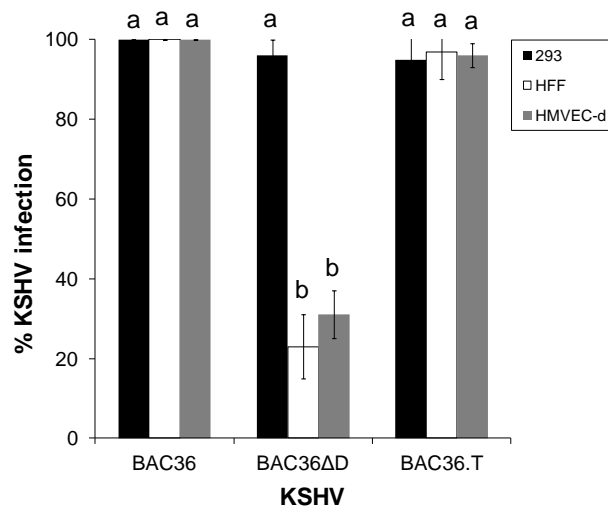


Figure 7

Table 1. List of primers.

Primer Name	Sequence
α 9.FW2.Q.F	GATGAGTGGATGGGGGTGAG
α 9.FWQ.R	CCGTGTCCTCTCCGTA
DLD-M2(F)	TCGATCACCGGGGAGGCGGCGGCGGCGAACCTGGAGCAGACG
DLD-M2(R)	CGTCTGCTCCAGGTTCCGCGCCGCGCCTCCCCGGTGATCGA
pHHV8gB(F)	AGTGAGGATCCACAATGACTCCCAGG
ORF8.HIS(R)	TCCGAATTCTCAATGATGATGATGATGATGGCCACCCAGGTCCGCCACTATCTC
ORF8.RD(F)	ATGACTCCCAGGTCTAGATT
ORF8.D(F)	AAGCATCTGGTCCTAAGAGT
ORF8.RD(R)	TCGTTGGCCACAAAGTGGA
ORF50P8.ChIP.OD(F)	CTACCGGCGACTCATTAAGC
ORF50P8.ChIP.OD(R)	GTGGCTGCCTGGACAGTATT
T1(F)	GTGACGCTGGCTCAGTGCTTCGAGGCTGCGGGCATGCTT
T1(R)	TCGAATCATATGTCCTCCCCGTTTCCGGACTGATGTC
T2(F)	GAGTGACATATGATTTCGAGGTTATTGTTTGATGTAAATT
T2(R)	CGCGTTGGGAAAACCTTCTCGCCCATACATTCTATATC
Tet (F)	CATATGGCCGATTATGGTGCCTCTCAGTAC
Tet (R)	CATATGTGGTGAATCCGTTAGCGAGGTGCC

Table 2. Amino acid sequences of the phage-displayed peptides isolated by screening against DLD in gB.

Name	Sequence	Frequency
L3	P K A D G R V	9
L5	M T A E N I R	1
F1	D C K P K P D G R L R D	6
F3	Q A M S D K F R C G W A	2
F5	P K A D G H V	5
F9	C N H P L E C	1
S6	P Y H D Q I A	1
S8	L R P R A D G P T E F W	2
S9	S W A D T T I Q Y V V L	1
S4	R F I Y P E D P F I E C	1

**CHAPTER 3: $\alpha 9\beta 1$ INTEGRIN MEDIATES POST-INTERNALIZATION STEP OF
KSHV ENTRY**

Lia R. Walker, Hosni A.M. Hussein, Shaw M. Akula*
**Department of Microbiology & Immunology, Brody School of Medicine at East Carolina
University, Greenville, NC 27834.**

This manuscript is under revision.

Running head: Integrins assist KSHV escape from late endosome

Keywords: disintegrins, KSHV, integrins, entry

Word count: Summary (235); Main text (5573)

Journal's contents category: Animal viruses – Large DNA

Address correspondence to: Shaw M. Akula, Department of Microbiology & Immunology, Brody
School of Medicine, East Carolina University, Greenville, North Carolina, USA 27834. Phone:
(252)744-2702; Fax: (252) 744-3104; Email: akulas@ecu.edu

SUMMARY

Virus entry is a complex, multi-step, and highly orchestrated event on which successful virus infection collectively depends. In terms of herpesviruses, viral envelope glycoproteins have been widely reported to engage target cell surface receptors, such as integrins, in interactions leading to entry and subsequent infection. Integrins are known to physically interact with Kaposi's sarcoma-associated herpesvirus (KSHV) envelope glycoprotein B (gB) to promote virus entry into cells. Our recent study identified KSHV gB to interact with cell surface expressed $\alpha 9\beta 1$ integrin crucial to promoting viral infection of cells. KSHV enters human foreskin fibroblast (HFF) cells via clathrin-mediated endocytosis. In this study, the role of disintegrin-like domain (DLD)-binding integrin, $\alpha 9\beta 1$, in KSHV entry into HFF cells was analyzed. Incubating cells with antibodies to $\alpha 9$ integrin subunit or soluble $\alpha 9\beta 1$ integrin with the virus significantly inhibited virus infection of cells but not the internalization of the virus. This was true in both the permissive human foreskin fibroblast (HFF) and the non-permissive Chinese hamster ovary (CHO) cells that stably expressed human $\alpha 9$ integrin subunit. Therefore, the trafficking of KSHV via endosomes was analyzed using a subcellular fractionation method which was supported by traditional imaging techniques. Incubating KSHV with soluble $\alpha 9\beta 1$ significantly blocked the ability of the viral capsid to escape the late endosomes into the cytoplasm. These results support the fact that $\alpha 9\beta 1$ integrin may play a crucial role in mediating endosomal escape of the viral capsid into cytoplasm.

INTRODUCTION

As pathogenic hijackers of cellular machinery, viruses enter target cells via diverse, complex, and still fairly enigmatic processes that are presumed to be cell type dependent. It is widely accepted that herpesviruses access a target cell's interior via interactions between viral envelope glycoproteins and host cell surface receptors. Such glycoprotein:receptor interactions function in attachment and binding at the cell surface, successive internalization (uptake into the host cell), membrane fusion, and trafficking of the virus (Zhang & Gao, 2012). The *gamma*-2-herpesvirus, Kaposi's sarcoma-associated herpesvirus (KSHV) is no different in this respect. KSHV, otherwise known as human herpesvirus-8 (HHV-8), has an extensive cellular tropism both *in vivo* and *in vitro* and can infect a plethora of different cell types (Hertel, 2011) presumably due to its ability to bind ubiquitous molecules expressed on target cells such as heparan sulfate (HS) (Akula *et al.*, 2001b).

KSHV binding to HS is thought to bring the virus in closer proximity to target cells such that perhaps more meaningful interactions with other receptor molecules, such as integrins, can occur to promote the actual entry process (Akula *et al.*, 2001b). In fact, KSHV sets precedence as the first herpesvirus shown to interact with adherent target cell integrins in a step initiating the entry process (Akula *et al.*, 2002). For instance, KSHV envelope associated glycoprotein B (gB) is said to interact with integrins via its RGD (Arg-Gly-Asp) (Akula *et al.*, 2002; Chakraborty *et al.*, 2012) and disintegrin-like domain (DLD) integrin recognition motifs (Walker *et al.*, 2014) to facilitate virus entry and infection. Aside from integrins, other receptors shown to have a role in KSHV entry are ephrin receptor tyrosine kinase A2 (EphA2) (Hahn *et al.*, 2012), dendritic cell-specific intercellular adhesion molecule-3-grabbing non-integrin (DC-SIGN) (Rappocciolo *et al.*, 2006), and human cysteine transporter xCT (Zhang & Gao, 2012). After binding to receptors (i.e

proteins, carbohydrates, or lipids; (Dimitrov, 2004)), the vast majority of viruses utilize endocytic routes to enter target cells (Yamauchi & Helenius, 2013a).

The mechanism of endocytosis is thought to leave no trace of the virus at the plasma membrane presumably causing delayed detection by the host immune system. Upon uptake into the cell, viruses utilize cellular processes for their own infectious agenda (Mercer *et al.*, 2010). Several reports have described KSHV to utilize what is often deemed as the receptor-mediated endocytic pathway (Chaudhary *et al.*, 2014; Dutta *et al.*, 2013; Raghu *et al.*, 2009; Veettil *et al.*, 2014). Specifically, KSHV enters human foreskin fibroblast (HFF) cells via clathrin-mediated endocytosis (Akula *et al.*, 2003). Recent studies by us (Walker *et al.*, 2014) demonstrated KSHV to interact with $\alpha 9\beta 1$ integrins expressed on the surface of cells to mediate infection of cells. Entry processes are commonly analyzed by monitoring internalized virus particles via Western blotting, polymerase chain reaction (PCR), and imaging techniques that allow scientists to track their intracellular location. Such studies have provided abundant direct evidence on how viruses interact with receptor molecules on the cell surface, induce cell signaling at the point of initial contact with the cell to facilitate internalization, and exploit existing endocytic mechanisms of the cell for their ultimate infectious agenda. However, there is dearth of knowledge in regards to trafficking of a virus via endosomes. In this study, we attempted to analyze the role of $\alpha 9\beta 1$ integrin in the intracellular trafficking of the virus. We utilized subcellular fractionation to understand the transit of KSHV via endosomes. Our study defines a critical role for $\alpha 9\beta 1$ integrin in the ability of KSHV to escape late endosomes in HFF cells.

RESULTS

Anti- $\alpha 9$ and $\beta 1$ integrin antibodies and soluble $\alpha 9\beta 1$ integrins do not inhibit KSHV internalization but do inhibit KSHV infectivity

Integrins are known to alter different stages of the virus entry process. KSHV envelope associated gB is shown to interact with RGD-binding integrins $\alpha 3\beta 1$, $\alpha V\beta 3$, and $\alpha V\beta 5$ (Chakraborty *et al.*, 2012; Fotiadis *et al.*, 2013; Hahn & Desrosiers, 2013; Veettil *et al.*, 2008), as well as integrin $\alpha 9\beta 1$ (Walker *et al.*, 2014), a DLD-binding integrin, to aid in initiating the internalization of KSHV. A lot of work has been done to establish a role for RGD-binding integrins in regulating KSHV infection, with only very little known about the role of DLD-binding integrins in KSHV infection. To further investigate the involvement of DLD-binding integrins during the initial stages of KSHV infection, we first conducted infection-based studies in HFF cells using appropriate anti-integrin antibodies or soluble integrins (Fig. 1). Monolayers of HFF cells were incubated with 20 μ g/ml of antibodies against integrin subunits $\alpha 9$, $\beta 1$, or $\alpha 5$, for 1h at 4 $^{\circ}$ C prior to infection with KSHV (Fig. 1A). As per earlier studies (Dyson *et al.*, 2010; Krishnan *et al.*, 2004), expression of *orf50* in cells (as monitored by qRT-PCR) was considered an indicator for establishment of infection. Antibodies to $\alpha 9$ and $\beta 1$ integrins significantly inhibited KSHV infection of HFF cells compared to antibodies to $\alpha 5$ and a pre-immune IgG (Fig. 1A). For further authentication of the above results, the effect of pre-incubating KSHV with human soluble $\alpha 9\beta 1$ for 1h at 4 $^{\circ}$ C prior to infecting cells was tested (Fig. 1B). In this case, a dose dependent inhibition of KSHV infection of HFF cells was observed when the virus was incubated with increasing concentrations of soluble $\alpha 9\beta 1$ versus bovine serum albumin (BSA) prior to infection (Fig. 1B). As a positive control, soluble heparin was used as a known inhibitor of KSHV binding and infection of HFF cells (Fig. 1B).

To assess the roles of these integrins in KSHV internalization, HFF cells were first treated with antibodies (20 μ g/ml) against integrin subunits α 9, β 1, or α 5 prior to infection with KSHV (Fig. 1C). In a separate experiment, KSHV was pre-incubated with different doses of soluble α 9 β 1 integrin (0, 0.1, 1, 10 μ g/ml) prior to infection of cells (Fig. 1D). Upon quantification of internalized KSHV *orf50* gene copies via qPCR, we observed neither the anti-integrin antibodies nor the soluble integrin to have an effect on the internalization of KSHV in HFF cells (Fig. 1C, D). Expectedly however, soluble heparin inhibited KSHV internalization in a dose dependent fashion (Fig. 1D). Pre-treatment of KSHV with soluble heparin is shown to impede the initial attachment of the virus to HS on the cell surface (Bandyopadhyay *et al.*, 2014), thus blocking binding, signal induction, entry, and successful infection of target cells (Akula *et al.*, 2001b; Chakraborty *et al.*, 2012).

To further authenticate the above effects of integrins on KSHV internalization and infection of cells, we used Chinese hamster ovary (CHO) cells. CHO cells are not permissive to KSHV infection (Akula *et al.*, 2002). CHO cells do not express α 9 integrins (Chen *et al.*, 2006) but do express the β 1 subunit of integrins (Wu *et al.*, 1995). To determine the biological role of α 9 β 1 integrin in the virus internalization and infection, we stably expressed the human α 9 integrin subunit in the deficient CHO cells to obtain CHO- α 9 cells (Fig. 2A). The human α 9 subunit expressed by these cells associated with hamster β 1 subunit on the cell surface as shown by immunoprecipitation of the integrin complex with anti- α 9 antibodies from lysates of surface biotinylated cells (Fig. 2B). CHO- α 9 cells were permissive to KSHV infection of cells when compared to CHO cells (Fig. 2C). The KSHV infection of CHO- α 9 cells was significantly lowered when the cells were incubated with antibodies to integrin α 9 prior to conducting infection compared to incubating cells with antibodies to α 5 integrins (Fig. 2C). However, internalization

of KSHV was not significantly altered in these cells by incubating them with antibodies to integrin $\alpha 9$ (Fig. 2D). These results implicate a possible role for $\alpha 9\beta 1$ integrins at a stage beyond cellular uptake of virus.

KSHV particles are trafficked beyond the early endosome for late endosomal escape

We first attempted to conduct subcellular fractionation in untreated HFF cells via sucrose density gradient centrifugation for isolation/detection of organelles associated with the endocytic pathway. Typically, cargo internalized by clathrin-mediated endocytosis (e.g. KSHV into HFF cells) is thought to be directed from early endosomes (EEs) to late endosomes (LEs) then lysosomes to undergo degradation or changes to conformation (Vonderheit & Helenius, 2005). To begin with, untreated HFF cells grown to 80% confluency were cooled (incubated at 30min at 4°C), infected with KSHV or incubated with DMEM alone (15min at 37°C), collected and lysed in homogenization buffer; after which, centrifugation was performed to derive the post-nuclear supernatant (PNS) containing intracellular organelles in suspension (Fig. 3). The PNS adjusted to a concentration of 25% sucrose and 1mM EDTA was then subjected to sucrose density gradient centrifugation followed by fraction collection (Fig. 3).

Collected gradient fractions 1-6 of untreated HFF cells were analyzed for the distribution of endosome markers, Rab5 (EE marker) and Rab7 (LE marker) (Harley *et al.*, 2001; Wolf *et al.*, 2012), by SDS-PAGE and Western blotting (Fig. 4A). Fractions 1-3 contained the LEs with the majority being concentrated in fraction 1 as detected by Rab7, and fractions 4-6 contained the EEs with the majority being concentrated in fraction 5 as detected by Rab5 expression (Fig. 4A). Interestingly, KSHV infection of HFF cells did not seem to alter this distribution of EEs and LEs (Fig. 4A). LEs (sometimes referred to as pre-lysosomes; (Braulke & Bonifacino, 2009),

lysosomes, and the endolysosome hybrid organelle—from where mature lysosomes bud—are said to be difficult to distinguish (Repnik *et al.*, 2013), as basic sucrose gradient centrifugation procedures are shown to forgo total separation of such organelles (Waugh *et al.*, 2011). Here, acid phosphatase (an established enzyme marker for identifying lysosomes in subcellular fractions; (Zhao *et al.*, 2013) activity was analyzed to detect the level of lysosome enrichment in collected gradient fractions (Fig. 4B). Upon fraction comparison, acid phosphatase activity in both the uninfected and KSHV infected HFF cells was detected in fractions 1-3 with fraction 1 displaying the highest phosphatase activity. Activity of acid phosphatase foreseeably coincided with the LE fractions (fractions 1-3; Fig. 4A); although acid hydrolases (e.g. acid phosphatase) majorly localize in lysosomes, these enzymes can be found in LEs as well (Repnik *et al.*, 2013). Therefore, such findings provide a second line of evidence for the presence of LEs in the said fractions.

Having established the fractions that contain early and late endosomes, we purified endosomes via a sucrose flotation gradient to quantitatively track KSHV in infected HFF cells post-internalization and to characterize possible role(s) for DLD-binding integrins during this stage of the entry process via qPCR (Fig. 4C). Earlier studies described KSHV entry as a rapid process wherein the capsid delivers the genetic material to the nucleus allowing eventual expression of viral transcripts in as early as 30min post infection (PI) (Dyson *et al.*, 2010; Krishnan *et al.*, 2004). Therefore, we monitored KSHV particles in endosomes 15min PI. In the case of cells infected with KSHV, there was notably more KSHV DNA detected in EE containing fractions compared to the fractions containing LEs (Fig. 4C). Similar results were observed in cells infected with a mixture of KSHV and BSA (Fig. 4C). Though incubating soluble integrin $\alpha 9\beta 1$ with KSHV did not significantly alter the levels of KSHV in EEs, it significantly impeded the ability of KSHV to escape the LEs (Fig. 4C). These results suggest a possible role for $\alpha 9\beta 1$ integrin in virus-mediated

endosomal escape. Additionally, infection in the presence of our positive control, heparin, results in a significant drop in the number of virus particles observed in both EE and LE containing fractions (Fig. 4C). Based on these results, as it pertains to HFF cells, we presume KSHV to be a late penetrating virus that exits from the LE into the cytosol. We could not detect HSV-2 in either the early or late endosome (data not shown), as earlier studies demonstrated HSV-2 to enter target cells via fusion at the cell membrane (Akula *et al.*, 2003).

To further confirm the presence of KSHV in endosome containing gradient fractions, fractions collected at different early time points (1, 5, or 15min) during the course of infection were resolved by SDS-PAGE and subsequently Western blotted with antibodies directed against minor capsid protein KSHV ORF62-encoded triplex component I (TRI-1) for detecting the presence of viral capsids (Fig. 5). Expression of TRI-1 is ideal for detection of the virus, as the virus envelope is lost upon fusion/penetration. At 1 min post KSHV infection, significantly more virus was observed in EE containing fractions 4-6 versus LE fractions with most virus being detected in fraction 5 (Fig. 5). Similar patterns were observed at 1min PI when the virus was incubated with BSA or soluble $\alpha 9\beta 1$ (Fig. 5). Incubating KSHV with heparin lowered the percentage of virus being internalized as detected by limited staining for TRI-1 in EEs (Fig. 5). By 5min PI, a significant portion of the virus had reached LEs in KSHV infected cells or cells infected with a mixture of KSHV that was incubated with BSA or $\alpha 9\beta 1$ (Fig. 5). Heparin blocked KSHV internalization effectively as described at 1min PI. By 15min PI, there was a marked drop in the levels of virus in LEs (especially LE fraction 1) in cells that were infected with KSHV or a mixture of KSHV and BSA (Fig. 5). Surprisingly, we found an increase in the levels of virus associated with LEs of cells that were infected with a mixture of KSHV and soluble $\alpha 9\beta 1$. Overall, Western blotting results monitoring TRI-1 expression as an indicator of KSHV in collected

gradient fractions of virus infected HFF cells (Fig. 5) mimic qPCR results (Fig. 4C), thus confirming escape of KSHV from the LE to the cytoplasm in HFF cells.

Immunofluorescence microscopy demonstrates KSHV to localize in EEs and LEs

For further confirmation, we employed the traditional method of immunofluorescence imaging with FITC-KSHV and TRITC labeled antibodies to Rab5 and Rab7 to monitor the trafficking of KSHV into the target cells. By as early as 1min PI of cells, KSHV was associated with EEs as observed by co-localization of the FITC-KSHV with Rab5 expression (Fig. 6A). Treating cells with antibodies to $\alpha 9\beta 1$ or pre-immune IgGs did not significantly alter this co-localization (Fig. 6A). At 15min PI, a fraction of KSHV was associated with LEs as observed by co-localization of the FITC-KSHV with Rab7 expression (Fig. 6B). A similar result was observed when the cells were treated with pre-immune IgGs (Fig. 6B). However, the number of co-localizing events substantially increased when the cells were treated with antibodies to $\alpha 9\beta 1$ prior to infection (Fig. 6B). For further authentication, subsequent intracellular trafficking of KSHV upon cytosolic delivery (post-late endosomal penetration) was similarly analyzed via immunofluorescence microscopy using KSHV and antibodies directed against minor capsid protein TRI-1 (Fig 7). By 30min PI, KSHV was shown to accumulate at the perinuclear region as observed by TRI-1 positive viral capsids (similar results were observed in cells treated with pre-immune IgGs) (Fig. 7). However, when cells were treated with antibodies against integrin subunits ($\alpha 9$ or $\beta 1$), a substantial reduction in perinuclear TRI-1 expression corresponding to KSHV nucleocapsids was observed (Fig. 7). This reduction in the number of capsids positive for TRI-1 was not observed when the cells were treated with antibodies to integrin subunit $\alpha 5$ that served as a negative control (Fig. 7). These results clearly denote the ability of integrin antibodies to block virus infection by preventing

the escape of KSHV from LEs. Overall, we conclude virus: $\alpha 9\beta 1$ integrin interactions to play a key role in trafficking of KSHV via endosomes to eventually escape into the cytoplasm.

DISCUSSION

“Highly orchestrated, but complex” is typically the concluding remarks regarding the still very much enigmatic process of virus entry. Eukaryotic cellular uptake mechanisms under the endocytosis umbrella include phagocytosis, macropinocytosis, caveolae-mediated endocytosis, and the most well characterized mechanism, clathrin-mediated endocytosis (Ivanov, 2008). KSHV enter HFF cells via endocytosis (Akula *et al.*, 2003).

Receptors are considered necessary cell surface molecules instrumental for successful virus infection (Grove & Marsh, 2011). Herpesvirus entry occurs via viral glycoprotein engagement of target cell receptor molecules. Those receptors considered valuable for KSHV entry into HFF cells are binding receptor, HS, RGD-binding integrins ($\alpha 3\beta 1$, $\alpha V\beta 3$, $\alpha V\beta 5$; (Akula *et al.*, 2001a; 2002; Akula *et al.*, 2001b; Veettil *et al.*, 2008), and DLD-binding $\alpha 9\beta 1$ integrin (Walker *et al.*, 2014). The present study, for the first time, has employed subcellular fractionation to decipher a role for $\alpha 9\beta 1$ integrin in regulating KSHV entry.

KSHV infection-based studies using antibodies against integrin subunits ($\alpha 9$, $\beta 1$, or $\alpha 5$) as well as human soluble $\alpha 9\beta 1$ integrin were implemented to assess the role of DLD-binding integrins in KSHV internalization and overall infection of HFF cells (Fig. 1). Similar to previous studies (Veettil *et al.*, 2008; Walker *et al.*, 2014), KSHV infection of HFF cells was significantly blocked (between 40 and 50%) by antibodies to integrin subunits (Fig. 1A); along the same lines, soluble DLD-binding $\alpha 9\beta 1$ inhibited KSHV infection in a dose dependent fashion according to expression of *orf50* transcripts in HFF cells (Fig. 1B). However, qPCR (monitoring internalized KSHV *orf50*

gene copies) results revealed KSHV internalization into HFF cells to be greatly unaffected by the aforementioned anti-integrin antibodies and soluble integrin (Fig 1C, D). Unlike soluble $\alpha 9\beta 1$, heparin was shown to have a significant inhibitory effect on both KSHV internalization and infection of HFF cells, again supporting claims implicating HS as the initial attachment receptor for subsequent virus binding, entry, and eventual infection (Fig. 1B, D). We observed identical results with anti- $\alpha 9$ antibodies on KSHV internalization and infection of CHO and CHO- $\alpha 9$ cells (Fig. 2). The effective inhibition of infection but distinct inability to block internalization by antibodies to integrin subunits ($\alpha 9$ or $\beta 1$) and soluble $\alpha 9\beta 1$ alludes to DLD-binding receptors having a role post-internalization during KSHV infection of HFF cells.

A sucrose flotation gradient assay to track the endocytosed viral cargo through the EEs, LEs, and lysosomes via subcellular fractionation was used (Fig. 3). Determining at which interface a particular membrane will be detected depends on the lipid to protein content ratio. Endosomal membranes are considered low density and lipid-rich (Huber *et al.*, 2003). LEs as well as lysosomes were expected to be recovered from the interface between 8 and 25% sucrose, whereas the EEs were expected between 25 and 35% sucrose (Yang *et al.*, 2006; Yu & Lai, 2005). In this study, the PNS derived from KSHV infected HFF cells untreated or treated with soluble $\alpha 9\beta 1$, heparin, or BSA was subjected to high-speed sucrose density gradient centrifugation (Fig. 4C, 5). Mutually, qPCR and Western blotting results revealed significantly lower levels of KSHV in LE fractions obtained from KSHV infected cells 15min PI compared to cells that were infected with KSHV incubated in the presence of soluble $\alpha 9\beta 1$ (Fig. 4C, 5). In other words, incubating KSHV with soluble $\alpha 9\beta 1$ blocked the escape of KSHV from LEs to the cytoplasm. Taken together, these results suggest integrin $\alpha 9\beta 1$ to have a role in escape of KSHV from the LE for cytosolic delivery.

Presuming KSHV to be a late penetrating virus, immunofluorescence microscopy verified that though FITC-KSHV co-localizes with both early (Fig. 6A) and late endosome markers (TRITC labeled anti-Rab5 and anti-Rab7, respectively), there was notably less virus association with LEs by 15min PI (Fig. 6B). This significant decrease in the association of KSHV with LEs was because capsids containing the viral genome had escaped into the cytoplasm (Fig. 7). Interestingly, treating cells with antibodies to integrins significantly blocked viral escape from the LEs (Fig. 6B, 7). Thus, these results provided additional evidence that post-internalization, $\alpha 9\beta 1$ interactions have a role in mediating the LE escape of KSHV into the cytoplasm for subsequent infection.

These findings have taken our current knowledge of KSHV entry a step further, delineating a dynamic role for $\alpha 9\beta 1$ integrins in a post-internalization stage of KSHV infection of HFF cells. Based on results from this quantitative study we can conclude that heparin has a role at the initial binding stage and DLD-binding integrin $\alpha 9\beta 1$ aids in mediating late endosomal escape. Earlier studies implicate RGD-binding integrins to have a role in the actual internalization of the virus. With further studies, we seek to resolve the direct role of $\alpha 9\beta 1$ integrin in the conformational changes to KSHV gB that may result in the endosomal escape of the viral capsid.

METHODS

Cells. HFF and CHO cells were propagated as per standard laboratory protocols (Akula *et al.*, 2005; Akula *et al.*, 2002).

Antibodies. Human $\alpha 9$ (H-198) rabbit polyclonal antibodies (Santa Cruz Biotechnology, Inc., Santa Cruz, CA), monoclonal anti-human antibody anti- $\alpha 9\beta 1$ (clone Y9A2; Millipore, Darmstadt,

Germany), $\alpha 5$ monoclonal mouse IgG (clone P1D6; Millipore), and $\beta 1$ monoclonal mouse IgG (clone 6S6; Millipore) were used in this study. Rab5 rabbit polyclonal antibody, Rab7 (D95F2) XPTM rabbit monoclonal antibody (Cell Signaling Technology, Beverly, MA), and mouse monoclonal antibody (5B7B6) to KSHV *orf62* encoded minor capsid protein, TRI-1 (Thermo Scientific, Rockford, IL) were used for Western blotting experiments and/or immunofluorescence.

Proteins and Reagents. Recombinant human integrin $\alpha 9\beta 1$ used in this study was obtained from R & D Systems, Inc., Minneapolis, MN. Heparin and fluorescein isothiocyanate (FITC) were purchased from Sigma, St. Louis, MO. Lipofectamine 2000 and G418, Geneticin[®] were obtained from Life Technologies, Grand Island, NY.

Generating stable CHO cell line expressing human $\alpha 9$. Transfection of $\alpha 9$ /pcDNA3.1+ expression plasmid into CHO cells grown in 6-well plates was performed using Lipofectamine 2000. Twenty-four hours after transfection, the cells were cultured in DMEM supplemented with 10% heat-inactivated FBS, 2mM L-glutamine, streptomycin and penicillin, and 1mg/mL G418/Geneticin. Cells were grown under selection pressure for 3-4 weeks to avoid contamination with non-resistant cells after which the expression of human $\alpha 9$ integrin was confirmed by flow cytometry and RT-PCR.

Flow cytometry. The expression of cell surface $\alpha 9$ integrins on CHO and CHO- $\alpha 9$ cells was analyzed via flow cytometric techniques. Cells were washed, incubated in growth medium at 37°C for 30min, centrifuged and resuspended in cold PBS. The entire procedure involved the use of cold reagents and temperatures of 4°C. Cells were incubated with integrin $\alpha 9$ (H-198) rabbit polyclonal antibody at 4°C for 30min, washed, incubated with FITC-conjugated appropriate

secondary IgG at 4°C for 30min, washed, and analyzed in a FACScan flow cytometer (Becton Dickinson) with appropriate gating parameters.

Virus infection of cells. Monolayers of HFF, CHO, or CHO- $\alpha 9$ cells were incubated with different antibodies to integrins for 1h at 4°C prior to infection with wild type KSHV (MOI of 5 DNA copies/cell) at 4°C for 1h. The unadsorbed viruses were washed with DMEM and the cells were further incubated for different time points. In another set of experiments, KSHV was incubated with soluble $\alpha 9\beta 1$ or control proteins (heparin or BSA) for 1h at 4°C prior to incubating it on HFF monolayers for 1h at 4°C. The unadsorbed viruses were washed with DMEM and the cells were further incubated for different time points. Herpes virus simplex-2 (HSV-2) infection of cells was performed as per early studies (Akula *et al.*, 2003).

qRT-PCR. After 2h of KSHV infection of HFF, CHO, and CHO- $\alpha 9$ cells, RNA was extracted, cDNA synthesized, and the expression of *orf50* was monitored by qRT-PCR using specific primers (Dyson *et al.*, 2010). As a benchmark for successful infection, *orf50* was monitored; *orf50* is said to be expressed within 30min of successful KSHV infection (Dyson *et al.*, 2010; Krishnan *et al.*, 2004). As per earlier studies, relative copy numbers of *orf50* transcripts were computed based on the standard graph plotted using *Ct* values for different dilutions of *in vitro* transcribed *orf50* (via the *orf50*/pGEM-T plasmid), and these values were normalized against β -*actin* controls. HSV-2 infection of cells was determined by qRT-PCR using primers corresponding to immediate early gene, UL5, as per earlier studies (Tang *et al.*, 2012). The lowest limit of detection for the standards was 6–60 *orf50* gene copies (Dyson *et al.*, 2010).

Monitoring KSHV by qPCR. After 10min of KSHV infection of HFF, CHO, and CHO- α 9 cells, total genomic DNA was extracted via QIAamp DNA Mini Kit (Qiagen, Valencia, CA) as per recommendations of the manufacturer. Isolated DNA was used to estimate the number of KSHV *orf50* gene copies by performing real time PCR (qPCR) using appropriate primers as per our earlier studies (Grange *et al.*, 2012). As an external standard, the KSHV *orf50* promoter gene cloned in the pGEM-T vector was used alongside test samples in the reaction mixtures (Deng *et al.*, 2000). The standard graph was plotted using the Ct values which are critical to calculating the relative copy numbers of viral DNA in the samples. A similar approach was used to monitor KSHV levels in different fractions collected after gradient centrifugation. HSV-2 levels in gradient fractions were monitored by qPCR using primers corresponding to immediate early gene, UL5, as per earlier studies (Tang *et al.*, 2012).

Immunoprecipitation. Cell surface proteins of HFF, CHO, and CHO- α 9 were biotinylated as previously described (Wu *et al.*, 1995). Cell lysates were incubated with 20 μ g/ml integrin α 9 (H-198) rabbit polyclonal antibody or pre-immune IgG antibodies for 1h at 4°C followed by precipitation with Protein A-Sepharose beads at 4°C for 1h. The beads were washed four times with Gold lysis buffer, boiled in sample-loading buffer without 2-mercaptoethanol, and the proteins were resolved on a 10% SDS-PAGE gel and Western blotted. The biotinylated cell surface proteins were detected by horseradish peroxidase-conjugated streptavidin and chemiluminescence.

Sucrose flotation gradient. Confluent monolayers of adherent HFF cells were cooled (4°C for 30min) and either remained uninfected (undergoing incubation at 37°C for 15min) or were infected

(undergoing incubation 37°C for 1, 5, or 15min) with wild type KSHV (MOI of 5 DNA copies/cell) in the presence of DMEM only or 10µg/ml α 9 β 1, BSA, or heparin. After the designated time point, cells were washed thrice with DMEM followed by the application of 0.5ml of homogenization buffer (250mM sucrose, 1mM EDTA, 1mM phenylmethylsulfonyl fluoride (PMSF), in which cells were gently detached using a cell scraper, lysed, and further processed for examination by a sucrose flotation assay as previously described (Yu & Lai, 2005). Specifically, after centrifugation (1,000 x g), the PNS was collected and adjusted to a concentration of 25% sucrose and 1mM EDTA in 1ml total volume. In 1ml increments, 2.4ml of 45% sucrose was transferred to the bottom of a SW41Ti tube and successively overlaid with 5.2ml of 35% sucrose, 3.9ml of 25% sucrose, and 1ml of PNS in 25% sucrose. Following centrifugation (100,000 x g), 2ml fractions were collected from top to bottom. These fractions were further analyzed using endosomal markers and KSHV. Herpes simplex virus-2 (HSV-2) was used as control in this study.

Western blotting/marker analysis. Equal protein concentrations (5µg) from different fractions obtained from sucrose floatation gradient centrifugation were resolved on a 12% SDS-PAGE gel, transferred to a polyvinylidene difluoride (PVDF) membrane, and probed with antibodies to proteins Rab5, Rab7, and KSHV TRI-1.

Acid phosphatase activity assay. Acid phosphatase activity for lysosome identification was analyzed by using Acid Phosphatase Assay Kit (Sigma) according to the manufacturer's instructions. In brief, after fractionation, 50µl of each sample was transferred to triplicate wells of a 96-well plate followed by the addition of substrate solution (50µl). The reaction was mixed for

10min using a horizontal shaker and incubated for 20min at 37°C. Next, stop solution (0.5N NaOH) was added and the absorption was measured at 405nm using a spectrophotometer.

FITC-KSHV. KSHV labeling was conducted as per earlier protocols (Akula *et al.*, 2003). Specifically, density gradient-purified wild type KSHV (50µl; 2mg/ml) was incubated at room temperature for 8h with a solution of FITC (50µl; 5mg/ml) dissolved in dimethyl sulfoxide (DMSO; Sigma). To rid the virus preparation of free dye, FITC-KSHV was purified by centrifugation (70,000 x g) over a 30% sucrose cushion (8.5ml) for 90min at 4°C in a Beckman SW41Ti rotor. The FITC-KSHV band was resuspended in phosphate-buffered saline (PBS) and subsequently dialyzed against PBS (pH 7.2). FITC-HSV-2 was generated on the same lines.

Immunofluorescence microscopy. In order to map the endosomal location of KSHV, HFF cells (75% confluent) cultured in 8 well chamber slides were either uninfected or infected with FITC-KSHV for 1 or 15min at 37°C. Post-infection, cells were washed in phosphate-buffered saline (PBS) and fixed with 3.7% formaldehyde in PBS for 10min. After fixing, cells were washed, permeabilized using 0.1% Triton X-100 in PBS for 3min, washed again, and incubated for 20min at room temperature with PBS containing 1% bovine serum albumin (BSA) to block non-specific binding sites. Post-washing, cells were then incubated successfully (1h at 37°C) with the appropriate primary (anti-Rab5, or anti-Rab7) and secondary (goat anti-rabbit TRITC) antibodies. Immunostained cells were washed in PBS and imaged with a Nikon fluorescent microscope using appropriate filters. To study the escape of KSHV from the LEs, we infected cells with KSHV for 30min, fixed the cells as described above, and sequentially stained with anti-KSHV TRI-1

antibodies and goat anti-mouse TRITC antibodies prior to examining under a fluorescent microscope.

Author contributions

Conceived the idea: SMA; Designed experiments: LRW; performed experiments: LRW, HAH.

FIGURE LEGENDS

Figure 1. Effect of anti-integrin antibodies and soluble $\alpha 9\beta 1$ on KSHV infection (A, B) and internalization (C, D). (A, C) Monolayers of HFF cells were incubated with antibodies to $\alpha 9$, $\beta 1$, $\alpha 5$, or a pre-immune IgG for 1h at 4°C prior to infection with KSHV (MOI of 5 DNA copies/cell). In another set of experiments (B, D), KSHV was mixed with increasing concentrations (0, 0.1, 1, 10 μ g/ml) of soluble $\alpha 9\beta 1$, heparin, or BSA for 1h at 4°C prior to being added to cells. (A, B) At 2h PI, cells were washed, lysed, RNA extracted, cDNA synthesized, and the expression of *orf50* was monitored by qRT-PCR using specific primers. (C, D) At 10min PI, cells were lysed and the genomic DNA extracted. To quantitate internalized viral DNA, KSHV *orf50* copy numbers were monitored by performing qPCR. The data are presented as percentages of inhibition of KSHV infection (A, B) or viral DNA internalization (C, D). Data represent the average \pm SD (error bars) of three experiments.

Figure 2. Antibodies to integrin $\alpha 9$ inhibit KSHV infection of CHO- $\alpha 9$ cells, but not internalization. (A) Flow cytometry analysis of the surface expression of $\alpha 9$ integrin subunit in CHO and CHO- $\alpha 9$ cells was performed following staining with integrin $\alpha 9$ (H-198) rabbit polyclonal antibody and subsequent incubation with goat anti-rabbit FITC. The average percentage of cells positive for $\alpha 9$ expression from three independent experiments is shown above the marker in the representative histogram plots. (B) **Cell surface expression of $\alpha 9\beta 1$ integrin in CHO- $\alpha 9$ and HFF cells.** Integrin $\alpha 9\beta 1$ was immunoprecipitated from cell lysates of surface biotinylated HFF and CHO- $\alpha 9$ cells with integrin $\alpha 9$ (H-198) rabbit polyclonal antibody and Protein A-Sepharose beads. Precipitated protein samples were resolved on a 10% SDS-PAGE gel and Western blotted. The biotinylated proteins were detected by horseradish peroxidase-

conjugated streptavidin and chemiluminescence. **(C,D)** Monolayers of CHO and CHO- $\alpha 9$ cells were untreated or incubated with antibodies to $\alpha 9$ or $\alpha 5$ for 1h at 4°C prior to infection with KSHV (MOI of 5 DNA copies/cell). **(C)** At 2h PI, cells were washed, lysed, RNA extracted, cDNA synthesized, and the expression of *orf50* was monitored by qRT-PCR using specific primers. **(D)** At 10min PI, cells were lysed and the genomic DNA extracted. To quantitate internalized viral DNA, KSHV *orf50* copy numbers were monitored by performing qPCR. The data are presented as percentages of KSHV infection **(C)** or internalization **(D)**. Data represent the average \pm SD (error bars) of three experiments.

Figure 3. Schematic representation of the sucrose flotation assay for endosome purification.

This study used uninfected and KSHV (MOI of 5 DNA copies/cell) infected HFF cells.

Figure 4. Detection of KSHV in endosomal fractions. **(A)** Distribution of endosomal membranes was determined from uninfected and KSHV infected HFF cells using sucrose gradient fractions. Equal-volume aliquots from each gradient fraction were separated by SDS-PAGE and probed by Western blotting against organelle markers: Rab5 (EE marker) and Rab7 (LE marker). **(B)** Lysosome detection in sucrose gradient fractions of uninfected and KSHV infected HFF cells. Acid phosphatase activity was analyzed by using Acid Phosphatase Assay Kit (Sigma). **(C) KSHV escapes from the LE.** Following gradient centrifugation, viral genomic DNA was extracted from each recovered fraction. Fractions were then quantified for the content of internalized viral DNA by performing qPCR using specific primers. Data (panels

B, C) represent the average \pm SD (error bars) of three experiments. Columns with different alphabets indicate statistical significance ($P < 0.05$) by Least Significant Difference (LSD).

Figure 5. Confirming the presence of KSHV in sucrose gradient fractions at different early time points. Fractions (5 μ g protein) collected at different early time points (1, 5, or 15min) during the course of infection were resolved by SDS-PAGE followed by Western blot analysis with anti-KSHV TRI-1 antibodies.

Figure 6. Antibodies to integrin $\alpha 9\beta 1$ inhibit KSHV escape from the late endosome. (A) KSHV is present in Rab5-positive EEs and Rab7-positive LEs. HFF cells were either uninfected or pre-treated (1h at 37°C) with antibodies (20 μ g/ml) to $\alpha 9\beta 1$ or pre-immune IgG prior to infection with FITC-KSHV for 1min (A) and 15min (B) at 37°C. Cells were washed, fixed, and subsequently immunostained with TRITC labeled anti-Rab5 antibodies (A) and TRITC labeled anti-Rab7 antibodies (B) prior to mounting using an anti-fade reagent containing DAPI and examining under a fluorescent microscope. Representative images are provided at 1,000x magnification. The white circles indicate co-localization of FITC-KSHV with the respective endosome marker within the cell (panels A and B).

Figure 7. Antibodies against $\alpha 9$ and $\beta 1$ integrin subunits block KSHV nucleocapsid trafficking to the perinuclear region by 30min PI. HFF cells were untreated or pre-treated (1h at 37°C) with antibodies (20 μ g/ml) to $\alpha 9$, $\beta 1$, $\alpha 5$ or a pre-immune IgG prior to infection with KSHV for 30min at 37°C. Cells were washed, fixed, and subsequently immunostained for TRI-1

minor capsid protein. Representative fluorescence imaging depicting TRI-1 positive viral capsids in infected HFF cells are shown. Mag: 1,000x.

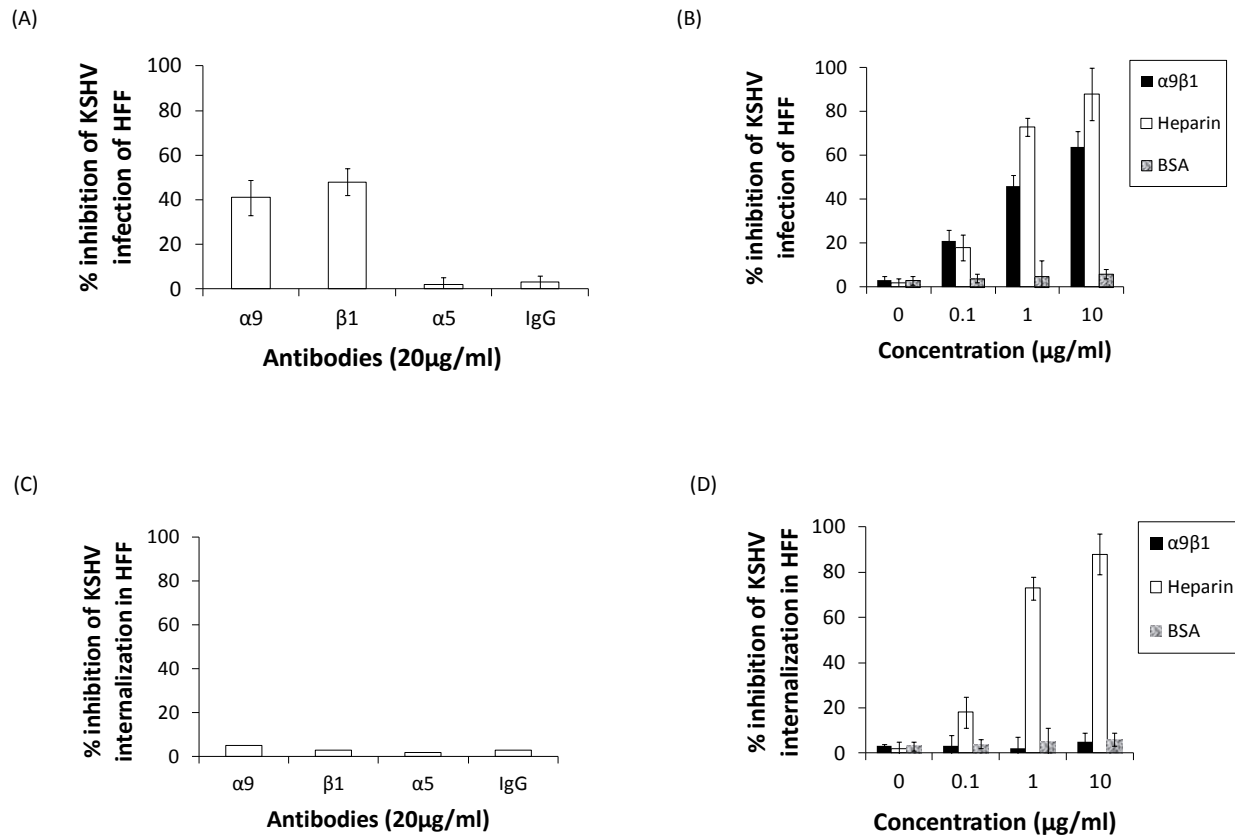


Figure 1

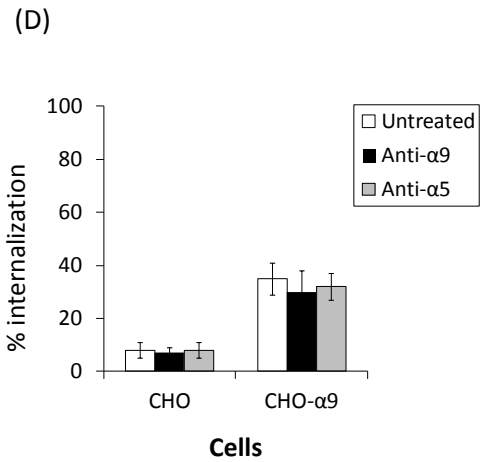
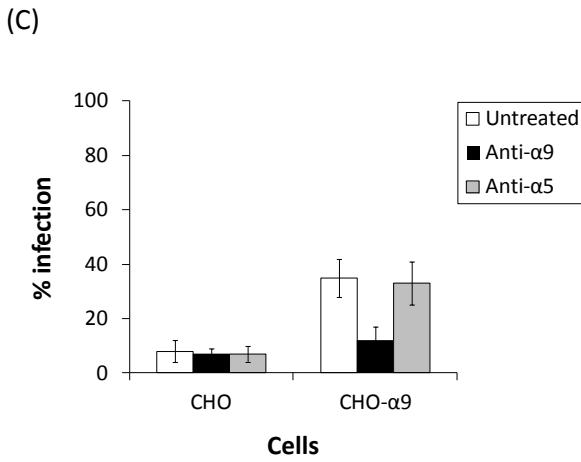
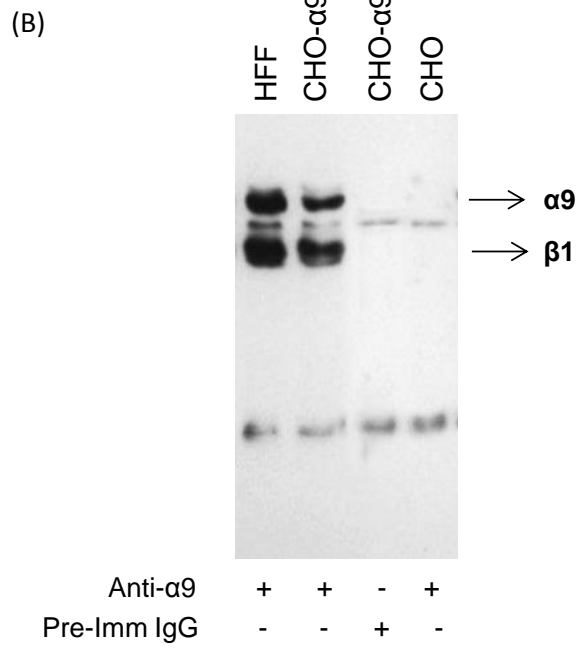
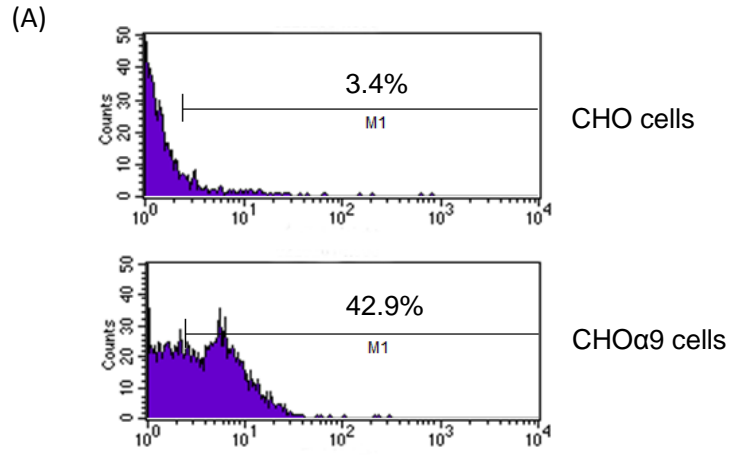


Figure 2

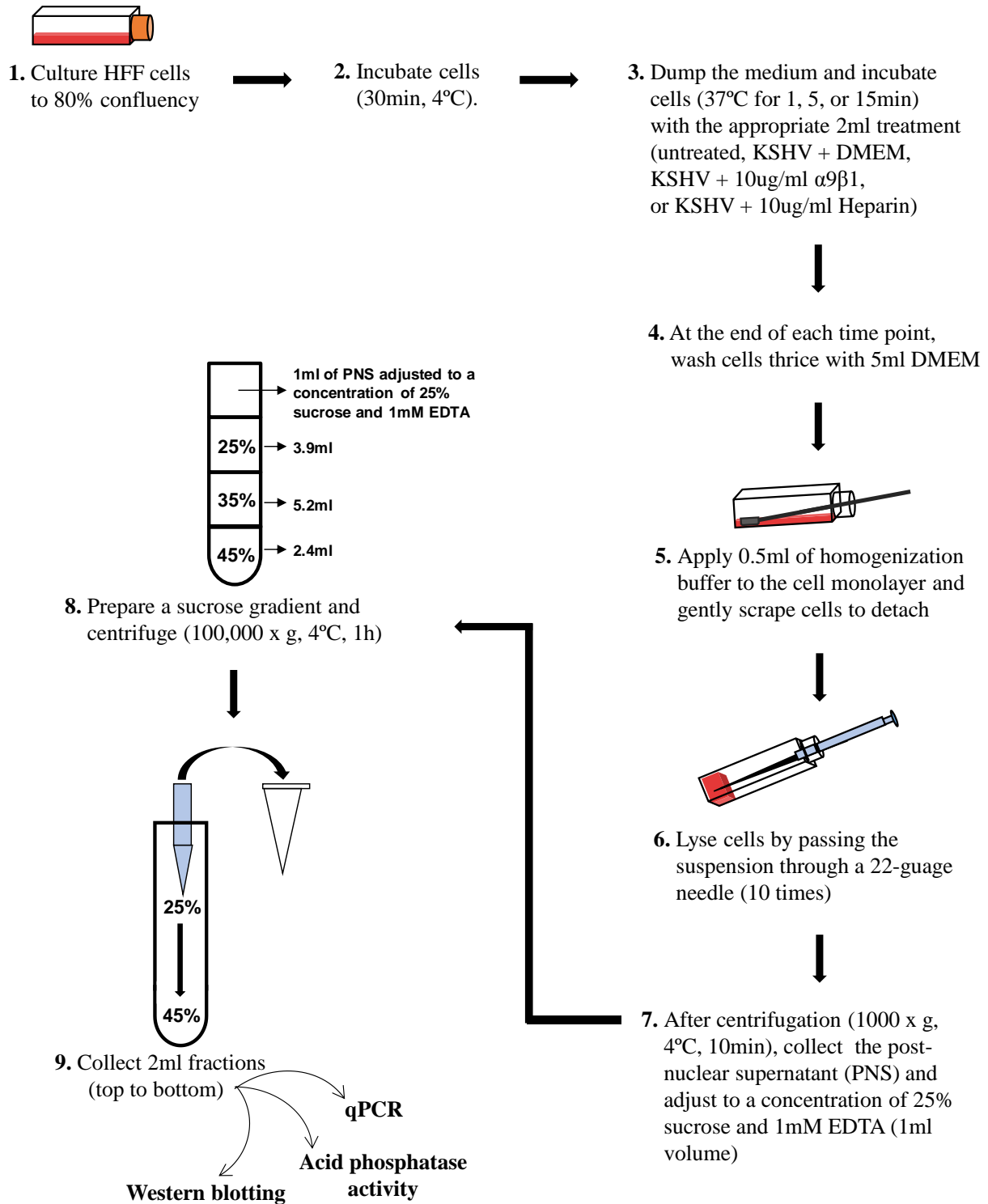


Figure 3

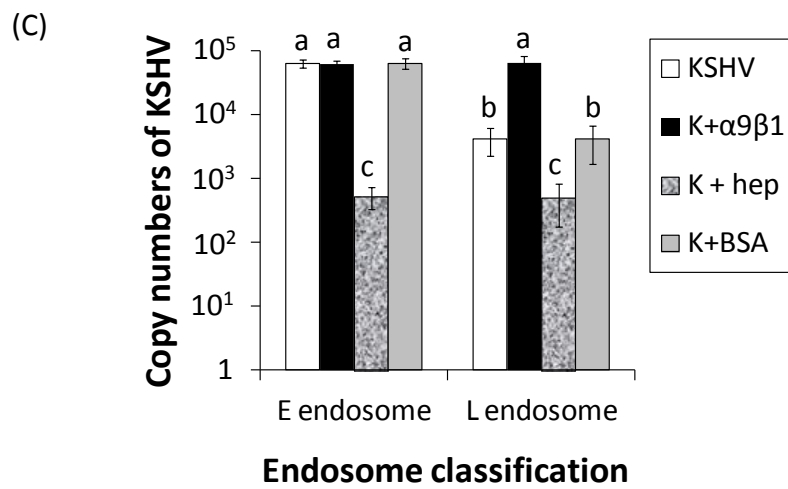
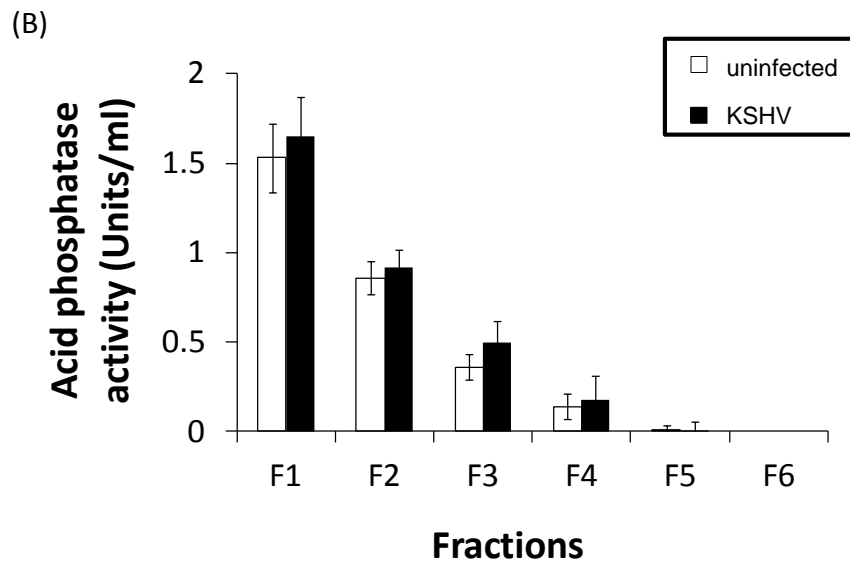
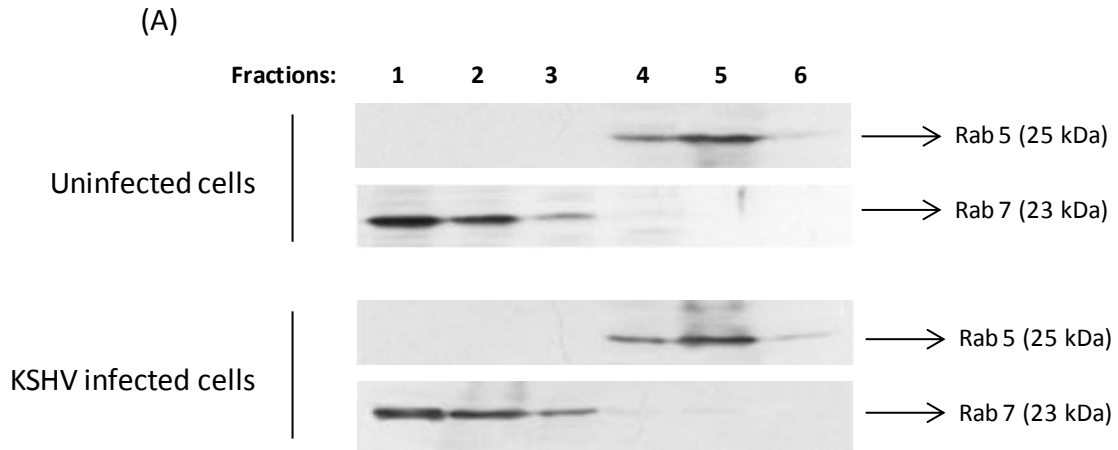


Figure 4

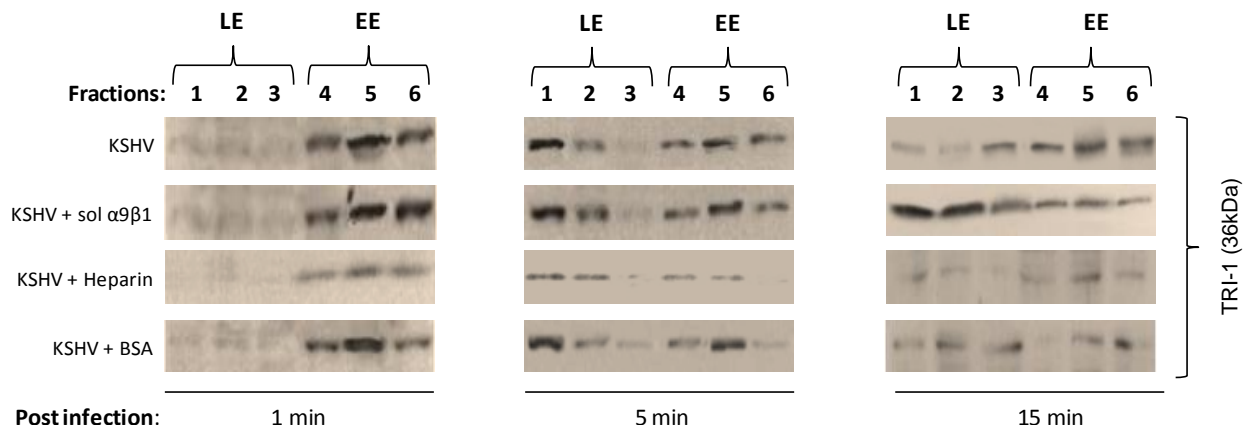


Figure 5

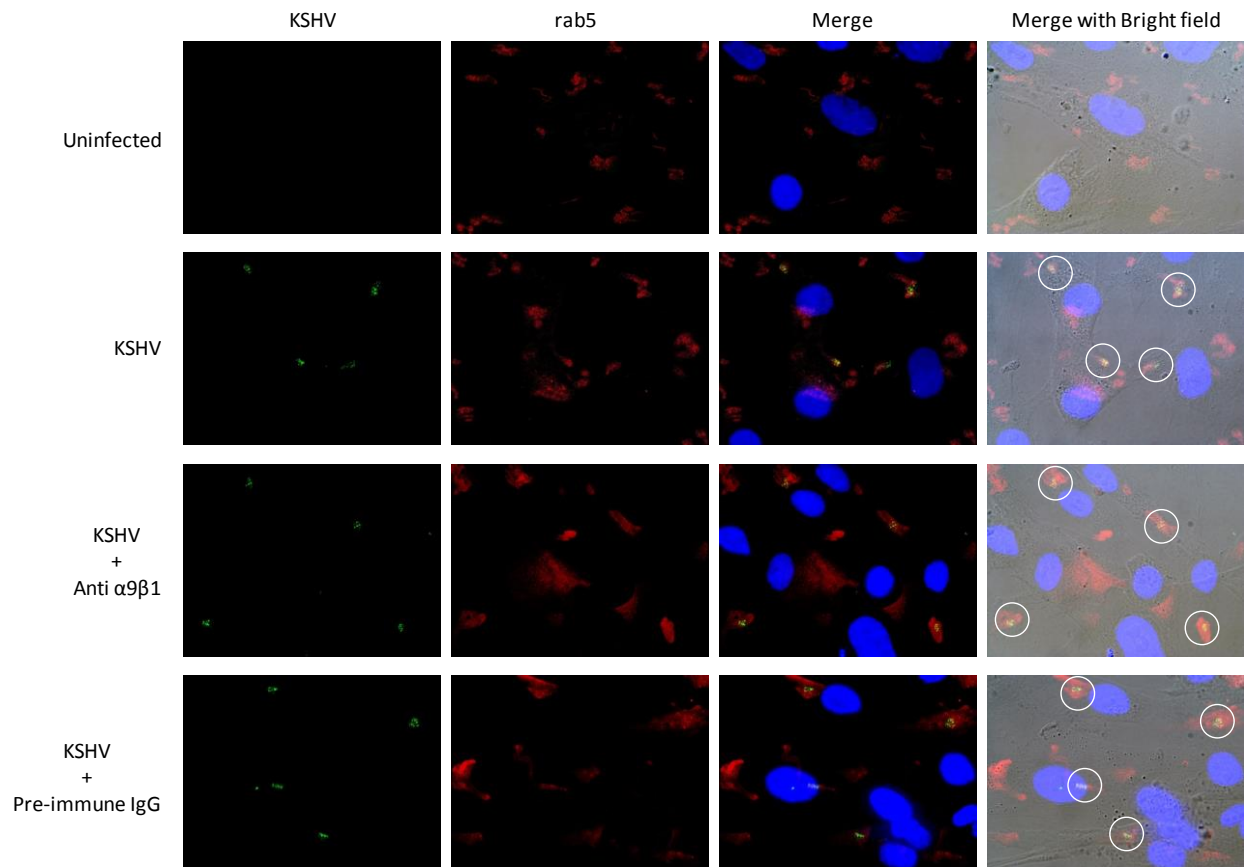


Figure 6A

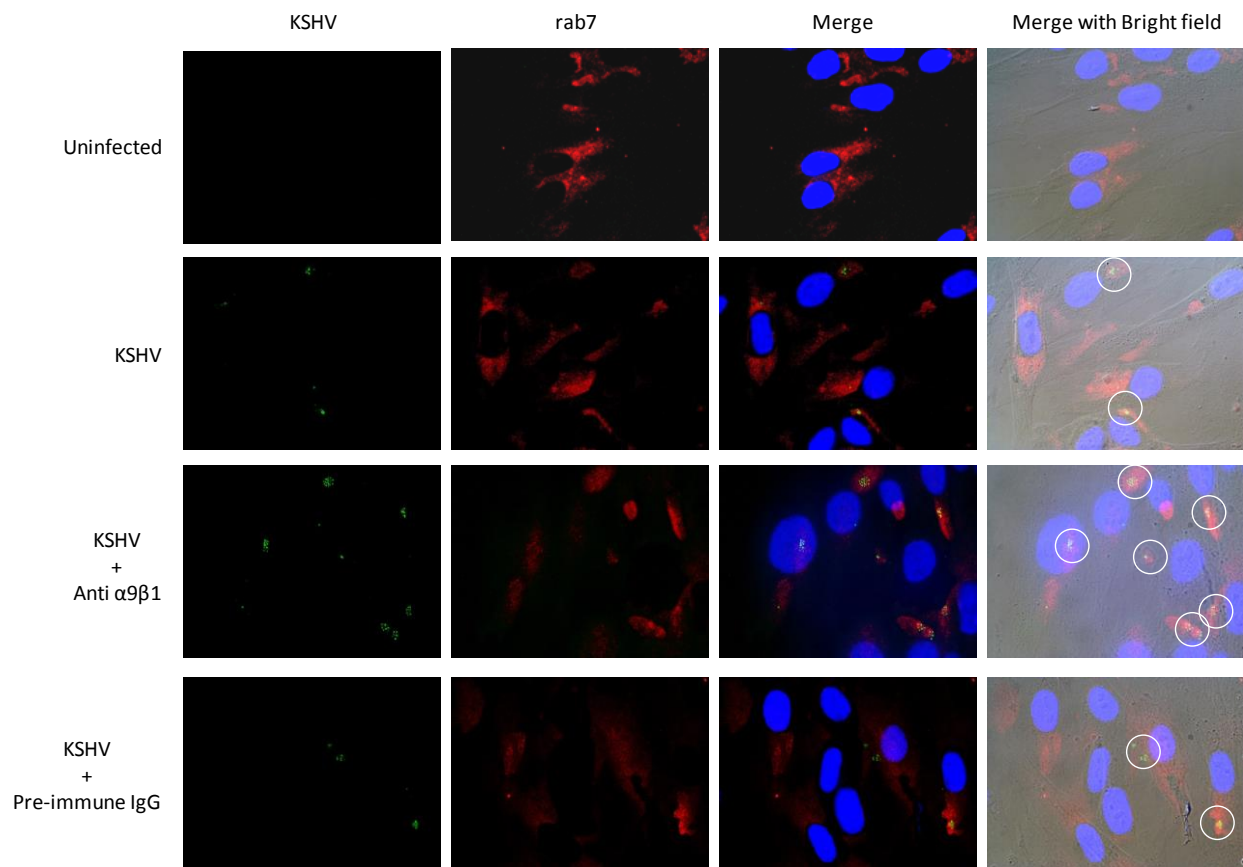


Figure 6B

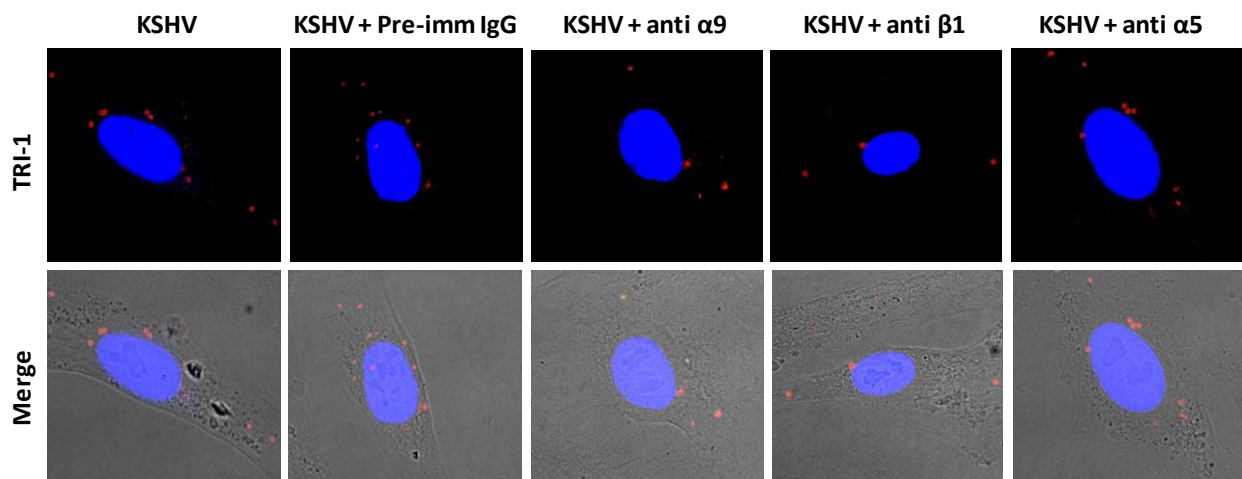


Figure 7

SUMMARY

To date, many aspects of the intricate KSHV entry process are still enigmatic. Like other viruses, KSHV has evolved to utilize combinations of host cell receptor molecules for the infection of target cells. KSHV is the first herpesvirus identified to functionally interact with adherent target cell integrins. KSHV gB is the only gB homolog possessing the most common integrin binding domain, RGD. KSHV envelope associated gB interacts with RGD-binding $\alpha 3\beta 1$, $\alpha V\beta 3$, and $\alpha V\beta 5$ integrins for the initiation of virus entry processes. Apart from RGD, KSHV gB also harbors the less common integrin recognition motif, DLD (**Summary Figure**). Though DLD is highly conserved among herpesviruses, its role in virus entry has been majorly unexplored outside of HCMV. Thus, initially seeking to determine a role for DLD of KSHV gB, we hypothesized that this lesser studied integrin binding domain would also play a critical role in KSHV entry and subsequent infection of cells (**Chapter 2**).

In the first study (**Chapter 2**) phage display peptide library screening identified integrin $\alpha 9$ as a plausible receptor for DLD of KSHV gB; non-RGD binding integrin $\alpha 9$ forms a heterodimer with the $\beta 1$ subunit to yield $\alpha 9\beta 1$. Binding specificity was confirmed between DLD of KSHV gB and integrin $\alpha 9\beta 1$ using soluble proteins. Inhibition of the DLD: $\alpha 9\beta 1$ interactions significantly lowered wild type KSHV infection of HFF and HMVEC-d cells (cells express integrin $\alpha 9\beta 1$ on their surfaces) versus 293 cells which do not express $\alpha 9\beta 1$. The physiological relevance of the interaction was explored by performing infection assays using a recombinant virus lacking a functional DLD (BAC36 Δ D-KSHV). Recombinant viruses were constructed via use of a BAC system harboring the KSHV genome, BAC36. BAC36 Δ D-KSHV infection rates were significantly lower in HFF and HMVEC-d cells compared to the comparable infection rates observed in BAC36.T-KSHV (containing an intact DLD sequence and an introduced tetracycline

cassette) and wild type BAC36-KSHV infected cells. These findings provided substantial proof that interactions between DLD of KSHV gB and $\alpha 9\beta 1$ play an important role in virus infection of cells independent of RGD (**Summary Figure**).

As a continuation of this work, our next study further investigated a role for DLD-binding $\alpha 9\beta 1$ during the initial stages of KSHV infection (**Chapter 3**). Integrins are known to alter various stages of virus entry, but there has been very little analysis of the role of DLD-binding integrins during early KSHV infection. Both antibodies against the $\alpha 9$ and $\beta 1$ integrin subunits as well as soluble $\alpha 9\beta 1$ inhibited KSHV infection of HFF cells but failed to inhibit virus uptake. These findings were reproduced in CHO cells that are $\alpha 9$ integrin deficient and non-permissive to KSHV infection. CHO cells stably transfected to express human $\alpha 9$ (CHO- $\alpha 9$) were permissive to infection compared to CHO cells. As in HFF cells, antibodies against the $\alpha 9$ integrin subunit inhibited KSHV infection of CHO- $\alpha 9$ cells but not internalization. Such findings alluded to a possible role for $\alpha 9\beta 1$ at an entry step beyond KSHV internalization.

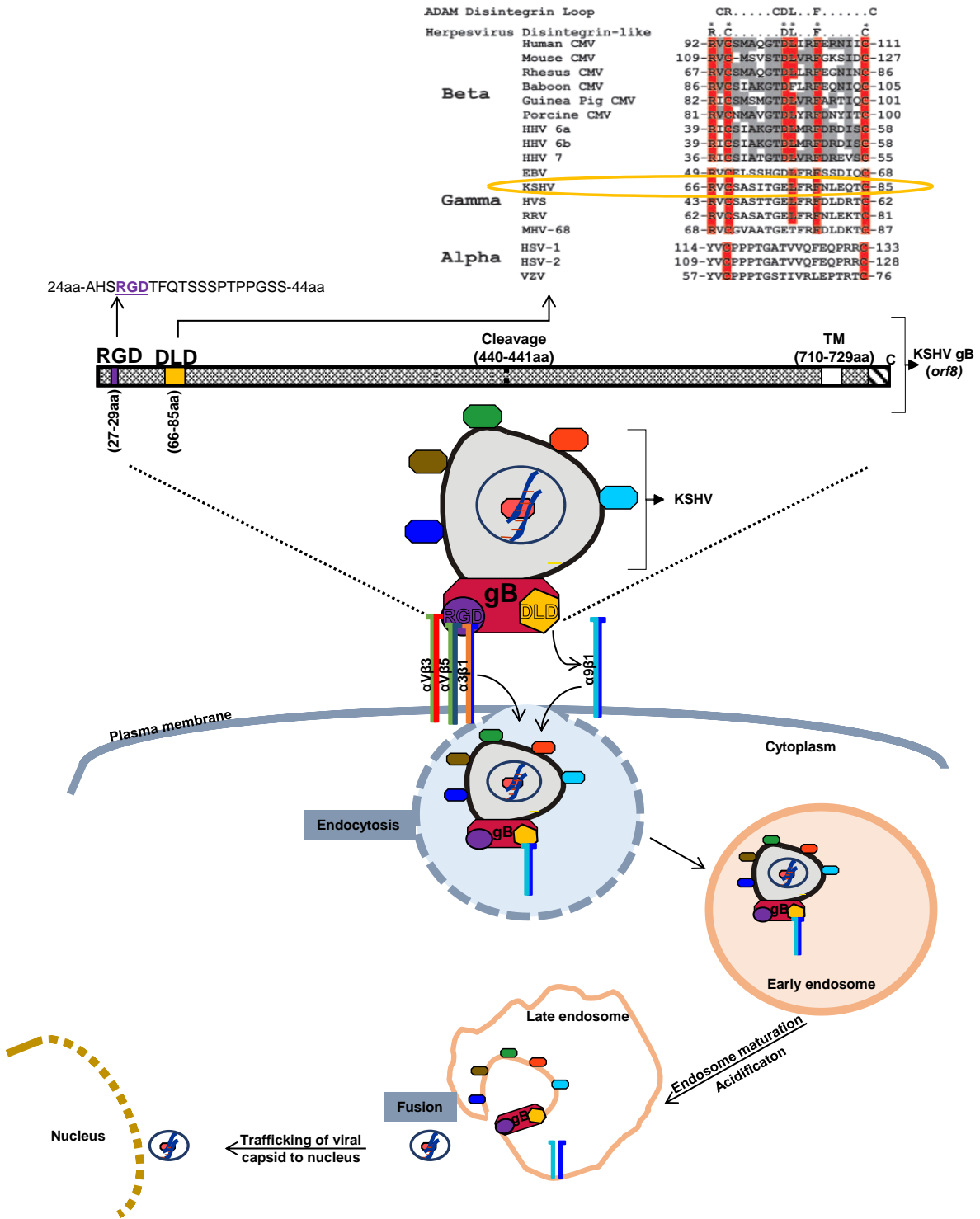
For entry into target cells, KSHV is known to utilize the endocytic pathway (**Summary Figure**). Unconventionally, we used subcellular fractionation via sucrose density gradient centrifugation to isolate intact endosomes from uninfected and KSHV infected HFF cells; endocytosed cargo is typically first delivered to endosomes. Upon confirming gradient fractions containing early and late endosomes, we were able to track KSHV in infected HFF cells for characterization of possible post-internalization roles for $\alpha 9\beta 1$. Virus particles in endosomes were monitored at early time points. By 15min PI, significantly more KSHV was present in EE fractions versus fractions containing LEs; this decline in late endosomal levels of KSHV was blocked in the presence of soluble $\alpha 9\beta 1$.

Immunofluorescence microscopy provided confirmation of $\alpha 9\beta 1$ integrin's role in late endosomal escape of the KSHV capsid into the cytoplasm. By 30min PI of HFF cells, an accumulation of KSHV was observed at the perinuclear region. However, treatment of HFF cells with antibodies blocked KSHV nucleocapsid trafficking by preventing the escape of KSHV from LEs. In all, such findings confirm a role for DLD-binding $\alpha 9\beta 1$ in mediating a late endosomal escape of KSHV into the cytosol for subsequent infection (**Summary Figure**).

Entry processes are commonly analyzed by monitoring internalized virus particles via inhibitor-based infection assays, Western blotting, polymerase chain reaction, and imaging techniques that allow scientists to track their intracellular location. To study intracellular trafficking of a virus via endosomes, it is imperative to use an approach that will allow us to specifically isolate intact early and late endosomes. Accordingly, we standardized a subcellular fractionation method in our laboratory (**Chapter 3**). Subcellular fractionation aids in specifically isolating virus containing early and late endosomes by performing a series of centrifugation steps. In the future, employing such an assay will be a boon to characterize the manner by which KSHV traverses via endosomes to successively establish infection. The future studies will focus on the following:

- (i) What is the role for $\alpha 9\beta 1$ integrin in endosome trafficking?
- (ii) What happens to the virus as it is being trafficked within the endosomes?
- (iii) What is effect of acidic pH and protease activity on KSHV envelope gB within the endosomes, and how do they promote a successful infection?

SUMMARY FIGURE



Summary Figure: Role of RGD and DLD binding integrins in KSHV biology. KSHV gB possesses two integrin recognition motifs: RGD and DLD. RGD interacts with $\alpha 3\beta 1$, $\alpha V\beta 3$, and $\alpha V\beta 5$ integrins to initiate entry processes. DLD of KSHV gB interacts with integrin $\alpha 9\beta 1$ in an interaction critical for entry and subsequent infection. Post-internalization, KSHV: $\alpha 9\beta 1$ interactions play a role in virus trafficking via endosomes for eventual escape into the cytoplasm. The portion of this figure depicting conservation of the gB DLD was derived from (Feire *et al.*, 2004).
TM: transmembrane region; C: carboxyl domain

CHAPTER 4: ADDITIONAL DATA

REACTIVATION OF VIRUSES IN RENAL TRANSPLANT RECIPIENTS

ABSTRACT

Objective: Post-transplantation immunosuppression renders transplant recipients vulnerable to reactivation of opportunistic viral infections. Unfortunately, immunosuppression cannot be avoided as it is a preventative measure to combat allograft damage. Several viruses are said to be a threat in renal transplant patients and they include Kaposi's sarcoma-associated herpesvirus (KSHV), cytomegalovirus (CMV), Epstein-Barr virus (EBV), BK virus (BKV), and JC virus (JCV). Therefore, we attempted to establish a direct correlation between immunosuppression in renal transplantation to viral lytic replication. **Methods:** A cohort of 10 renal transplantation patients receiving a combination of immunosuppressive and an anti-viral drugs were categorized into two groups (n=5) based on their prior CMV sero-status. Each study patient provided pre- (day 0) and post-transplantation (days 45 and 90) blood (8ml) and urine samples (5ml) for analysis. Peripheral blood mononuclear cells (PBMCs) separated from whole blood samples were quantitatively monitored (via qRT-PCR) for the expression of KSHV, CMV, and EBV transcripts. BKV and JCV DNA levels in urine were also quantitatively monitored (via qPCR). **Conclusions:** There was no significant KSHV, CMV, or EBV reactivation in any of the study patients. There was reactivation of BKV and JCV in the renal transplant patients but no immediate pathologies were associated with it. We believe that the administered treatment regimen that included a cocktail of immunosuppression, anti-inflammatory, and anti-viral drugs is effective within the early months post-transplantation.

INTRODUCTION

Throughout the years, commendable advancements have been made to improve renal transplantation, as it is now the go-to therapeutic method for survivability and improving quality of life in those battling end-stage renal disease (ESRD) (Abecassis *et al.*, 2008). However, successful renal transplantations are not without grave risks. Unfortunately, viral, non-viral, and co-infections as well as allograft dysfunction/failure raise great concern post-solid organ transplantation (Cukuranovic *et al.*, 2012). Contributing to the severe morbidity and mortality risk (Weikert & Blumberg, 2008), viruses are among the most common post-transplant infections (Snyder *et al.*, 2009). Some of the typical viral pathogens affecting renal transplant recipients include: Kaposi's sarcoma-associated herpesvirus (KSHV; human herpesvirus-8/HHV-8), cytomegalovirus (CMV; human herpesvirus-5/HHV-5), Epstein-Barr virus (EBV; human herpesvirus-4/ HHV-4), and urine shedded polyomaviruses, BK virus (BKV) and JC virus (JCV/John Cunningham virus) (Kotton & Fishman, 2005). Incidentally, CMV is considered the most common opportunistic pathogen afflicting renal transplant and other allograft recipients (Karuthu & Blumberg, 2012; Weikert & Blumberg, 2008).

After an allotransplant, patients receive a cocktail of both immunosuppressive and anti-viral drugs. Immunosuppressant therapies are vital for preventing immunological damage to and rejection of the transplanted kidney, but on the other hand, these drugs promote reactivation of latent viral infection (Cukuranovic *et al.*, 2012; Ketteler *et al.*, 2003) which prompts the need for antivirals. This dual treatment approach is not infallible, however. For instance, viruses can develop resistance to anti-viral drugs (Biron, 2006; Einollahi, 2007). Also, immunosuppressive therapy is deemed a potential risk factor for the onset of polyomavirus-associated nephropathy (PVAN) for which there is a void of established polyomavirus-specific anti-viral drugs (Wiseman,

2009) and the suggested treatment is immunosuppression reduction (Garces, 2010). Thus, a conundrum ensues.

For those who are recipients of an allograft, viral infections result majorly from reactivation of preexisting latent (i.e. dormant; (Weinberger & Weinberger, 2013)) infections in the host or the graft itself (Cukuranovic *et al.*, 2012; Jenkins *et al.*, 2003; Kotton & Fishman, 2005; Weikert & Blumberg, 2008). With the ability to establish latent and/or persistent infections, herpesviruses and polyomaviruses generate much concern post-transplantation, as reactivation is frequently observed among immunosuppressed transplant recipients (Ling *et al.*, 2003; Tanenbaum *et al.*, 2007). Reactivation is the poorly understood molecular mechanism wherein a virus in latent phase of the complicated replication process shifts to the productive (lytic) phase of replication—a state of full viral gene expression with the production of infectious progeny (Speck & Ganem, 2010)—allowing cell-to-cell spread (Traylen *et al.*, 2011).

In this report, we conducted an *in vivo* pilot study in which a cohort of ten renal transplant recipients receiving treatment (immunosuppressant, anti-inflammatory, and anti-viral drugs) functioned as a means to analyze a correlation between immune suppression and virus reactivation. Over the course of this three-month study, pre- and post-transplantation blood or urine samples collected from enrolled study patients were quantitatively analyzed for reactivation of KSHV, CMV, EBV, BKV, and JCV. Results from our study demonstrate that the treatment strategy being followed at the Brody School of Medicine (East Carolina University, Greenville, NC) is effective in preventing reactivation of herpesviruses in renal transplant patients but not polyomaviruses.

METHODS

Study patients. A total of ten English speaking Vidant Medical Center (Greenville, NC) renal transplant patients above the age of 18 years and not considered high risk for acute allograft rejection were studied. All participants provided written consent for inclusion into the study prior to their transplantation, and the study was approved by East Carolina University's University and Medical Center Institutional Review Board (UMCIRB). Samples collected by clinical study team members on days 0 (pre-transplantation/check-in day for renal transplantation), 45, and 90 (post-transplantation/days of routine follow-up doctor's visits) included: blood (8ml) and urine (5ml). Donor:recipient history with respect to prior CMV exposure was taken under consideration, and the ten total participants were divided categorically into two groups (n=5): CMV-seropositive donor/CMV-seropositive recipient (D+/R+) and CMV-seropositive donor/CMV-seronegative recipient (D+/R-). All study patients were treated with a combination of tacrolimus and mycophenolate immunosuppressant drugs, along with the anti-inflammatory steroid, prednisone. They were also administered the anti-viral drug, valganciclovir to treat CMV infections.

Isolation of peripheral blood mononuclear cells (PBMCs). PBMC isolation from collected whole blood samples was performed by Ficoll-Paque PREMIUM (GE healthcare, Piscataway, NJ) density-gradient centrifugation as per earlier studies (Fidan *et al.*, 2014). Post-centrifugation, buffy coats (the fraction of anti-coagulated blood that contains most of the white blood cells and platelets) were collected, washed thrice in phosphate-buffered saline (PBS), and resuspended at a concentration of 2×10^6 cells/ml. All study participants' blood samples (8ml) from days 0, 45, and 90 were processed within 1-2h post-collection to obtain PBMCs.

qRT-PCR. As per standard laboratory protocols, RNA was extracted from 2×10^6 PBMCs, cDNA synthesized, and qRT-PCR was conducted (Dyson *et al.*, 2010) to monitor the expression of viral transcripts using primers specific to KSHV, CMV, and EBV (Table 1). Serial dilutions of each plasmid control containing PCR products amplified by the respective primer set (Table 1) were tested, and standard curves were constructed from the Ct values. The number of viral copies were calculated from these standard curves (values were normalized against β -actin controls) and expressed as copies/ml. The lowest limit of detection for the standards was 6-60 gene copies (Dyson *et al.*, 2010).

DNA preparation and qPCR monitoring reactivation of BKV and JCV. The extraction of genomic DNA from urine was performed as previously described (Bergallo *et al.*, 2006) using the phenol/chloroform/iso-amyl method. DNA was precipitated using 3M sodium acetate (1/10 volume; pH 5) and isopropanol, pelleted, washed with 70% ethanol, and following centrifugation (room temperature for 2min at 13,000rpm), the pellet was air-dried and rehydrated with 20 μ l TE buffer (10mM TrisCl, 1mM EDTA pH 8).

Per standard protocols (Grange *et al.*, 2012), genomic DNA was used to quantify viral DNA in a real-time PCR (qPCR) assay using previously validated primer sets for BKV and JCV (Table 1). Plasmid DNA containing BKV or JCV genomes served to generate standard curves against which samples were analysed. The standard graph was plotted using Ct values which are critical to calculating the relative copy numbers of viral DNA in the samples. All qPCR results were calculated as copies/ml, and the detection cut-off of the assay was 1×10^7 copies/ml in urine.

RESULTS AND DISCUSSION

I. Reactivation of herpesviruses post-renal transplantation.

Though the mechanism supporting virus reactivation is fairly enigmatic, the potential for virus reactivation from latency is significantly enhanced during a state of immunosuppression (Gill *et al.*, 2014) (i.e. during renal transplantation). A 2001 study by Andreoni *et al.* concluded that the level of KSHV reactivation among renal transplant recipients—presumably due to drug-induced immunosuppression—resulted in increased incidence of Kaposi’s sarcoma (KS) (Andreoni *et al.*, 2001), a malignancy caused by KSHV (Moore & Chang, 1995). Maximum immunosuppression is believed to occur within the first three months post-transplantation (Cukuranovic *et al.*, 2012; Weikert & Blumberg, 2008), the exact time frame after transplantation in which there is maximal disease incidence (Manz *et al.*, 2001). For instance, EBV reactivation/infection is commonly observed between months two and three post-transplantation (Allen & Preiksaitis, 2013). Befittingly, in this three month prospective study, herpesvirus (KSHV, CMV, and EBV) reactivation was initially monitored in all ten, presumably immunocompromised, renal transplant recipients (two patient groups; n=5: D+/R+ and D+/R-).

Specifically, PBMCs (comprised of blood cells that regulate the immune system; (Koncarevic *et al.*, 2014) separated from the blood samples (8mL) of each study participant pre- (day 0) and post-transplantation (days 45 and 90) were quantitatively monitored for the expression of viral transcripts (via qRT-PCR) using published primer sets for KSHV, CMV, and EBV (Table 1). In all of the allograft recipients (100% of patients from the D+/R+ and D+/R- groups), herpesviruses were present at undetectable levels (on days 0, 45, and 90), as neither KSHV, CMV, nor EBV lytic replication occurred within the time span of this study.

It is likely that the observed negligible herpesviral loads in all members of our study cohort are a result of an effectively adapted treatment regimen that includes anti-viral and anti-inflammatory drugs in addition to the administered immunosuppressant drugs. In terms of CMV for instance, studies have reported that during the period in which antivirals are being administered, the incidence of post-transplantation CMV infection and related complications is reduced—in the absence of drug toxicity and/or viral resistance. This reduction in CMV incidence was observed despite the fact that the serologically mismatched D+/R- demographic is considered high risk for CMV disease (Liu *et al.*, 2013; Singh, 2005). According to some reports, valganciclovir used for CMV prophylaxis can reduce the incidence of non-CMV herpesvirus infections, as well (Razonable *et al.*, 2005). Work by Casper *et al.* involving KSHV positive patients, demonstrated valganciclovir to effectively reduce KSHV replication, *in vivo* (Casper *et al.*, 2008). Similarly, valganciclovir has been shown to control EBV replication in CMV D+/R-solid organ transplant recipients (Razonable *et al.*, 2005).

II. Incidence of polyomaviruses post-renal transplantation.

After primary infection, both BK and JC polyomaviruses persist latently within the reno-urinary tract (Behzad-Behbahani *et al.*, 2004; Costa & Cavallo, 2012), and although asymptomatic viruria *may* occur as a response to reactivation in ‘normal’ individuals, it is known to precede PVAN in renal transplant patients (Bohl & Brennan, 2007; Costa & Cavallo, 2012). BKV is considered the primary causative agent for PVAN (Hirsch & Randhawa, 2013) which causes kidney graft dysfunction in 60-90% of affected patients and premature allograft loss in approximately 50% of cases (Acott, 2013). Notably, JCV, the etiological agent of progressive multifocal leukoencephalopathy (PML), is estimated to contribute to about 5% of PVAN incidents (Costa &

Cavallo, 2012). Previous studies have considered the ability to quantify viral load in urine (via qPCR) an advantageous means for early detection of polyomavirus reactivation prior to the occurrence of tissue damage (Marinic *et al.*, 2014), as significant and persisting viruria poses a cause for concern given the typical clinical progression from viruria to viremia and later PVAN (Costa & Cavallo, 2012).

In this study, to initially evaluate reactivation of BKV and/or JCV in our cohort of ten total renal transplant recipients, BK and JC viruria was quantitatively investigated pre- (day 0) and post-transplantation (days 45 and 90) via qPCR using appropriate primer sets (Table 1). On day 0, 100% of the renal transplantation study participants from both the D+/R+ and D+/R- groups were negative for BK and JC viruria (two patients from both the D+/R+ and D+/R- groups were unable to provide a day 0 urine sample). Interestingly, seemingly sudden polyomavirus reactivation occurred on day 45. Though no D+/R+ group patients (day 45) were positive for BK viruria, four out of five kidney graft recipients from this group were positive for JC viruria. In the D+/R- group (day 45), one patient was positive for BK viruria, and two were positive for JC viruria (one patient from the D+/R- group was unable to provide a day 45 urine sample). On day 90, there was again no apparent BK viral shedding among the D+/R+ patients. However, in terms of JC viral shedding, by day 90, only one patient from this group (D+/R+) exhibited JC viruria (one patient from the D+/R+ group was unable to provide a day 90 urine sample). In the D+/R- group (day 90), BK viruria was apparent in one patient, as was JC viruria (one patient from this group was unable to provide a day 90 urine sample). Taken together, qPCR results revealed a sudden onset in the reactivation of both these polyomaviruses with a gradual decline in the occurrence of urinary BKV and JCV shedding.

In the case of our experimentation, one patient (from the D+/R- group; day 45) presented a urine BK viral load at approximately 10^3 copies/mL which was the highest number of polyomavirus copies observed throughout the study among all 10 participants. However, because the observed urinary BK viral load was under 10^7 copies/mL (the urine DNA level deemed significant and potentially predictive of a high risk for PVAN development; (Randhawa *et al.*, 2004; Saundh *et al.*, 2010; Tremolada *et al.*, 2010; Varella *et al.*, 2014)), there is no immediate cause for concern; unfortunately, this particular patient was unable to provide day 0 and 90 urine samples for further evaluation.

Perhaps the observed BKV and JCV replication was due to fluctuations in immune status; reportedly, within the first three months following transplantation (i.e. during the time of maximum immune suppression), kidney graft recipients are prone to polyomavirus reactivation (Vilchez & Kusne, 2006). Notably, despite the observed polyomavirus shedding on day 45 and to a lesser degree, day 90, there has been no indication of adverse effects in any of our pilot study participants. Likewise, donor:recipient CMV status did not appear to make a noticeable difference in regards to lytic polyomavirus replication, and with such a small sample cohort for this pilot study, the possibility of drawing any statistical conclusions from our results was ruled out. Furthermore, due to predominantly minimal and unsustained polyomaviruria among our renal transplant patient cohort, the analysis of cell surface receptors—associated with BKV and JCV entry and infection—was again waived.

CONCLUDING REMARKS

(i) BK and JC virus reactivation was observed with no immediately associated pathologies.

(ii) The currently adapted treatment regimen significantly limits herpesvirus reactivation within the first three months post-renal transplantation.

(iii) Renal transplant recipients do not serve as an adequate model to study herpesvirus reactivation.

Table 1. List of primers.

Primer	Sequence	Reference
ORF50P8.ChIP.OD(F) ORF50P8.ChIP.OD(R)	CTA CCG GCG ACT CAT TAA GC GTG GCT GCC TGG ACA GTA TT	(Dyson <i>et al.</i> , 2010)
qCMV.gB.F qCMV.gB.R	ACG ACC CGT GGT CAT CTT TA GCG GTG GTT GCC CAA CAG GA	(Habbal <i>et al.</i> , 2009)
qEBV.BALF5.F qEBV.BALF5.R	CGG AAG CCC TCT GGA CTT C CCC TGT TTA TCC GAT GGA ATG	(Fadavi, 2013)
BKV2.1.F BKV2.1.R	GCA GCT CCC AAA AAG CCA AA CTG GGT TTAGGA AGC ATT CTA	(Randhawa <i>et al.</i> , 2004)
JC-F1 JC-R1	GAA GAA CCC AAA AAC TAT TTG TTG AAA GCC TAA CTG GAG ACA ATC TAG AAT AAT AGT C	(Holman <i>et al.</i> , 2003)

Table 2. Urinary viral loads.

Renal Transplant Study Patients	BKV Copies (copies/mL)			JCV Copies (copies/mL)		
	Day 0	Day 45	Day 90	Day 0	Day 45	Day 90
D+/R+ 1	*No urine output			*No urine output	12.0	
D+/R+ 2						
D+/R+ 3			*No urine output		9.0	*No urine output
D+/R+ 4					19.0	
D+/R+ 5	*No urine output			*No urine output	516.0	32.0
D+/R- 1						
D+/R- 2					85.0	10.0
D+/R- 3	*No urine output	*No urine output		*No urine output	*No urine output	
D+/R- 4			314.0			
D+/R- 5	*No urine output	1206.0	*No urine output	*No urine output	6.0	*No urine output
*No urine output = no sample processed						
denotes viruria negative sample						

REFERENCES

- Abecassis, M., Bartlett, S. T., Collins, A. J., Davis, C. L., Delmonico, F. L., Friedewald, J. J., Hays, R., Howard, A., Jones, E., Leichtman, A. B., Merion, R. M., Metzger, R. A., Pradel, F., Schweitzer, E. J., Velez, R. L. & Gaston, R. S. (2008). Kidney transplantation as primary therapy for end-stage renal disease: a National Kidney Foundation/Kidney Disease Outcomes Quality Initiative (NKF/KDOQITM) conference. *Clin J Am Soc Nephrol* 3, 471-480.
- Acott, P. D. (2013). Natural killer cell response to BK virus infection in polyoma virus-associated nephropathy of renal transplant recipients. *Kidney Int* 84, 233-235.
- Akula, S. M., Ford, P. W., Whitman, A. G., Hamden, K. E., Bryan, B. A., Cook, P. P. & McCubrey, J. A. (2005). B-Raf-dependent expression of vascular endothelial growth factor-A in Kaposi sarcoma-associated herpesvirus-infected human B cells. *Blood* 105, 4516-4522.
- Akula, S. M., Ford, P. W., Whitman, A. G., Hamden, K. E., Shelton, J. G. & McCubrey, J. A. (2004). Raf promotes human herpesvirus-8 (HHV-8/KSHV) infection. *Oncogene* 23, 5227-5241.
- Akula, S. M., Naranatt, P. P., Walia, N. S., Wang, F. Z., Fegley, B. & Chandran, B. (2003). Kaposi's sarcoma-associated herpesvirus (human herpesvirus 8) infection of human fibroblast cells occurs through endocytosis. *J Virol* 77, 7978-7990.
- Akula, S. M., Pramod, N. P., Wang, F. Z. & Chandran, B. (2001a). Human herpesvirus 8 envelope-associated glycoprotein B interacts with heparan sulfate-like moieties. *Virology* 284, 235-249.

- Akula, S. M., Pramod, N. P., Wang, F. Z. & Chandran, B. (2002). Integrin alpha3beta1 (CD 49c/29) is a cellular receptor for Kaposi's sarcoma-associated herpesvirus (KSHV/HHV-8) entry into the target cells. *Cell* 108, 407-419.
- Akula, S. M., Wang, F. Z., Vieira, J. & Chandran, B. (2001b). Human herpesvirus 8 interaction with target cells involves heparan sulfate. *Virology* 282, 245-255.
- Alibek, K., Baiken, Y., Kakpenova, A., Mussabekova, A., Zhussupbekova, S., Akan, M. & Sultankulov, B. (2014). Implication of human herpesviruses in oncogenesis through immune evasion and suppression. *Infect Agent Cancer* 9, 3.
- Allen, U. D. & Preiksaitis, J. K. (2013). Epstein-Barr virus and posttransplant lymphoproliferative disorder in solid organ transplantation. *Am J Transplant* 13 Suppl 4, 107-120.
- Andreoni, M., Goletti, D., Pezzotti, P., Pozzetto, A., Monini, P., Sarmati, L., Farchi, F., Tisone, G., Piazza, A., Pisani, F., Angelico, M., Leone, P., Citterio, F., Ensoli, B. & Rezza, G. (2001). Prevalence, incidence and correlates of HHV-8/KSHV infection and Kaposi's sarcoma in renal and liver transplant recipients. *J Infect* 43, 195-199.
- Andrews, M. R., Czvitkovich, S., Dassie, E., Vogelaar, C. F., Faissner, A., Blits, B., Gage, F. H., French-Constant, C. & Fawcett, J. W. (2009). Alpha9 integrin promotes neurite outgrowth on tenascin-C and enhances sensory axon regeneration. *J Neurosci* 29, 5546-5557.
- Azadmanesh, K., Norouzfard, Z. S., Sohrabi, A., Safaie-Naraghi, Z., Moradi, A., Yaghmaei, P., Naraghi, M. M., Arashkia, A. & Eslamifar, A. (2012). Characterization of human herpes virus 8 genotypes in Kaposi's sarcoma patients in Tehran, Iran. *Int J Mol Epidemiol Genet* 3, 144-152.

- Backovic, M., Longnecker, R. & Jardetzky, T. S. (2009). Structure of a trimeric variant of the Epstein-Barr virus glycoprotein B. *Proc Natl Acad Sci U S A* 106, 2880-2885.
- Bandyopadhyay, C., Valiya-Veetil, M., Dutta, D., Chakraborty, S. & Chandran, B. (2014). CIB1 synergizes with EphrinA2 to regulate Kaposi's sarcoma-associated herpesvirus macropinocytic entry in human microvascular dermal endothelial cells. *PLoS Pathog* 10, e1003941.
- Barczyk, M., Carracedo, S. & Gullberg, D. (2010). Integrins. *Cell Tissue Res* 339, 269-280.
- Behzad-Behbahani, A., Klapper, P. E., Vallely, P. J., Cleator, G. M. & Khoo, S. H. (2004). Detection of BK virus and JC virus DNA in urine samples from immunocompromised (HIV-infected) and immunocompetent (HIV-non-infected) patients using polymerase chain reaction and microplate hybridisation. *J Clin Virol* 29, 224-229.
- Bergallo, M., Costa, C., Gribaudo, G., Tarallo, S., Baro, S., Negro Ponzi, A. & Cavallo, R. (2006). Evaluation of six methods for extraction and purification of viral DNA from urine and serum samples. *New Microbiol* 29, 111-119.
- Betsem, E., Cassar, O., Afonso, P. V., Fontanet, A., Froment, A. & Gessain, A. (2014). Epidemiology and genetic variability of HHV-8/KSHV in Pygmy and Bantu populations in Cameroon. *PLoS Negl Trop Dis* 8, e2851.
- Bhattacharyya, S., Warfield, K. L., Ruthel, G., Bavari, S., Aman, M. J. & Hope, T. J. (2010). Ebola virus uses clathrin-mediated endocytosis as an entry pathway. *Virology* 401, 18-28.
- Bhutani, M., Polizzotto, M. N., Uldrick, T. S. & Yarchoan, R. (2015). Kaposi sarcoma-associated herpesvirus-associated malignancies: epidemiology, pathogenesis, and advances in treatment. *Semin Oncol* 42, 223-246.

- Birkmann, A., Mahr, K., Ensser, A., Yaguboglu, S., Titgemeyer, F., Fleckenstein, B. & Neipel, F. (2001). Cell surface heparan sulfate is a receptor for human herpesvirus 8 and interacts with envelope glycoprotein K8.1. *J Virol* 75, 11583-11593.
- Biron, K. K. (2006). Antiviral drugs for cytomegalovirus diseases. *Antiviral Res* 71, 154-163.
- Bohannon, K. P., Jun, Y., Gross, S. P. & Smith, G. A. (2013). Differential protein partitioning within the herpesvirus tegument and envelope underlies a complex and variable virion architecture. *P Natl Acad Sci USA* 110, E1613-E1620.
- Bohl, D. L. & Brennan, D. C. (2007). BK virus nephropathy and kidney transplantation. *Clin J Am Soc Nephrol* 2 Suppl 1, S36-46.
- Boulant, S., Stanifer, M. & Lozach, P. Y. (2015). Dynamics of virus-receptor interactions in virus binding, signaling, and endocytosis. *Viruses* 7, 2794-2815.
- Braulke, T. & Bonifacino, J. S. (2009). Sorting of lysosomal proteins. *Biochim Biophys Acta* 1793, 605-614.
- Brown, J. C. & Newcomb, W. W. (2011). Herpesvirus capsid assembly: insights from structural analysis. *Curr Opin Virol* 1, 142-149.
- Bruce, A. G., Thouless, M. E., Haines, A. S., Pallen, M. J., Grundhoff, A. & Rose, T. M. (2015). Complete genome sequence of Pig-tailed macaque rhadinovirus 2 and its evolutionary relationship with rhesus macaque rhadinovirus and human herpesvirus 8/Kaposi's sarcoma-associated herpesvirus. *J Virol* 89, 3888-3909.
- Bryan, B. A., Dyson, O. F., McCubrey, J. A. & Akula, S. M. (2005). Biology of Kaposi's sarcoma-associated herpesvirus. *Front Biosci* 10, 2882-2891.

- Cabello, J., Esperon, F., Napolitano, C., Hidalgo, E., Davila, J. A. & Millan, J. (2013). Molecular identification of a novel gammaherpesvirus in the endangered Darwin's fox (*Lycalopex fulvipes*). *J Gen Virol* 94, 2745-2749.
- Cai, Q., Verma, S. C., Lu, J. & Robertson, E. S. (2010). Molecular biology of Kaposi's sarcoma-associated herpesvirus and related oncogenesis. *Adv Virus Res* 78, 87-142.
- Cancian, L., Hansen, A. & Boshoff, C. (2013). Cellular origin of Kaposi's sarcoma and Kaposi's sarcoma-associated herpesvirus-induced cell reprogramming. *Trends Cell Biol* 23, 421-432.
- Carbone, A., De Paoli, P., Gloghini, A. & Vaccher, E. (2015). KSHV-associated multicentric Castleman disease: A tangle of different entities requiring multitarget treatment strategies. *Int J Cancer* 137, 251-261.
- Casper, C., Krantz, E. M., Corey, L., Kuntz, S. R., Wang, J., Selke, S., Hamilton, S., Huang, M. L. & Wald, A. (2008). Valganciclovir for suppression of human herpesvirus-8 replication: a randomized, double-blind, placebo-controlled, crossover trial. *J Infect Dis* 198, 23-30.
- Cesarman, E., Chang, Y., Moore, P. S., Said, J. W. & Knowles, D. M. (1995). Kaposi's sarcoma-associated herpesvirus-like DNA sequences in AIDS-related body-cavity-based lymphomas. *N Engl J Med* 332, 1186-1191.
- Chakraborty, S., Veettil, M. V. & Chandran, B. (2012). Kaposi's Sarcoma Associated Herpesvirus Entry into Target Cells. *Front Microbiol* 3, 6.
- Chandran, B. (2010a). Early Events in Kaposi's Sarcoma-Associated Herpesvirus Infection of Target Cells. *Journal of Virology* 84, 2188-2199.

- Chandran, B. (2010b). Early events in Kaposi's sarcoma-associated herpesvirus infection of target cells. *J Virol* 84, 2188-2199.
- Chang, P. C. & Kung, H. J. (2014). SUMO and KSHV Replication. *Cancers (Basel)* 6, 1905-1924.
- Chang, Y., Cesarman, E., Pessin, M. S., Lee, F., Culpepper, J., Knowles, D. M. & Moore, P. S. (1994). Identification of herpesvirus-like DNA sequences in AIDS-associated Kaposi's sarcoma. *Science* 266, 1865-1869.
- Chang, Y. & Moore, P. (2014). Twenty years of KSHV. *Viruses* 6, 4258-4264.
- Chaudhary, N., Gomez, G. A., Howes, M. T., Lo, H. P., McMahon, K. A., Rae, J. A., Schieber, N. L., Hill, M. M., Gaus, K., Yap, A. S. & Parton, R. G. (2014). Endocytic crosstalk: cavins, caveolins, and caveolae regulate clathrin-independent endocytosis. *PLoS Biol* 12, e1001832.
- Chen, C., Huang, X., Atakilit, A., Zhu, Q. S., Corey, S. J. & Sheppard, D. (2006). The Integrin alpha9beta1 contributes to granulopoiesis by enhancing granulocyte colony-stimulating factor receptor signaling. *Immunity* 25, 895-906.
- Chen, J., Jiang, L., Lan, K. & Chen, X. (2015). Celecoxib Inhibits the Lytic Activation of Kaposi's Sarcoma-Associated Herpesvirus through Down-Regulation of RTA Expression by Inhibiting the Activation of p38 MAPK. *Viruses* 7, 2268-2287.
- Chen, K. H., Chen, T. D., Chen, C. W. & Lee, L. Y. (2014). Iatrogenic Kaposi's sarcoma in nasal cavity: a case report. *World J Surg Oncol* 12, 172.
- Costa, C. & Cavallo, R. (2012). Polyomavirus-associated nephropathy. *World J Transplant* 2, 84-94.

- Crabtree, K. L., Wojcicki, J. M., Minhas, V., Smith, D. R., Kankasa, C., Mitchell, C. D. & Wood, C. (2014). Risk factors for early childhood infection of human herpesvirus-8 in Zambian children: the role of early childhood feeding practices. *Cancer Epidemiol Biomarkers Prev* 23, 300-308.
- Cukuranovic, J., Ugrenovic, S., Jovanovic, I., Visnjic, M. & Stefanovic, V. (2012). Viral infection in renal transplant recipients. *ScientificWorldJournal* 2012, 820621.
- Davison, A. J. (2010). Herpesvirus systematics. *Vet Microbiol* 143, 52-69.
- Davison, A. J. (2011). Evolution of sexually transmitted and sexually transmissible human herpesviruses. *Annals of the New York Academy of Sciences* 1230, E37-49.
- Davison, A. J., Eberle, R., Ehlers, B., Hayward, G. S., McGeoch, D. J., Minson, A. C., Pellett, P. E., Roizman, B., Studdert, M. J. & Thiry, E. (2009). The order Herpesvirales. *Arch Virol* 154, 171-177.
- Deng, H., Young, A. & Sun, R. (2000). Auto-activation of the rta gene of human herpesvirus-8/Kaposi's sarcoma-associated herpesvirus. *J Gen Virol* 81, 3043-3048.
- Desiderio, U. V., Zhu, X. & Evans, J. P. (2010). ADAM2 interactions with mouse eggs and cell lines expressing alpha4/alpha9 (ITGA4/ITGA9) integrins: implications for integrin-based adhesion and fertilization. *PLoS One* 5, e13744.
- DiMaio, T. A., Gutierrez, K. D. & Lagunoff, M. (2011). Latent KSHV infection of endothelial cells induces integrin beta3 to activate angiogenic phenotypes. *PLoS Pathog* 7, e1002424.
- Dimitrov, D. S. (2004). Virus entry: molecular mechanisms and biomedical applications. *Nat Rev Microbiol* 2, 109-122.
- Dreyfus, D. H. (2013). Herpesviruses and the microbiome. *The Journal of allergy and clinical immunology* 132, 1278-1286.

- Dutta, D., Chakraborty, S., Bandyopadhyay, C., Valiya Veetil, M., Ansari, M. A., Singh, V. V. & Chandran, B. (2013). EphrinA2 regulates clathrin mediated KSHV endocytosis in fibroblast cells by coordinating integrin-associated signaling and c-Cbl directed polyubiquitination. *PLoS Pathog* 9, e1003510.
- Dyson, O. F., Oxendine, T. L., Hamden, K. E., Ford, P. W. & Akula, S. M. (2008). Differential regulation of the attachment of Kaposi's sarcoma-associated herpesvirus (KSHV)-infected human B cells to extracellular matrix by KSHV-encoded gB and cellular alphaV integrins. *Cell Microbiol* 10, 1546-1558.
- Dyson, O. F., Traylen, C. M. & Akula, S. M. (2010). Cell membrane-bound Kaposi's sarcoma-associated herpesvirus-encoded glycoprotein B promotes virus latency by regulating expression of cellular Egr-1. *J Biol Chem* 285, 37491-37502.
- Dyson, O. F., Walker, L. R., Whitehouse, A., Cook, P. P. & Akula, S. M. (2012). Resveratrol Inhibits KSHV Reactivation by Lowering the Levels of Cellular EGR-1. *PLoS One* 7, e33364.
- Einollahi, B. (2007). Kaposi sarcoma after kidney transplantation. *Iran J Kidney Dis* 1, 2-11.
- Engel, E. A., Song, R., Koyuncu, O. O. & Enquist, L. W. (2015). Investigating the biology of alpha herpesviruses with MS-based proteomics. *Proteomics* 15, 1943-1956.
- Estep, R. D. & Wong, S. W. (2013). Rhesus macaque rhadinovirus-associated disease. *Curr Opin Virol* 3, 245-250.
- Eto, K., Huet, C., Tarui, T., Kupriyanov, S., Liu, H. Z., Puzon-McLaughlin, W., Zhang, X. P., Sheppard, D., Engvall, E. & Takada, Y. (2002). Functional classification of ADAMs based on a conserved motif for binding to integrin alpha 9beta 1: implications for sperm-egg binding and other cell interactions. *J Biol Chem* 277, 17804-17810.

- Fadavi, P., Rostamian, M., Arashkia, A., Shafaghi, B., Niknam, H.M. (2013). Epstein-barr virus may not be associated with breast cancer in Iranian patients. *Oncology Discovery* 1.
- Fatahzadeh, M. (2012). Kaposi sarcoma: review and medical management update. *Oral Surg Oral Med Oral Pathol Oral Radiol* 113, 2-16.
- Fatahzadeh, M. & Schwartz, R. A. (2013). Oral Kaposi's sarcoma: a review and update. *Int J Dermatol* 52, 666-672.
- Feire, A. L., Koss, H. & Compton, T. (2004). Cellular integrins function as entry receptors for human cytomegalovirus via a highly conserved disintegrin-like domain. *Proc Natl Acad Sci U S A* 101, 15470-15475.
- Feire, A. L., Roy, R. M., Manley, K. & Compton, T. (2010). The glycoprotein B disintegrin-like domain binds beta 1 integrin to mediate cytomegalovirus entry. *J Virol* 84, 10026-10037.
- Fidan, I., Yesilyurt, E., Kalkanci, A., Aslan, S. O., Sahin, N., Ogan, M. C. & Dizbay, M. (2014). Immunomodulatory Effects of Voriconazole and Caspofungin on Human Peripheral Blood Mononuclear Cells Stimulated by *Candida albicans* and *Candida krusei*. *Am J Med Sci*.
- Fishman, J. A. (2013). Overview: cytomegalovirus and the herpesviruses in transplantation. *Am J Transplant* 13 Suppl 3, 1-8; quiz 8.
- Fotiadis, D., Kanai, Y. & Palacin, M. (2013). The SLC3 and SLC7 families of amino acid transporters. *Mol Aspects Med* 34, 139-158.
- Frappier, L. (2015). Regulation of herpesvirus reactivation by host microRNAs. *J Virol* 89, 2456-2458.

- Fu, B., Sun, F., Li, B., Yang, L., Zeng, Y., Sun, X., Xu, F., Rayner, S., Guadalupe, M., Gao, S. J. & Wang, L. (2009). Seroprevalence of Kaposi's sarcoma-associated herpesvirus and risk factors in Xinjiang, China. *J Med Virol* 81, 1422-1431.
- Fukumoto, H., Kanno, T., Hasegawa, H. & Katano, H. (2011). Pathology of Kaposi's Sarcoma-Associated Herpesvirus Infection. *Front Microbiol* 2, 175.
- Ganem, D. (1997). KSHV and Kaposi's sarcoma: the end of the beginning? *Cell* 91, 157-160.
- Ganem, D. (2010). KSHV and the pathogenesis of Kaposi sarcoma: listening to human biology and medicine. *J Clin Invest* 120, 939-949.
- Garces, J. C. (2010). BK Virus-Associated Nephropathy in Kidney Transplant Recipients. *Ochsner J* 10, 245-249.
- Garrigues, H. J., Rubinchikova, Y. E., Dipersio, C. M. & Rose, T. M. (2008). Integrin alphaVbeta3 Binds to the RGD motif of glycoprotein B of Kaposi's sarcoma-associated herpesvirus and functions as an RGD-dependent entry receptor. *J Virol* 82, 1570-1580.
- Garrigues, H. J., Rubinchikova, Y. E. & Rose, T. M. (2014). KSHV cell attachment sites revealed by ultra sensitive tyramide signal amplification (TSA) localize to membrane microdomains that are up-regulated on mitotic cells. *Virology* 452-453, 75-85.
- Gbabe, O. F., Okwundu, C. I., Dedicat, M. & Freeman, E. E. (2014). Treatment of severe or progressive Kaposi's sarcoma in HIV-infected adults. *Cochrane Database Syst Rev* 9, CD003256.
- Giffin, L. & Damania, B. (2014). KSHV: pathways to tumorigenesis and persistent infection. *Adv Virus Res* 88, 111-159.

- Gill, H., Hwang, Y. Y., Chan, T. S., Pang, A. W., Leung, A. Y., Tse, E. & Kwong, Y. L. (2014). Valganciclovir suppressed Epstein Barr virus reactivation during immunosuppression with alemtuzumab. *J Clin Virol* 59, 255-258.
- Grange, P. A., Gressier, L., Williams, J. F., Dyson, O. F., Akula, S. M. & Dupin, N. (2012). Cloning a Human Saliva-Derived Peptide for Preventing KSHV Transmission. *J Invest Dermatol*.
- Griffin, B. D., Verweij, M. C. & Wiertz, E. J. (2010). Herpesviruses and immunity: the art of evasion. *Vet Microbiol* 143, 89-100.
- Grose, C. & Adams, H. P. (2014). Reassessing the link between herpes zoster ophthalmicus and stroke. *Expert Rev Anti Infect Ther* 12, 527-530.
- Grove, J. & Marsh, M. (2011). The cell biology of receptor-mediated virus entry. *J Cell Biol* 195, 1071-1082.
- Guito, J. & Lukac, D. M. (2015). KSHV reactivation and novel implications of protein isomerization on lytic switch control. *Viruses* 7, 72-109.
- Guttman-Yassky, E., Dubnov, J., Kra-Oz, Z., Friedman-Birnbaum, R., Silbermann, M., Barchana, M., Bergman, R. & Sarid, R. (2006). Classic Kaposi sarcoma. Which KSHV-seropositive individuals are at risk? *Cancer* 106, 413-419.
- Habbal, W., Monem, F. & Gartner, B. C. (2009). Comparative evaluation of published cytomegalovirus primers for rapid real-time PCR: which are the most sensitive? *J Med Microbiol* 58, 878-883.
- Hahn, A., Birkmann, A., Wies, E., Dorer, D., Mahr, K., Sturzl, M., Titgemeyer, F. & Neipel, F. (2009). Kaposi's sarcoma-associated herpesvirus gH/gL: glycoprotein export and interaction with cellular receptors. *J Virol* 83, 396-407.

- Hahn, A. S. & Desrosiers, R. C. (2013). Rhesus monkey rhadinovirus uses eph family receptors for entry into B cells and endothelial cells but not fibroblasts. *PLoS Pathog* 9, e1003360.
- Hahn, A. S. & Desrosiers, R. C. (2014). Binding of the Kaposi's sarcoma-associated herpesvirus to the ephrin binding surface of the EphA2 receptor and its inhibition by a small molecule. *J Virol* 88, 8724-8734.
- Hahn, A. S., Kaufmann, J. K., Wies, E., Naschberger, E., Panteleev-Ivlev, J., Schmidt, K., Holzer, A., Schmidt, M., Chen, J., Konig, S., Ensser, A., Myoung, J., Brockmeyer, N. H., Sturzl, M., Fleckenstein, B. & Neipel, F. (2012). The ephrin receptor tyrosine kinase A2 is a cellular receptor for Kaposi's sarcoma-associated herpesvirus. *Nat Med* 18, 961-966.
- Hamden, K. E., Whitman, A. G., Ford, P. W., Shelton, J. G., McCubrey, J. A. & Akula, S. M. (2005). Raf and VEGF: emerging therapeutic targets in Kaposi's sarcoma-associated herpesvirus infection and angiogenesis in hematopoietic and nonhematopoietic tumors. *Leukemia* 19, 18-26.
- Hanson, L., Dishon, A. & Kotler, M. (2011). Herpesviruses that infect fish. *Viruses* 3, 2160-2191.
- Harley, C. A., Dasgupta, A. & Wilson, D. W. (2001). Characterization of herpes simplex virus-containing organelles by subcellular fractionation: role for organelle acidification in assembly of infectious particles. *J Virol* 75, 1236-1251.
- Hengge, U. R., Ruzicka, T., Tying, S. K., Stuschke, M., Roggendorf, M., Schwartz, R. A. & Seeber, S. (2002). Update on Kaposi's sarcoma and other HHV8 associated diseases. Part 1: epidemiology, environmental predispositions, clinical manifestations, and therapy. *Lancet Infect Dis* 2, 281-292.

- Hernaiz, B. & Alonso, C. (2010). Dynamin- and clathrin-dependent endocytosis in African swine fever virus entry. *J Virol* 84, 2100-2109.
- Hertel, L. (2011). Herpesviruses and intermediate filaments: close encounters with the third type. *Viruses* 3, 1015-1040.
- Hirsch, H. H. & Randhawa, P. (2013). BK polyomavirus in solid organ transplantation. *Am J Transplant* 13 Suppl 4, 179-188.
- Holman, C. J., van Burik, J. A., Hinrichs, S. H. & Balfour Jr, H. H., Jr. (2003). Specific detection of human BK polyomavirus in urine samples of immunocompromised patients. *Clin Diagn Lab Immunol* 10, 66-69.
- Huber, L. A., Pfaller, K. & Vietor, I. (2003). Organelle proteomics: implications for subcellular fractionation in proteomics. *Circ Res* 92, 962-968.
- Hussein, H. A., Walker, L. R., Abdel-Raouf, U. M., Desouky, S. A., Montasser, A. K. & Akula, S. M. (2015). Beyond RGD: virus interactions with integrins. *Arch Virol*.
- Ivanov, A. I. (2008). Pharmacological inhibition of endocytic pathways: is it specific enough to be useful? *Methods Mol Biol* 440, 15-33.
- Jenkins, F. J., Rowe, D. T. & Rinaldo, C. R., Jr. (2003). Herpesvirus infections in organ transplant recipients. *Clin Diagn Lab Immunol* 10, 1-7.
- Jenner, R. G. & Boshoff, C. (2002). The molecular pathology of Kaposi's sarcoma-associated herpesvirus. *Biochim Biophys Acta* 1602, 1-22.
- Jenner, R. G., Maillard, K., Cattini, N., Weiss, R. A., Boshoff, C., Wooster, R. & Kellam, P. (2003). Kaposi's sarcoma-associated herpesvirus-infected primary effusion lymphoma has a plasma cell gene expression profile. *Proc Natl Acad Sci U S A* 100, 10399-10404.

- Jha, H. C., Lu, J., Verma, S. C., Banerjee, S., Mehta, D. & Robertson, E. S. (2014). Kaposi's sarcoma-associated herpesvirus genome programming during the early stages of primary infection of peripheral blood mononuclear cells. *MBio* 5.
- Jin, L., Lohr, C. V., Vanarsdall, A. L., Baker, R. J., Moerdyk-Schauwecker, M., Levine, C., Gerlach, R. F., Cohen, S. A., Alvarado, D. E. & Rohrmann, G. F. (2008). Characterization of a novel alphaherpesvirus associated with fatal infections of domestic rabbits. *Virology* 378, 13-20.
- Kajumbula, H., Wallace, R. G., Zong, J. C., Hokello, J., Sussman, N., Simms, S., Rockwell, R. F., Pozos, R., Hayward, G. S. & Boto, W. (2006). Ugandan Kaposi's sarcoma-associated herpesvirus phylogeny: evidence for cross-ethnic transmission of viral subtypes. *Intervirology* 49, 133-143.
- Kaleeba, J. A. & Berger, E. A. (2006). Kaposi's sarcoma-associated herpesvirus fusion-entry receptor: cystine transporter xCT. *Science* 311, 1921-1924.
- Kaplan, L. D. (2013). Human herpesvirus-8: Kaposi sarcoma, multicentric Castleman disease, and primary effusion lymphoma. *Hematology Am Soc Hematol Educ Program* 2013, 103-108.
- Karamanou, M., Antoniou, C., Stratigos, A. J., Saridaki, Z. & Androutsos, G. (2013). The eminent dermatologist Moriz Kaposi (1837-1902) and the first description of idiopathic multiple pigmented sarcoma of the skin. *J BUON* 18, 1101-1105.
- Karuthu, S. & Blumberg, E. A. (2012). Common infections in kidney transplant recipients. *Clin J Am Soc Nephrol* 7, 2058-2070.

- Kati, S., Tsao, E. H., Gunther, T., Weidner-Glunde, M., Rothamel, T., Grundhoff, A., Kellam, P. & Schulz, T. F. (2013). Activation of the B cell antigen receptor triggers reactivation of latent Kaposi's sarcoma-associated herpesvirus in B cells. *J Virol* 87, 8004-8016.
- Ketteler, M., Kunter, U. & Floege, J. (2003). An update on herpes virus infections in graft recipients. *Nephrol Dial Transplant* 18, 1703-1706.
- Klepfish, A., Zuckermann, B. & Schattner, A. (2015). Primary effusion lymphoma in the absence of HIV infection--clinical presentation and management. *QJM* 108, 481-488.
- Koncarevic, S., Lossner, C., Kuhn, K., Prinz, T., Pike, I. & Zucht, H. D. (2014). In-depth profiling of the peripheral blood mononuclear cells proteome for clinical blood proteomics. *Int J Proteomics* 2014, 129259.
- Kotton, C. N. & Fishman, J. A. (2005). Viral infection in the renal transplant recipient. *J Am Soc Nephrol* 16, 1758-1774.
- Kramer, T. & Enquist, L. W. (2013). Directional spread of alphaherpesviruses in the nervous system. *Viruses* 5, 678-707.
- Krishnan, H. H., Naranatt, P. P., Smith, M. S., Zeng, L., Bloomer, C. & Chandran, B. (2004). Concurrent expression of latent and a limited number of lytic genes with immune modulation and antiapoptotic function by Kaposi's sarcoma-associated herpesvirus early during infection of primary endothelial and fibroblast cells and subsequent decline of lytic gene expression. *J Virol* 78, 3601-3620.
- Krug, L. T. & Pellett, P. E. (2014). Roseolovirus molecular biology: recent advances. *Curr Opin Virol* 9, 170-177.
- Kumari, P., Narayanan, S. & Kumar, H. (2015). Herpesviruses: interfering innate immunity by targeting viral sensing and interferon pathways. *Rev Med Virol* 25, 187-201.

- La Ferla, L., Pinzone, M. R., Nunnari, G., Martellotta, F., Lleshi, A., Tirelli, U., De Paoli, P., Berretta, M. & Cacopardo, B. (2013). Kaposi's sarcoma in HIV-positive patients: the state of art in the HAART-era. *Eur Rev Med Pharmacol Sci* 17, 2354-2365.
- Labo, N., Miley, W., Benson, C. A., Campbell, T. B. & Whitby, D. (2015). Epidemiology of Kaposi's sarcoma-associated herpesvirus in HIV-1-infected US persons in the era of combination antiretroviral therapy. *AIDS* 29, 1217-1225.
- Labo, N., Miley, W., Marshall, V., Gillette, W., Esposito, D., Bess, M., Turano, A., Uldrick, T., Polizzotto, M. N., Wyvill, K. M., Bagni, R., Yarchoan, R. & Whitby, D. (2014). Heterogeneity and breadth of host antibody response to KSHV infection demonstrated by systematic analysis of the KSHV proteome. *PLoS Pathog* 10, e1004046.
- Laskowski, R. A., Gerick, F. & Thornton, J. M. (2009). The structural basis of allosteric regulation in proteins. *FEBS Lett* 583, 1692-1698.
- Lepa, A. & Siwicki, A. K. (2012). Fish herpesvirus diseases: a short review of current knowledge. *Acta Veterinaria Brno* 81, 383-389.
- Li, J., Zhang, Q., Pang, Z., Wang, Y., Liu, Q., Guo, L. & Jiang, X. (2011). Identification of peptide sequences that target to the brain using in vivo phage display. *Amino Acids*.
- Li, Q., He, M., Zhou, F., Ye, F. & Gao, S. J. (2014). Activation of Kaposi's sarcoma-associated herpesvirus (KSHV) by inhibitors of class III histone deacetylases: identification of sirtuin 1 as a regulator of the KSHV life cycle. *J Virol* 88, 6355-6367.
- Li, Q., Wilkie, A. R., Weller, M., Liu, X. & Cohen, J. I. (2015). THY-1 Cell Surface Antigen (CD90) Has an Important Role in the Initial Stage of Human Cytomegalovirus Infection. *PLoS Pathog* 11, e1004999.

- Ling, P. D., Lednicky, J. A., Keitel, W. A., Poston, D. G., White, Z. S., Peng, R., Liu, Z., Mehta, S. K., Pierson, D. L., Rooney, C. M., Vilchez, R. A., Smith, E. O. & Butel, J. S. (2003). The dynamics of herpesvirus and polyomavirus reactivation and shedding in healthy adults: a 14-month longitudinal study. *J Infect Dis* 187, 1571-1580.
- Liu, X. F., Wang, X., Yan, S., Zhang, Z., Abecassis, M. & Hummel, M. (2013). Epigenetic control of cytomegalovirus latency and reactivation. *Viruses* 5, 1325-1345.
- Lopper, M. & Compton, T. (2002). Disulfide bond configuration of human cytomegalovirus glycoprotein B. *J Virol* 76, 6073-6082.
- Lu, D., Scully, M., Kakkar, V. & Lu, X. (2010). ADAM-15 disintegrin-like domain structure and function. *Toxins (Basel)* 2, 2411-2427.
- Lu, J., Jha, H. C., Verma, S. C., Sun, Z., Banerjee, S., Dzeng, R. & Robertson, E. S. (2014). Kaposi's sarcoma-associated herpesvirus-encoded LANA contributes to viral latent replication by activating phosphorylation of survivin. *J Virol* 88, 4204-4217.
- Makharoblidze, E., Goishvili, N., McHedlishvili, M. & Jangavadze, M. (2015). Primary Kaposi's sarcoma of the heart in non-immunodeficient patient: case report and literature review. *Diagn Pathol* 10, 111.
- Malope-Kgokong, B. I., Macphail, P., Mbisa, G., Ratshikhopha, E., Maskew, M., Stein, L., Sitas, F. & Whitby, D. (2010). Kaposi's Sarcoma Associated-Herpes Virus (KSHV) Seroprevalence in Pregnant Women in South Africa. *Infect Agent Cancer* 5, 14.
- Manz, T., Grotz, W., Orszagh, M., Volk, B., Kirste, G. & Neumann, H. P. (2001). A patient with neurological deficits and seizures after renal transplantation. *Nephrol Dial Transplant* 16, 631-633.

- Marinic, K., Sinchi, J., Gomez, M., Diaz, R., Grillo, S. & Habegger-de Sorrentino, A. (2014). Monitoring of BK virus in transplant patients of the renal unit of the Perrando Hospital, Chaco, Argentina. *Nefrologia* 34, 799-800.
- Mercer, J. & Greber, U. F. (2013). Virus interactions with endocytic pathways in macrophages and dendritic cells. *Trends Microbiol* 21, 380-388.
- Mercer, J., Schelhaas, M. & Helenius, A. (2010). Virus entry by endocytosis. *Annu Rev Biochem* 79, 803-833.
- Mettenleiter, T. C., Klupp, B. G. & Granzow, H. (2009). Herpesvirus assembly: an update. *Virus Res* 143, 222-234.
- Minhas, V. & Wood, C. (2014). Epidemiology and transmission of Kaposi's sarcoma-associated herpesvirus. *Viruses* 6, 4178-4194.
- Moore, P. S. & Chang, Y. (1995). Detection of herpesvirus-like DNA sequences in Kaposi's sarcoma in patients with and without HIV infection. *N Engl J Med* 332, 1181-1185.
- Moore, P. S. & Chang, Y. (2014). The conundrum of causality in tumor virology: the cases of KSHV and MCV. *Semin Cancer Biol* 26, 4-12.
- Morrison, B. J., Labo, N., Miley, W. J. & Whitby, D. (2015). Serodiagnosis for tumor viruses. *Semin Oncol* 42, 191-206.
- Mosam, A., Aboobaker, J. & Shaik, F. (2010). Kaposi's sarcoma in sub-Saharan Africa: a current perspective. *Curr Opin Infect Dis* 23, 119-123.
- Munawwar, A., Sharma, S. K., Gupta, S. & Singh, S. (2014). Seroprevalence and determinants of Kaposi sarcoma-associated human herpesvirus 8 in Indian HIV-infected males. *AIDS Res Hum Retroviruses* 30, 1192-1196.

- Myers, M. A., Davies, J. M., Tong, J. C., Whisstock, J., Scealy, M., Mackay, I. R. & Rowley, M. J. (2000). Conformational epitopes on the diabetes autoantigen GAD65 identified by peptide phage display and molecular modeling. *J Immunol* 165, 3830-3838.
- Nalwoga, A., Cose, S., Wakeham, K., Miley, W., Ndibazza, J., Drakeley, C., Elliott, A., Whitby, D. & Newton, R. (2015). Association between malaria exposure and Kaposi's sarcoma-associated herpes virus seropositivity in Uganda. *Trop Med Int Health* 20, 665-672.
- Naranatt, P. P., Akula, S. M., Zien, C. A., Krishnan, H. H. & Chandran, B. (2003). Kaposi's sarcoma-associated herpesvirus induces the phosphatidylinositol 3-kinase-PKC-zeta-MEK-ERK signaling pathway in target cells early during infection: implications for infectivity. *J Virol* 77, 1524-1539.
- Narayanan, K., Sim, E. U., Ravin, N. V. & Lee, C. W. (2009). Recombination between linear double-stranded DNA substrates in vivo. *Anal Biochem* 387, 139-141.
- Neipel, F., Albrecht, J. C. & Fleckenstein, B. (1998). Human herpesvirus 8--the first human Rhadinovirus. *J Natl Cancer Inst Monogr*, 73-77.
- Ohye, T., Inagaki, H., Ihira, M., Higashimoto, Y., Kato, K., Oikawa, J., Yagasaki, H., Niizuma, T., Takahashi, Y., Kojima, S., Yoshikawa, T. & Kurahashi, H. (2014). Dual roles for the telomeric repeats in chromosomally integrated human herpesvirus-6. *Sci Rep* 4, 4559.
- Orend, G. & Chiquet-Ehrismann, R. (2006). Tenascin-C induced signaling in cancer. *Cancer Lett* 244, 143-163.
- Ouyang, X., Zeng, Y., Fu, B., Wang, X., Chen, W., Fang, Y., Luo, M. & Wang, L. (2014). Genotypic analysis of Kaposi's sarcoma-associated herpesvirus from patients with Kaposi's sarcoma in Xinjiang, China. *Viruses* 6, 4800-4810.

- Owen, C. B., Hughes, D. J., Baquero-Perez, B., Berndt, A., Schumann, S., Jackson, B. R. & Whitehouse, A. (2014). Utilising proteomic approaches to understand oncogenic human herpesviruses (Review). *Mol Clin Oncol* 2, 891-903.
- Penkert, R. R. & Kalejta, R. F. (2011). Tegument protein control of latent herpesvirus establishment and animation. *Herpesviridae* 2, 3.
- Pinzone, M. R., Berretta, M., Cacopardo, B. & Nunnari, G. (2015). Epstein-barr virus- and Kaposi sarcoma-associated herpesvirus-related malignancies in the setting of human immunodeficiency virus infection. *Semin Oncol* 42, 258-271.
- Polizzotto, M. N., Uldrick, T. S., Hu, D. & Yarchoan, R. (2012). Clinical Manifestations of Kaposi Sarcoma Herpesvirus Lytic Activation: Multicentric Castleman Disease (KSHV-MCD) and the KSHV Inflammatory Cytokine Syndrome. *Front Microbiol* 3, 73.
- Purushothaman, P., Uppal, T. & Verma, S. C. (2015). Molecular biology of KSHV lytic reactivation. *Viruses* 7, 116-153.
- Radu, O. & Pantanowitz, L. (2013). Kaposi sarcoma. *Arch Pathol Lab Med* 137, 289-294.
- Raghu, H., Sharma-Walia, N., Veettil, M. V., Sadagopan, S. & Chandran, B. (2009). Kaposi's sarcoma-associated herpesvirus utilizes an actin polymerization-dependent macropinocytic pathway to enter human dermal microvascular endothelial and human umbilical vein endothelial cells. *J Virol* 83, 4895-4911.
- Randhawa, P., Ho, A., Shapiro, R., Vats, A., Swalsky, P., Finkelstein, S., Uhrmacher, J. & Weck, K. (2004). Correlates of quantitative measurement of BK polyomavirus (BKV) DNA with clinical course of BKV infection in renal transplant patients. *J Clin Microbiol* 42, 1176-1180.

- Rappocciolo, G., Hensler, H. R., Jais, M., Reinhart, T. A., Pegu, A., Jenkins, F. J. & Rinaldo, C. R. (2008). Human herpesvirus 8 infects and replicates in primary cultures of activated B lymphocytes through DC-SIGN. *J Virol* 82, 4793-4806.
- Rappocciolo, G., Jenkins, F. J., Hensler, H. R., Piazza, P., Jais, M., Borowski, L., Watkins, S. C. & Rinaldo, C. R., Jr. (2006). DC-SIGN is a receptor for human herpesvirus 8 on dendritic cells and macrophages. *J Immunol* 176, 1741-1749.
- Razonable, R. R., Brown, R. A., Humar, A., Covington, E., Alecock, E. & Paya, C. V. (2005). Herpesvirus infections in solid organ transplant patients at high risk of primary cytomegalovirus disease. *J Infect Dis* 192, 1331-1339.
- Regnier-Rosencher, E., Guillot, B. & Dupin, N. (2013). Treatments for classic Kaposi sarcoma: a systematic review of the literature. *J Am Acad Dermatol* 68, 313-331.
- Repnik, U., Cesen, M. H. & Turk, B. (2013). The endolysosomal system in cell death and survival. *Cold Spring Harb Perspect Biol* 5, a008755.
- Rescigno, P., Di Trolino, R., Buonerba, C., De Fata, G., Federico, P., Bosso, D., Virtuoso, A., Izzo, M., Policastro, T., Vaccaro, L., Cimmino, G., Perri, F., Matano, E., Delfino, M., De Placido, S., Palmieri, G. & Di Lorenzo, G. (2013). Non-AIDS-related Kaposi's sarcoma: A single-institution experience. *World J Clin Oncol* 4, 52-57.
- Restrepo, C. S. & Ocazonez, D. (2011). Kaposi's sarcoma: imaging overview. *Semin Ultrasound CT MR* 32, 456-469.
- Robey, R. C. & Bower, M. (2015). Facing up to the ongoing challenge of Kaposi's sarcoma. *Curr Opin Infect Dis* 28, 31-40.
- Ruoslahti, E. (1996). RGD and other recognition sequences for integrins. *Annu Rev Cell Dev Biol* 12, 697-715.

- Russo, J. J., Bohenzky, R. A., Chien, M. C., Chen, J., Yan, M., Maddalena, D., Parry, J. P., Peruzzi, D., Edelman, I. S., Chang, Y. & Moore, P. S. (1996). Nucleotide sequence of the Kaposi sarcoma-associated herpesvirus (HHV8). *Proc Natl Acad Sci U S A* 93, 14862-14867.
- Saggar, S., Zeichner, J. A., Brown, T. T., Phelps, R. G. & Cohen, S. R. (2008). Kaposi's sarcoma resolves after sirolimus therapy in a patient with pemphigus vulgaris. *Arch Dermatol* 144, 654-657.
- Sakakibara, S. & Tosato, G. (2014). Contribution of viral mimics of cellular genes to KSHV infection and disease. *Viruses* 6, 3472-3486.
- Saundh, B. K., Tibble, S., Baker, R., Sasnauskas, K., Harris, M. & Hale, A. (2010). Different patterns of BK and JC polyomavirus reactivation following renal transplantation. *J Clin Pathol* 63, 714-718.
- Schwartz, R. A., Micali, G., Nasca, M. R. & Scuderi, L. (2008). Kaposi sarcoma: a continuing conundrum. *J Am Acad Dermatol* 59, 179-206; quiz 207-178.
- Selistre-de-Araujo, H. S., Pontes, C. L., Montenegro, C. F. & Martin, A. C. (2010). Snake venom disintegrins and cell migration. *Toxins (Basel)* 2, 2606-2621.
- Shiels, M. S., Pfeiffer, R. M., Hall, H. I., Li, J., Goedert, J. J., Morton, L. M., Hartge, P. & Engels, E. A. (2011). Proportions of Kaposi sarcoma, selected non-Hodgkin lymphomas, and cervical cancer in the United States occurring in persons with AIDS, 1980-2007. *JAMA* 305, 1450-1459.
- Simonart, T. (2006). Role of environmental factors in the pathogenesis of classic and African-endemic Kaposi sarcoma. *Cancer Lett* 244, 1-7.

- Sin, S. H. & Dittmer, D. P. (2013). Viral latency locus augments B-cell response in vivo to induce chronic marginal zone enlargement, plasma cell hyperplasia, and lymphoma. *Blood* 121, 2952-2963.
- Singh, N. (2005). Late-onset cytomegalovirus disease as a significant complication in solid organ transplant recipients receiving antiviral prophylaxis: a call to heed the mounting evidence. *Clin Infect Dis* 40, 704-708.
- Singh, P., Cartwright, L. & Visperas, C. (2014). African Kaposi's sarcoma in the light of global AIDS: antiblackness and viral visibility. *J Bioeth Inq* 11, 467-478.
- Sivakumar, R., Sharma-Walia, N., Raghu, H., Veetil, M. V., Sadagopan, S., Bottero, V., Varga, L., Levine, R. & Chandran, B. (2008). Kaposi's sarcoma-associated herpesvirus induces sustained levels of vascular endothelial growth factors A and C early during in vitro infection of human microvascular dermal endothelial cells: biological implications. *J Virol* 82, 1759-1776.
- Smith, C. M., Rosa, G. T., May, J. S., Bennett, N. J., Mount, A. M., Belz, G. T. & Stevenson, P. G. (2006). CD4+ T cells specific for a model latency-associated antigen fail to control a gammaherpesvirus in vivo. *Eur J Immunol* 36, 3186-3197.
- Snyder, J. J., Israni, A. K., Peng, Y., Zhang, L., Simon, T. A. & Kasiske, B. L. (2009). Rates of first infection following kidney transplant in the United States. *Kidney Int* 75, 317-326.
- Soulier, J., Grollet, L., Oksenhendler, E., Cacoub, P., Cazals-Hatem, D., Babinet, P., d'Agay, M. F., Clauvel, J. P., Raphael, M., Degos, L. & et al. (1995). Kaposi's sarcoma-associated herpesvirus-like DNA sequences in multicentric Castleman's disease. *Blood* 86, 1276-1280.

- Spadavecchia, S., Gonzalez-Lopez, O., Carroll, K. D., Palmeri, D. & Lukac, D. M. (2010).
Convergence of Kaposi's sarcoma-associated herpesvirus reactivation with Epstein-Barr
virus latency and cellular growth mediated by the notch signaling pathway in coinfecting
cells. *J Virol* 84, 10488-10500.
- Speck, S. H. & Ganem, D. (2010). Viral latency and its regulation: lessons from the gamma-
herpesviruses. *Cell Host Microbe* 8, 100-115.
- Spiller, O. B., Mark, L., Blue, C. E., Proctor, D. G., Aitken, J. A., Blom, A. M. & Blackbourn, D.
J. (2006). Dissecting the regions of virion-associated Kaposi's sarcoma-associated
herpesvirus complement control protein required for complement regulation and cell
binding. *J Virol* 80, 4068-4078.
- Steitz, J., Borah, S., Cazalla, D., Fok, V., Lytle, R., Mitton-Fry, R., Riley, K. & Samji, T. (2011).
Noncoding RNPs of viral origin. *Cold Spring Harb Perspect Biol* 3.
- Sun, R., Lin, S. F., Staskus, K., Gradoville, L., Grogan, E., Haase, A. & Miller, G. (1999).
Kinetics of Kaposi's sarcoma-associated herpesvirus gene expression. *J Virol* 73, 2232-
2242.
- Szajerka, T. & Jablecki, J. (2007). Kaposi's sarcoma revisited. *AIDS Rev* 9, 230-236.
- Tanenbaum, N. D., Alla, S. B. & Brennan, D. C. (2007). Herpesviruses and polyomaviruses in
renal transplantation. *Minerva Urol Nefrol* 59, 353-365.
- Tang, H. & Mori, Y. (2010). Human herpesvirus-6 entry into host cells. *Future Microbiol* 5,
1015-1023.
- Tang, Q., Qin, D., Lv, Z., Zhu, X., Ma, X., Yan, Q., Zeng, Y., Guo, Y., Feng, N. & Lu, C.
(2012). Herpes simplex virus type 2 triggers reactivation of Kaposi's sarcoma-associated
herpesvirus from latency and collaborates with HIV-1 Tat. *PLoS One* 7, e31652.

- Traylen, C. M., Patel, H. R., Fondaw, W., Mahatme, S., Williams, J. F., Walker, L. R., Dyson, O. F., Arce, S. & Akula, S. M. (2011). Virus reactivation: a panoramic view in human infections. *Future Virol* 6, 451-463.
- Tremolada, S., Delbue, S., Castagnoli, L., Allegrini, S., Miglio, U., Boldorini, R., Elia, F., Gordon, J. & Ferrante, P. (2010). Mutations in the external loops of BK virus VP1 and urine viral load in renal transplant recipients. *J Cell Physiol* 222, 195-199.
- Trempe, F., Gravel, A., Dubuc, I., Wallaschek, N., Collin, V., Gilbert-Girard, S., Morissette, G., Kaufer, B. B. & Flamand, L. (2015). Characterization of human herpesvirus 6A/B U94 as ATPase, helicase, exonuclease and DNA-binding proteins. *Nucleic Acids Res* 43, 6084-6098.
- Ueda, K., Ohsaki, E., Nakano, K. & Zheng, X. (2011). Characterization of Kaposi's Sarcoma-Associated Herpesvirus-Related Lymphomas by DNA Microarray Analysis. *Leuk Res Treatment* 2011, 726964.
- Uldrick, T. S., Polizzotto, M. N. & Yarchoan, R. (2012). Recent advances in Kaposi sarcoma herpesvirus-associated multicentric Castleman disease. *Curr Opin Oncol* 24, 495-505.
- Uppal, T., Banerjee, S., Sun, Z., Verma, S. C. & Robertson, E. S. (2014). KSHV LANA--the master regulator of KSHV latency. *Viruses* 6, 4961-4998.
- Uppal, T., Jha, H. C., Verma, S. C. & Robertson, E. S. (2015). Chromatinization of the KSHV Genome During the KSHV Life Cycle. *Cancers (Basel)* 7, 112-142.
- van Bogaert, L. J. (2012). Anogenital Lesions: Kaposi's Sarcoma and Its Mimicks. *ISRN AIDS* 2012, 486425.
- Van den Broeke, C., Jacob, T. & Favoreel, H. W. (2014). Rho'ing in and out of cells: viral interactions with Rho GTPase signaling. *Small GTPases* 5, e28318.

- Varella, R. B., Almeida, J. R., Lopes Pde, F., Matos, J. P., Menezes, P. & Lugon, J. R. (2014). BK polyomavirus in kidney transplant recipients: screening, monitoring and clinical management. *J Bras Nefrol* 36, 529-534.
- Veetil, M. V., Bandyopadhyay, C., Dutta, D. & Chandran, B. (2014). Interaction of KSHV with host cell surface receptors and cell entry. *Viruses* 6, 4024-4046.
- Veetil, M. V., Sadagopan, S., Sharma-Walia, N., Wang, F. Z., Raghu, H., Varga, L. & Chandran, B. (2008). Kaposi's sarcoma-associated herpesvirus forms a multimolecular complex of integrins (alphaVbeta5, alphaVbeta3, and alpha3beta1) and CD98-xCT during infection of human dermal microvascular endothelial cells, and CD98-xCT is essential for the postentry stage of infection. *J Virol* 82, 12126-12144.
- Vieira, J., O'Hearn, P., Kimball, L., Chandran, B. & Corey, L. (2001). Activation of Kaposi's sarcoma-associated herpesvirus (human herpesvirus 8) lytic replication by human cytomegalovirus. *J Virol* 75, 1378-1386.
- Vilchez, R. A. & Kusne, S. (2006). Molecular and clinical perspectives of polyomaviruses: emerging evidence of importance in non-kidney transplant populations. *Liver Transpl* 12, 1457-1463.
- Vlahakis, N. E., Young, B. A., Atakilit, A. & Sheppard, D. (2005). The lymphangiogenic vascular endothelial growth factors VEGF-C and -D are ligands for the integrin alpha9beta1. *J Biol Chem* 280, 4544-4552.
- Vonderheit, A. & Helenius, A. (2005). Rab7 associates with early endosomes to mediate sorting and transport of Semliki forest virus to late endosomes. *PLoS Biol* 3, e233.

- Walker, L. R., Hussein, H. A. & Akula, S. M. (2014). Disintegrin-like domain of glycoprotein B regulates Kaposi's sarcoma-associated herpesvirus infection of cells. *J Gen Virol* 95, 1770-1782.
- Wanas, E., Efler, S., Ghosh, K. & Ghosh, H. P. (1999). Mutations in the conserved carboxy-terminal hydrophobic region of glycoprotein gB affect infectivity of herpes simplex virus. *J Gen Virol* 80 (Pt 12), 3189-3198.
- Wang, F. Z., Akula, S. M., Pramod, N. P., Zeng, L. & Chandran, B. (2001). Human herpesvirus 8 envelope glycoprotein K8.1A interaction with the target cells involves heparan sulfate. *J Virol* 75, 7517-7527.
- Wang, F. Z., Akula, S. M., Sharma-Walia, N., Zeng, L. & Chandran, B. (2003). Human herpesvirus 8 envelope glycoprotein B mediates cell adhesion via its RGD sequence. *J Virol* 77, 3131-3147.
- Waugh, M. G., Chu, K. M., Clayton, E. L., Minogue, S. & Hsuan, J. J. (2011). Detergent-free isolation and characterization of cholesterol-rich membrane domains from trans-Golgi network vesicles. *J Lipid Res* 52, 582-589.
- Weikert, B. C. & Blumberg, E. A. (2008). Viral infection after renal transplantation: surveillance and management. *Clin J Am Soc Nephrol* 3 Suppl 2, S76-86.
- Weinberger, A. D. & Weinberger, L. S. (2013). Stochastic fate selection in HIV-infected patients. *Cell* 155, 497-499.
- Wen, V. W. & MacKenzie, K. L. (2013). Modeling human endothelial cell transformation in vascular neoplasias. *Dis Model Mech* 6, 1066-1079.

- White, T., Hagen, M., Gudza, I., White, I. E., Ndemera, B., Gwanzura, L., Borok, M. & Campbell, T. B. (2008). Genetic diversity of the Kaposi's sarcoma herpesvirus K1 protein in AIDS-KS in Zimbabwe. *J Clin Virol* 42, 165-171.
- Wiseman, A. C. (2009). Polyomavirus nephropathy: a current perspective and clinical considerations. *Am J Kidney Dis* 54, 131-142.
- Wolf, M., Deal, E. M. & Greenberg, H. B. (2012). Rhesus rotavirus trafficking during entry into MA104 cells is restricted to the early endosome compartment. *J Virol* 86, 4009-4013.
- Wolfsberg, T. G., Straight, P. D., Gerena, R. L., Huovila, A. P., Primakoff, P., Myles, D. G. & White, J. M. (1995). ADAM, a widely distributed and developmentally regulated gene family encoding membrane proteins with a disintegrin and metalloprotease domain. *Dev Biol* 169, 378-383.
- Wu, C., Chung, A. E. & McDonald, J. A. (1995). A novel role for alpha 3 beta 1 integrins in extracellular matrix assembly. *J Cell Sci* 108 (Pt 6), 2511-2523.
- Wu, X., Zhou, L., Zhao, X. & Tan, Z. (2014). The analysis of microsatellites and compound microsatellites in 56 complete genomes of Herpesvirales. *Gene (Amsterdam)* 551, 103-109.
- Yakushko, Y., Hackmann, C., Gunther, T., Ruckert, J., Henke, M., Koste, L., Alkharsah, K., Bohne, J., Grundhoff, A., Schulz, T. F. & Henke-Gendo, C. (2011). Kaposi's sarcoma-associated herpesvirus bacterial artificial chromosome contains a duplication of a long unique-region fragment within the terminal repeat region. *J Virol* 85, 4612-4617.
- Yamauchi, Y. & Helenius, A. (2013a). Virus entry at a glance. *Journal of cell science* 126, 1289-1295.
- Yamauchi, Y. & Helenius, A. (2013b). Virus entry at a glance. *J Cell Sci* 126, 1289-1295.

- Yang, J. Y., Zong, C. S., Xia, W., Wei, Y., Ali-Seyed, M., Li, Z., Broglio, K., Berry, D. A. & Hung, M. C. (2006). MDM2 promotes cell motility and invasiveness by regulating E-cadherin degradation. *Mol Cell Biol* 26, 7269-7282.
- Yang, W. S., Hsu, H. W., Campbell, M., Cheng, C. Y. & Chang, P. C. (2015). K-bZIP Mediated SUMO-2/3 Specific Modification on the KSHV Genome Negatively Regulates Lytic Gene Expression and Viral Reactivation. *PLoS Pathog* 11, e1005051.
- Ye, F., Lei, X. & Gao, S. J. (2011). Mechanisms of Kaposi's Sarcoma-Associated Herpesvirus Latency and Reactivation. *Adv Virol* 2011.
- Yokosaki, Y., Palmer, E. L., Prieto, A. L., Crossin, K. L., Bourdon, M. A., Pytela, R. & Sheppard, D. (1994). The integrin alpha 9 beta 1 mediates cell attachment to a non-RGD site in the third fibronectin type III repeat of tenascin. *J Biol Chem* 269, 26691-26696.
- Young, B. A., Taooka, Y., Liu, S., Askins, K. J., Yokosaki, Y., Thomas, S. M. & Sheppard, D. (2001). The cytoplasmic domain of the integrin alpha9 subunit requires the adaptor protein paxillin to inhibit cell spreading but promotes cell migration in a paxillin-independent manner. *Mol Biol Cell* 12, 3214-3225.
- Yu, G. Y. & Lai, M. M. (2005). The ubiquitin-proteasome system facilitates the transfer of murine coronavirus from endosome to cytoplasm during virus entry. *J Virol* 79, 644-648.
- Zaichick, S. V., Bohannon, K. P. & Smith, G. A. (2011). Alphaherpesviruses and the Cytoskeleton in Neuronal Infections. *Viruses-Basel* 3, 941-981.
- Zhang, T., Yang, Y., Yu, F., Zhao, Y., Lin, F., Minhas, V., Wood, C. & He, N. (2014). Kaposi's sarcoma associated herpesvirus infection among female sex workers and general population women in Shanghai, China: a cross-sectional study. *BMC Infect Dis* 14, 58.

- Zhang, W. & Gao, S. J. (2012). Exploitation of Cellular Cytoskeletons and Signaling Pathways for Cell Entry by Kaposi's Sarcoma-Associated Herpesvirus and the Closely Related Rhesus Rhadinovirus. *Pathogens* 1, 102-127.
- Zhang, X., Wang, J. F., Chandran, B., Persaud, K., Pytowski, B., Fingerroth, J. & Groopman, J. E. (2005). Kaposi's sarcoma-associated herpesvirus activation of vascular endothelial growth factor receptor 3 alters endothelial function and enhances infection. *J Biol Chem* 280, 26216-26224.
- Zhao, H., Ruberu, K., Li, H. & Garner, B. (2013). Analysis of subcellular [⁵⁷Co] cobalamin distribution in SH-SY5Y neurons and brain tissue. *J Neurosci Methods* 217, 67-74.
- Zong, J. C., Ciuffo, D. M., Alcendor, D. J., Wan, X., Nicholas, J., Browning, P. J., Rady, P. L., Tying, S. K., Orenstein, J. M., Rabkin, C. S., Su, I. J., Powell, K. F., Croxson, M., Foreman, K. E., Nickoloff, B. J., Alkan, S. & Hayward, G. S. (1999). High-level variability in the ORF-K1 membrane protein gene at the left end of the Kaposi's sarcoma-associated herpesvirus genome defines four major virus subtypes and multiple variants or clades in different human populations. *J Virol* 73, 4156-4170.

APPENDIX A: SUPPLEMENTARY DATA FROM CHAPTERS 2

METHODS

Cells. Human foreskin fibroblasts (HFF) and 293 cells were propagated in Dulbecco modified Eagle medium (DMEM) while, human vascular endothelial cells-dermal (HMVEC-Ds, CC-2543; Clonetics) were propagated in EGM MV-microvascular endothelial cell medium (Clonetics) (Akula *et al.*, 2005). *Spodoptera frugiperda* ovarian cells (Sf9) were routinely cultured in TNM-FH insect medium (BD Biosciences/PharMingen, San Diego, CA). For studies involving expression and purification of soluble gB proteins, cells were cultured in Gibco® Sf-900™ III SFM (Invitrogen, Carlsbad, CA).

Proteins. Heparan sulfate (HS), chondroitin sulfate A (CSA), chondroitin sulfate B (CSB) (Sigma, St. Louis, MO), human recombinant vascular endothelial growth factor (VEGF) (Calbiochem; EMD, Darmstadt, Germany), recombinant human tenascin C (R & D Systems, Inc., Minneapolis, MN), human laminin (Sigma), recombinant human integrin $\alpha 9\beta 1$, $\alpha V\beta 3$ (R & D Systems, Inc.) and $\alpha 5\beta 1$ for functional studies (Millipore) were used in various molecular biology and enzyme-linked immunosorbent assays (ELISAs)/binding assays performed in this study.

Peptides. Peptide sequence (geeasgpksvdfyqf**RVCSASITGELFRFNLEQTC**pdtkdkyhqegillv; DLD sequence is bolded) flanking the DLD in KSHV encoded gB protein (gBDLD); phage carrying peptides, PKADGRV, DCKPKPDGRLRD, PKADGHV; and a scrambled peptide sequence of GPDRVKA was synthesized at Pi Proteomics, LLC (Huntsville, AL). The gBDLD peptide was used in the screening of phage display peptide libraries and ELISA. GRGDSP and KQAGDV peptides from Sigma (St. Louis, MO) were also used in ELISAs.

Cloning and expression of recombinant gB Δ TM Δ D. His-tagged, recombinant, and soluble KSHV gB Δ TM (2106bp; encoding amino acids 1-702 lacking the transmembrane and cytoplasmic domains) was expressed and purified from Sf9 cells as per earlier studies (Dyson *et al.*, 2010; Wang *et al.*, 2003). The gB Δ TM lacking the DLD (gB Δ TM Δ D) mutant was generated by mutating four of the existing DLD amino acids (geeasgpksvdfyqf**RVCSASITGELFRFNLEQTC**pdtkdkyhqegillv; DLD sequence is in bold) of KSHV gB to alanine (GCG) (geeasgpksvdfyqfRVCSASITGE**AAA**ANLEQTCpdtkdkyhqegillv; alanine point mutations are bolded) (Fig. 1). The point mutations within the DLD sequence of KSHV gB were achieved by using the gB Δ TM/pCDNA3.1(+) plasmid as the dsDNA template and appropriate primers: DLD-M2 forward (5'-TCGATCACCGGGGAGG**CGGCGGCGGCG**GAACCTGGAGCAGACG-3'; bolded region depicts the alanine point mutations to DLD, coding strand) and DLD-M2 reverse (5'-CGTCTGCTCCAGGTTCCGCC**CGCCG**CCTCCCCGGTGATCGA-3'; bolded region depicts the alanine point mutations to DLD, non-coding strand); along with the QuikChange XL site-directed mutagenesis kit (Stratagene, La Jolla, CA) as per the manufacturer's recommendations to yield the gB Δ TM Δ DLD.M2/pCDNA3.1(+). To develop His-tagged (at the carboxy-terminal) gB Δ TM Δ D, the gB Δ TM Δ DLD.M2/ pCDNA3.1(+) plasmid was amplified using primers: pHHV8gB(F): 5'-AGTGAGGATCCACAATGACTCCCAGG-3' and ORF8.HIS(R): 5'-TCCGAATTCTCAATGATGATGATGATGATGGCCACCCAGGTCCGCCACTATCTC-3'. The amplified gene encoding his-tagged gB Δ TM Δ D was cloned into the pCR $\text{\textcircled{R}}$ 8/GW/TOPO $\text{\textcircled{R}}$ vector and expressed in a BaculoDirect TM baculovirus expression system using Gateway $\text{\textcircled{R}}$ technology (Invitrogen, Carlsbad, CA) according to the manufacturer's instructions. Recombinant viruses were passaged a minimum of two times before use. His-tagged

gBΔTMΔD was expressed in Sf9 cells, the supernatant was harvested on the fifth day, and the proteins were purified using a column containing nickel-nitrilotriacetic acid (Ni-NTA) agarose beads (5 Prime, Inc., Gaithersburg, MD) as per lab procedures. The protein purity was analyzed by Coomassie staining of sodium dodecyl sulfate (SDS)-10% polyacrylamide gel electrophoresis (PAGE) gels, and detection following standard Western blotting procedures.

Screening phage display peptide libraries to determine a novel receptor for gB. We used Ph.D phage display libraries (New England Biolabs, Ipswich, MA) to identify novel ligands for the DLD in KSHV gB. The system was constructed based on a M13 bacteriophage vector, in which displayed peptides were fused at the N terminus of the minor coat protein pIII. *E. coli* ER2738 (included in the kit) was used for M13 phage propagation (Li *et al.*, 2011). Three random peptide libraries (New England Biolabs), a linear (X)7, a cyclic Cys (X)7 Cys, and a linear (X)12 were screened by panning against the gBDLD peptide corresponding to the DLD in gB as per recommendations of the manufacturer. After 5 binding/amplification enrichment cycles, individual phage clones were analyzed by ELISA (Myers *et al.*, 2000) on wells containing the immobilized peptide representing the DLD in gB or negative wells containing an irrelevant peptide. For clones producing a signal only in receptor-containing wells, the phage DNA were sent for sequencing (Laragen, Inc., Culver City, CA).

Phage carrying peptides containing a majorly conserved sequence were further analyzed to determine their ability to bind soluble gB immobilized on 96 well plates. In brief, aliquots containing 2×10^{11} plaque forming units (PFU) were screened against immobilized proteins (1μg/ml of gBΔTM and the bovine serum albumin, BSA, as the negative control) as per recommendations of the manufacturer. Unbound phage particles were washed away with TBST

(TBS + 0.1% [v/v] Tween-20), and the bound phage were eluted in 100 μ l volumes and titrated in *E. coli* host strain ER2738.

ELISA. To characterize the binding interactions between soluble gB and integrin α 9, ELISA was performed. Briefly, high-binding 96-well plates were coated with gB Δ TM, gB Δ TM Δ D, or non-specific controls, BSA or glutathione-S-transferase (GST) in 100mM bicarbonate/carbonate coating buffer overnight at 4°C. Plates were washed five times with 0.1% Tween 20-PBS, blocked for 30min with 1% BSA blocking solution containing 0.1% Tween 20, washed five times, and incubated at room temperature (RT) for 30min with different concentrations of recombinant human integrin α 9 β 1 in PBS. Plates were again washed five times and incubated at RT for 1h with human integrin α 9 antibodies, followed by a 1h RT incubation with goat anti-rabbit horseradish peroxidase (or goat anti-mouse horseradish peroxidase). After reaction with 3,3',5,5'-Tetramethylbenzidine substrate, the reaction was stopped by 1N HCl and read at 450nm. For further analysis of the gB: α 9 β 1 binding interactions, various competition ELISAs were performed using different concentrations of HS, VEGF, tenascin C, and anti-DLD IgGs.

Generating recombinant KSHV. We generated recombinant KSHV with mutation in the *orf8* gene encoding gB by employing a combination of overlap PCR and site-directed mutagenesis in a BAC system. As schematically shown in Fig. 6A, a three step process was conducted to generate the 4005bp target-3 PCR product corresponding to the *orf8* gene with flanking sequences. Initially, target-1 and -2 were amplified using appropriate primers (Table 1) using Bac36 genome (*accession number HQ404500.1*) as the template. Overlap PCR was conducted to amplify target-3 (Fig. 6B) from elution-purified target-1 and target-2 (Fig. 6B) overlapping (17bp overlap) DNA fragments using appropriate primers (Table 1). Gel purified target-3 was cloned into the *PCR XL*

TOPO vector (Invitrogen) to yield *orfΔ7.8.Δ9/TOPO*, for which the correct orientation of the target-3 insert was confirmed via restriction mapping. A schematic flowchart depicting the molecular biology process to obtain the recombinant virus is provided in Figure 6C.

PCR based Site-directed mutagenesis was used to introduce point mutations to the gene fragment encoding DLD of gB. The point mutations within the DLD sequence of KSHV gB were achieved by using the *orfΔ7.8.Δ9/TOPO* plasmid as the dsDNA template as described under section titled '*Cloning and expression of recombinant gBATMADLD.H*' to yield *orf8ΔDLD/TOPO*.

For antibiotic selection purposes, PCR was conducted to amplify the tetracycline cassette region of *pEX18TC* using Advantage PCR kit (BD Biosciences Clontech). While amplifying the tetracycline cassette (Tet.NdeI), we engineered NdeI restriction enzyme sites on both the 5' and 3' ends using specific primers (Table 1). Elution-purified Tet.NdeI was cloned into the pGEM-T Easy vector (Promega Inc., Madison, WI). Blunt end ligation was performed using NdeI restriction enzyme digested tetracycline cassette and *orf8ΔDLD/TOPO* to yield *orf8ΔDLD.Tet^r/TOPO*. Advantage PCR kit was used to amplify the above mentioned 5698bp DNA fragment encoding gB with a mutation to the DLD along with the tetracycline cassette and the flanking sequences to yield *orf8ΔDLD.Tet^r* that was used to electroporate. The 5698bp elution purified *orf8ΔDLD.Tet^r* PCR product was electroporated at 1.8kV, 200Ω, and 25μF into into *E. coli* DH10B cells harboring the BAC36wt-KSHV and pGET-rec (Narayanan *et al.*, 2009) plasmids. The electroporated cells were suspended in 800μl of LB medium, incubated at 37°C for 1h with shaking, and plated onto LB agar plates containing 10μg/ml tetracycline. After 48h incubation at 37°C, plasmid DNA was extracted via alkaline lysis, colonies were screened for the presence of the tetracycline cassette, and further confirmed by sequencing to detect mutation to

the sequence encoding DLD of gB. Our experimentation confirmed BAC36 Δ DLD.Tet^r (clone#3.2) to contain both the mutation to DLD of gB and the correct orientation of the tetracycline cassette. On the same lines, we also generated a BAC36 episome with the correct orientation of the tetracycline cassette with no mutations to the *orf8* gene that was referred to as BAC36.Tet^r (clone#7.2). This was used as a control in all of the experiments involving generation of the recombinant virus. To make it easy for labeling purposes, from now on the wild-type, BAC36 Δ DLD.Tet^r (clone#3.2), and BAC36.Tet^r (clone#7.2) episomes will be referred to as BAC36, BAC36 Δ D, and BAC36.T, respectively. Authenticity of the above mentioned cloning was confirmed by sequencing and performing PCR (Fig. 7).

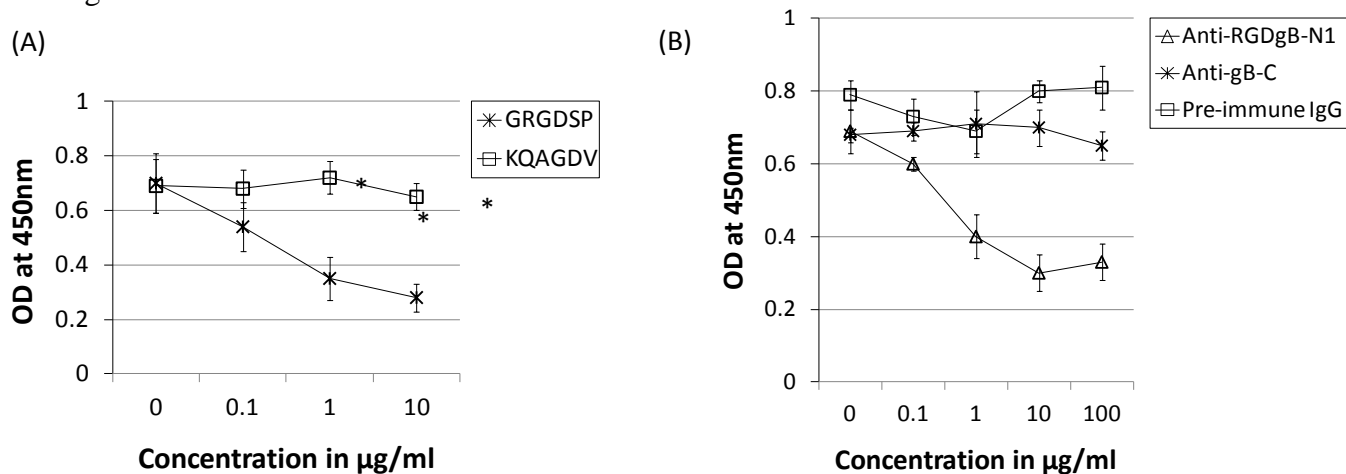
Purifying KSHV for infection studies. Transfection of BAC36, BAC36 Δ D, and BAC36.T plasmids into 293 cells grown in six-well plates was performed using Lipofectamine 2000 (Invitrogen, Carlsbad, CA). After 48h incubation, the cells were treated with TPA for 4 days prior to collecting the supernatant and infecting 50% confluent monolayers of 293 cells in a T25 flask. These cells were cultured in DMEM supplemented with 10% heat-inactivated FBS, 2mM-glutamine, streptomycin and penicillin, and 150 μ g/ml of hygromycin-B for a period of 3-4 weeks to select specifically for cells only harboring the BAC episomes. These cells were used to obtain BAC36-KSHV, BAC36 Δ D-KSHV, BAC36.T-KSHV, respectively, by specifically treating cells with 20ng/ml of TPA. At the end of 4 days post infection (PI), the supernatant was collected and the virus purified as per earlier studies (Akula *et al.*, 2004). The copy numbers of the purified KSHV from different transfected cell types were quantified by performing DNA PCR as per standard protocol (Naranatt *et al.*, 2003).

Monitoring KSHV infection of cells. The rKSHV.152 derived from BCBL-1 cells was used in most of the infection-based studies. The copy numbers of rKSHV.152 were determined by performing DNA PCR as mentioned above (Naranatt *et al.*, 2003). To test the effect of antibodies to integrins and the DLD peptide on virus infection of target cells, monolayers of cells cultured in 8-well chamber slides were incubated with different antibodies for 1h at 37°C prior to infection with 1 MOI of rKSHV.152 for 2h at 37°C. In another set of experiments, rKSHV.152 was incubated with 1µg/ml of heparin (a positive control) at 37°C for 1h prior to infecting. At the end of 2h incubation with the virus, cells were washed twice with DMEM and further incubated with appropriate growth medium for 72h prior to viewing under a fluorescent NIKON microscope. Cells expressing GFP were considered to be an indicator of a successful KSHV infection. The number of cells fluorescing green in five random fields using 20X objective within a particular well were counted and averaged. To avoid bias, the counting of green fluorescent cells for each experiment was performed by two different individuals and averaged. The data for plotting the graph was obtained from three different experiments. The above results were also authenticated by performing qRT-PCR using specific primers for *orf50*.

In all other experiments involving the use of BAC36-KSHV, confluent monolayers (70-80%) of target cells cultured in chamber slides were infected with 0.1 MOI of BAC36-KSHV, BAC36ΔD-KSHV, and BAC36.T-KSHV for 2h prior to washing the cells twice with DMEM to remove any unabsorbed virus particles followed by further incubation with growth medium. At the end of 72hPI, cells fluorescing green due to the expression of GFP was counted under a fluorescent microscope as per standard protocols.

Supplemental Figure 1

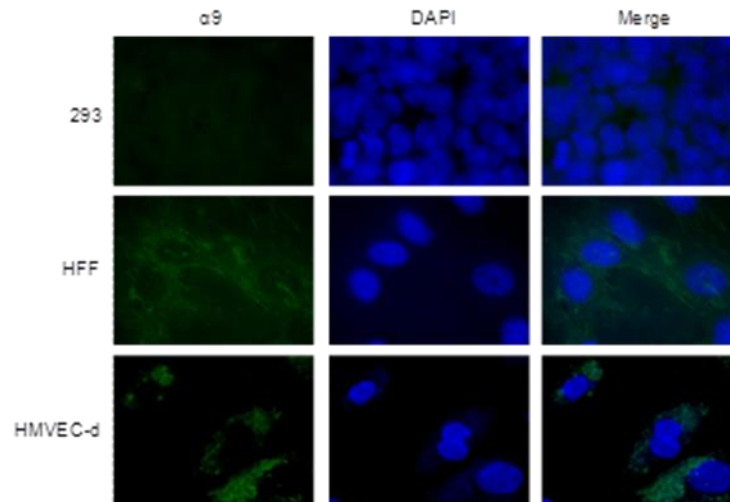
Effect of RGD peptides and anti-RGDgB-N1 antibodies in blocking $\alpha\beta3$ integrin interactions with gB.



SFig. 1: (A) Increasing concentrations of GRGDSP and KQAGDV (an irrelevant peptide) were incubated with $\alpha\beta3$ for 30min at room temperature (in an additional step) prior to their addition into gB Δ TM-coated wells and performing ELISA. (B) gB Δ TM-coated plates were incubated with anti-RGDgB-N1, anti-gB-C or pre-immune IgGs prior to incubation with $\alpha\beta3$ and performing ELISA. The results were read at 450nm (OD 450). Data presented in both the panels represent the average \pm S.D. (error bars) of three experiments. Asterisks on the data points denote the value to be statistically significant ($p < 0.05$) by LSD.

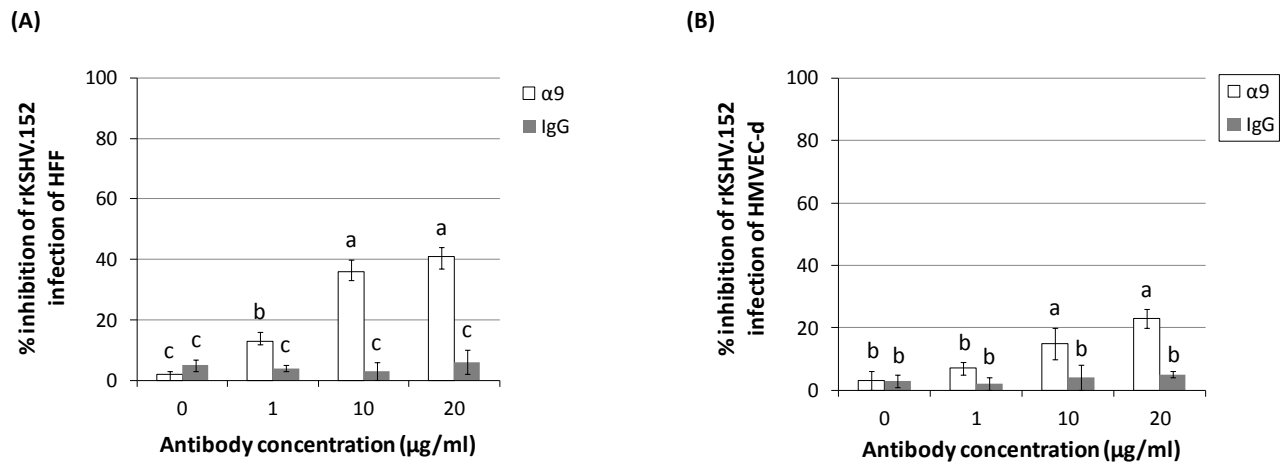
Supplemental Figure 2

Expression of integrin $\alpha 9$ on the surface of HFF and HMVEC-d cells.



SFig. 2: Surface Immunofluorescence assay (SIFA) was performed on 0.1% paraformaldehyde-fixed cells (Akula et al., 2001a) that were stained with Integrin $\alpha 9$ (H-198) rabbit polyclonal antibodies followed by incubation with goat anti-rabbit FITC, before examining under a fluorescent Nikon microscope using appropriate filters. A representative panel is depicted. Mag: 400X.

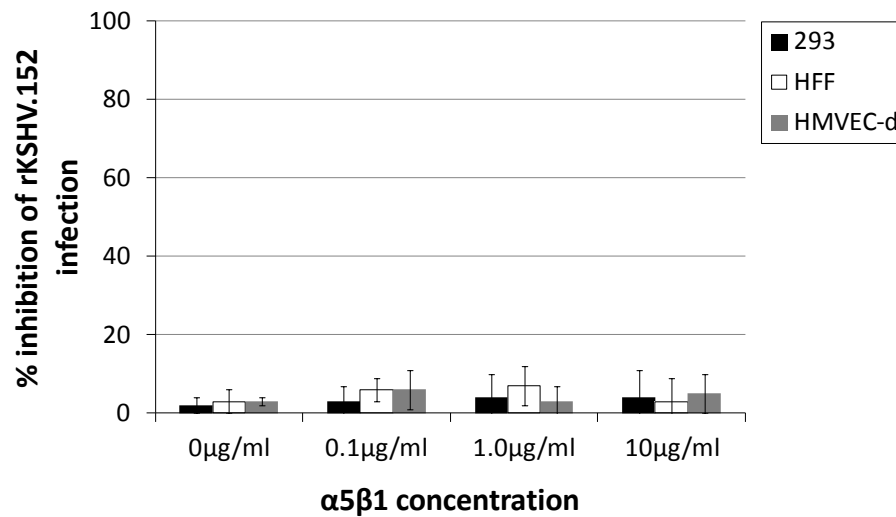
Supplemental Figure 3



SFig. 3: Inhibition of rKSHV.152 infection by different doses of antibodies to $\alpha 9$ is shown. In all of the above experiments, infection was monitored at 72hPI by recording the total number of cells expressing GFP under a fluorescent microscope. Data are presented as percentage of inhibition of virus infectivity obtained when the cells were preincubated with DMEM as control. Data represent the average \pm SD (*error bars*) of three experiments. Columns with different alphabets are statistically significant ($p < 0.05$) by LSD.

Supplemental Figure 4

$\alpha 5\beta 1$ integrin does not inhibit rKSHV.152 infection of cells.



SF4: Inhibition of rKSHV.152 infection by different concentrations of $\alpha 5\beta 1$ soluble integrin is shown. Infection was monitored at 72hPI by counting the number of GFP expressing cells under a fluorescent microscope indicative of rKSHV.152 infection. Data are presented as percentage of inhibition of virus infectivity obtained when the cells were preincubated with DMEM (minus antibodies) as control. Data represent the average \pm SD (*error bars*) of three experiments.

SF5: Molecular cloning and mutagenesis involved in derivation of BAC36 Δ D and BAC36.T via PCR and sequencing. **(A)** Plasmids *orf8 Δ DLD.Tet^r/TOPO* (clone#3.2) and *orf Δ 7.8. Δ 9.Tet^r/TOPO* (clone#7.2) contain correctly oriented tetracycline cassette. Prior to electroporation of *orf8 Δ DLD.Tet^r* or *orf8wtDLD.Tet^r* into *E. coli* DH10B cells harboring the BAC36wt-KSHV and pGET-rec plasmids, the correct orientation (~4235bp and 4958bp) of inserted Tet.NdeI in *orf8 Δ DLD.Tet^r/TOPO* and *orf Δ 7.8. Δ 9.Tet^r/TOPO* positive clones was confirmed by restriction enzyme digestion using BamHI and NheI as monitored by DNA agarose gel electrophoresis (0.8% agarose gel stained by ethidium bromide). **(B)** PCR using genomic BAC36, BAC36 Δ D, and BAC36.T DNA templates and specific primers (Tet(F), Tet(R); ORF8.RD(F), ORF8.RD(R); ORF8.D(F), ORF8.RD(R); Table 1) confirm presence of the tetracycline gene (~1.7kb; lanes 1 and 4) in recombinant BAC36 Δ D and BAC36.T. Likewise, *orf8* gene presence (1022bp, lanes 2 and 5; 865bp lanes 3 and 6) was confirmed in BAC36, BAC36 Δ D, and BAC36.T. **(C)** PCR using BAC36, BAC36 Δ D, and BAC36.T genomic DNA templates and specific primers (T1(F), T1(R); T2(F), T2(R)) confirm the presence of target-1 (2967bp) and target-2 (1055bp) in all three recombinant virus constructs. **(D)** PCR amplification of the target-3 DNA fragment from BAC36, BAC36 Δ D, and BAC36.T genomic DNA templates using specific primers (T1(F), T2(R)) confirm presence of Tet.NdeI cassette in BAC36 Δ D and BAC36.T (5698bp) versus BAC36 (4005bp). **(E)** Sequencing data (gathered via use of appropriate primers: ORF8.RD(F), ORF8.RD(R)) confirm presence of specifically introduced alanine point mutations within the DLD sequence of gB in BAC36 Δ D.

APPENDIX B: SUPPLEMENTARY DATA FROM CHAPTER 3

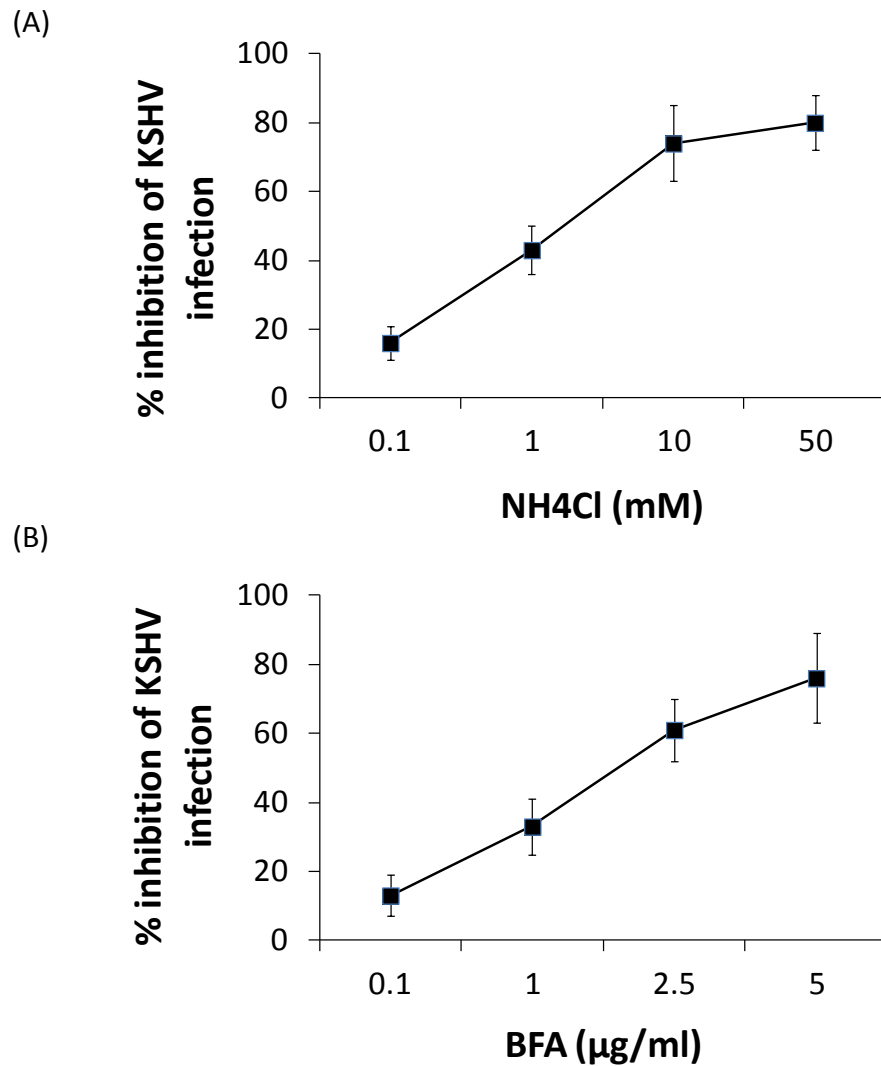
METHODS

Reagents. Ammonium chloride (NH₄Cl) was purchased from Sigma, St. Louis, MO; Brefeldin A (BFA) was purchased from Alfa Aesar, Ward Hill, MA.

Monitoring the effects of inhibitors on KSHV infection. Confluent monolayers of HFF cells grown in 6-well plates were incubated at 37°C for 1h with inhibitors diluted in DMEM: NH₄Cl (0.1, 1, 10, 50mM); BFA (0.1, 1, 2.5, 5µg/ml). Post-incubation, cells were infected with KSHV in the presence of inhibitors for 2h at 37°C, washed twice with DMEM, and further incubated with growth medium at 37°C. After 24h, cells were lysed, RNA extracted, cDNA synthesized, and the expression of *orf50* was monitored by qRT-PCR using specific primers (Dyson *et al.*, 2010) as previously mentioned.

Supplemental Figure 1

Disruption of 'normal' endosome function inhibits KSHV infectious entry into HFF cells.



SF1: HFF monolayers were incubated with DMEM containing increasing concentrations of NH₄Cl (A) or BFA (B) for 1h at 37°C. Cells were then infected with KSHV in the presence of inhibitors for 2h at 37°C, washed with DMEM, and further incubated for 24h at 37°C. Post-incubation, cells were lysed, RNA extracted, and cDNA synthesized. The expression of *orf50* was monitored by qRT-PCR using specific primers. The data are presented as percentages of inhibition of KSHV infection. Data represent the average \pm SD (error bars) of three experiments.

APPENDIX C: IRB APPROVAL



EAST CAROLINA UNIVERSITY
University & Medical Center Institutional Review Board Office
4N-70 Brody Medical Sciences Building · Mail Stop 682
600 Moyer Boulevard · Greenville, NC 27834
Office 252-744-2914 · Fax 252-744-2284 · www.ecu.edu/irb

Notification of Continuing Review Approval: Expedited

From: Biomedical IRB
To: [Shaw Akula](#)
CC:
[Karen Parker](#)
Date: 10/17/2014
Re: [CR00002347](#)
[UMCIRB 12-001158](#)
Cellular environment in renal transplant patients

The continuing review of your expedited study was approved. Approval of the study and any consent form(s) is for the period of 10/17/2014 to 10/16/2015. This research study is eligible for review under expedited category #1,2,3,5. The Chairperson (or designee) deemed this study no more than minimal risk.

Changes to this approved research may not be initiated without UMCIRB review except when necessary to eliminate an apparent immediate hazard to the participant. All unanticipated problems involving risks to participants and others must be promptly reported to the UMCIRB. The investigator must submit a continuing review/closure application to the UMCIRB prior to the date of study expiration. The Investigator must adhere to all reporting requirements for this study.

Approved consent documents with the IRB approval date stamped on the document should be used to consent participants (consent documents with the IRB approval date stamp are found under the Documents tab in the study workspace).

The approval includes the following items:

Document	Description
HIPAA authorization(0,01)	HIPAA Authorization
ICF(0,01)	Consent Forms
ICF,genetic testing(0,01)	Consent Forms
STUDY PROTOCOL(0,01)	Study Protocol or Grant Application

The Chairperson (or designee) does not have a potential for conflict of interest on this study.

